

ASSESSMENT OF 17BETA-ESTRADIOL-ESTROGEN RECEPTOR ALPHA
COMPLEX-MEDIATED CHANGES IN GENOME-WIDE METHYLATION
AND GENE EXPRESSION PROFILES

A THESIS SUBMITTED TO
THE GRADUATE SCHOOL OF NATURAL AND APPLIED SCIENCES
OF
MIDDLE EAST TECHNICAL UNIVERSITY

BY
SIRMA DAMLA USER

IN PARTIAL FULFILLMENT OF THE REQUIREMENTS
FOR
THE DEGREE OF MASTER OF SCIENCE
IN
BIOLOGY

MAY 2016

Approval of the Thesis:

**ASSESSMENT OF 17 β -ESTRADIOL-ESTROGEN RECEPTOR ALPHA
COMPLEX-MEDIATED CHANGES IN GENOME-WIDE METHYLATION
AND GENE EXPRESSION PROFILES**

submitted by **SIRMA DAMLA USER** in partial fulfillment of the requirements for
the degree of **Master of Science in Biology Department, Middle East Technical
University** by,

Prof. Dr. M. Gülbin Dural Ünver
Dean, Graduate School of **Natural and Applied Sciences** _____

Prof. Dr. Orhan Adalı
Head of Department, **Biology** _____

Prof. Dr. Mesut Muyan
Supervisor, **Biology Dept., METU** _____

Examining Committee Members:

Assoc. Prof. Dr. A. Elif Erson-Bensan
Biology Dept., METU _____

Prof. Dr. Mesut Muyan
Biology Dept., METU _____

Assoc. Prof. Dr. Tolga Can
Computer Engineering Dept., METU _____

Assoc. Prof. Dr. Çağdaş Devrim Son
Biology Dept., METU _____

Assist. Prof. Dr. Bala Gür Dedeoğlu
Biotechnology Institute, Ankara University _____

Date: 30.05.2016

I hereby declare that all information in this document has been obtained and presented in accordance with academic rules and ethical conduct. I also declare that, as required by these rules and conduct, I have fully cited and referenced all material and results that are not original to this work.

Name, Last name: Sırma Damla User

Signature :

ABSTRACT

ASSESSMENT OF 17BETA-ESTRADIOL-ESTROGEN RECEPTOR ALPHA COMPLEX-MEDIATED CHANGES IN GENOME-WIDE METHYLATION AND GENE EXPRESSION PROFILES

User, Sirma Damla
M.S., Biology Department
Supervisor: Prof. Dr. Mesut Muyan
May 2016, 142 pages

17 β -estradiol (E2), the most potent estrogen hormone, induces cellular responses primarily through Estrogen Receptor-alpha (ER α), which is a transcription factor. Interfering E2 signaling indicates that E2 is mitogenic for cells, exemplified by MCF7 cells derived from breast adenocarcinoma, synthesizing ER α endogenously.

Studies used exogenous expression of ER α in ER α -negative cell lines to examine structural/functional properties of the receptor. What was unexpected from these studies is the observation that E2 treatment represses cellular proliferation. However, mechanism(s) of this paradoxical phenomenon remains unknown.

Methylation is an important epigenetic DNA modification. Changes in methylation alter gene expressions critical for cellular proliferation/differentiation, embryonic development, genomic imprinting and cancer. We therefore hypothesize that distinct methylation statuses of responsive genes' regulatory regions underlie differential gene expressions, and hence, proliferative and anti-proliferative effects of E2 in cell models.

To test this prediction, we generated a cell model stably expressing ER α in MDAMB231 breast cancer cell line. Of the monoclonal synthesizing ER α , the MDA-ER α 5, based on expected ER α functions, was selected as the cell model to

comparatively assess the E2 effects on changes in methylome and transcriptome profiles to those observed in MCF7 cells.

Our studies suggest that cell models have cell-specific methylation patterns for the same genomic region at which E2 induces distinct alterations and differentially modulates gene expressions. However, due to the existence of variations among experimental replicates, establishing a correlation between the methylation statuses to gene expression profile of cell lines appears to be immature. An increase in sample size could circumvent this issue.

Keywords: estrogen, estrogen receptor, methylation, gene expression

ÖZ

17BETA-ÖSTRADİOL-ÖSTROJEN RESEPTÖR ALFA KOMPLEKSİ ARACILIĞI İLE GENOM ÇAPINDA OLUŞAN METİLASYON VE GEN İFADESİ DEĞİŞİKLERİNİN BELİRLENMESİ

User, Sırma Damla
Yüksek Lisans, Biyoloji Bölümü
Tez Yönetçisi: Prof. Dr. Mesut Muyan
Mayıs 2016, 142 sayfa

17 β -östradiol (E2), en güçlü östrojen hormonudur ve transkripsiyon faktörü olan Östrojen Reseptörü-alfa (ER α) aracılığıyla hücrede birçok yanıtın oluşmasına neden olur. E2 sinyal yolağına müdahale ile yapılan çalışmalarda, MCF7 gibi ER α 'yı endojen olarak sentezleyen hücrelerde E2'nin hücreyel çoğalma için gerekli olduğu gösterilmiştir.

ER α -negatif hücre hatlarında, ER α 'nın harici olarak sentezlenmesiyle reseptörün yapısal/fonksiyonel özellikleri çalışılmıştır. Beklenmedik olan ise E2'nin hücreyel çoğalmayı bu hücre hatlarında baskılamasıdır. Bu çelişkili gözlemlerin sebebi ise belirsizliğini korumaktadır.

Metilasyona önemli bir epigenetik modifikasyondur. Metilasyon sonucu oluşan gen ifadelerindeki değişiklikler, embryonik gelişim, genomik imprinting, kök hücre başkalaşımı ve kanser gibi birçok moleküler işlemde gereklidir. Bu nedenle, genlerin düzenleyici bölgelerindeki farklı metilasyon durumlarının, farklı gen ifadelerinin, bu nedenle de E2'nin endojen ya da harici olarak ER α sentezleyen hücrelerde, sırasıyla, hücre çoğalmasını destekleyen ya da engelleyen etkisinin sebebi olabileceğini varsayımında bulunuyoruz.

Farklı metilasyon durumlarını çalışabilmek adına MDAMB231 meme kanseri hücre hattında stabil olarak ER α sentezleyen bir model hücre hattı geliřtirdik. Harici olarak hücreye verilen reseptörün işlevliğini kontrol etmek için birçok fonksiyonel tarama yaptıktan sonra MDA-ER α 5 monoklon hücre hattının, genom çapında metilasyon farklılıklarını çalışmak için uygun olduğuna karar verdik. Ayrıca, metilasyonun gen ifadesi ile arasında bir bağıntı kurmak adına tüm transkriptomik profil analizi gerçekleřtirdik.

Genom çapında yapılan metilasyon profillemesi, aynı bölgeler için, her hücre hattının kendine özgü metilasyon desenleri olduğunu gösterdi. Ek olarak, E2 muamelesi ile bu deęişiklikler daha da artmıştır. Fakat, transkriptomik analizlerdeki varyasyonlar nedeniyle, sonuçlarımız metilasyon ve gen ifadesi arasında bir bağıntı kurmak için yetersiz kalmıştır.

Anahtar kelimeler: östrojen, östrojen reseptörü, metilasyon, gen ifadesi

ACKNOWLEDGEMENTS

I would like to thank my supervisor Prof. Dr. Mesut Muyan for, first of all, teaching me how to think critically and to question every single result. Also, for teaching me to mentally plan subsequent steps and anticipate the possible results. I have learned the beauty of scientific world thanks to him. There is no way to express my gratitude for all the guidance he has provided and the patience he has shown.

I am grateful to Assoc. Prof. Dr. A. Elif Erson-Bensan for her support and valuable inputs in this thesis work. I would like to thank Assoc. Prof. Dr. Tolga Can for his guidance and enormous input in analyzing the data.

I would like to thank all my thesis committee members; Prof. Dr. Mesut Muyan, Assoc. Prof. Dr. A. Elif Erson-Bensan, Assoc. Prof. Dr. Tolga Can, Assoc. Prof. Dr. Çağdaş Devrim Son, and Assist. Prof. Dr. Bala Gür Dedeoğlu once again for being here to provide critical feedbacks to my work.

I want to express my sincere thanks to my lab members Gamze Ayaz, Pelin Yaşar, Çağla Ece Olgun, Burcu Karakaya, and Gizem Kars as well as the former lab member Gizem Güpür for their endless help and comforting when I needed the most. Also, I would like to thank Bilge Aşkın for her help in numerous experiments. In addition, I want to thank all the members of Erson-Bensan Lab for their support and help. I would like to thank Bilgi Güngör and Ersin Gül for their invaluable help in Flow Cytometry. I also would like to thank Prof. Dr. Rengül Çetin Atalay and her lab members for their help in fluorescent microscope use.

My special thanks go to Berfin Karakeçili, Ece Öztürk, Ege Tuna, Gülce Çakman, Nazlı Ünal, and Pınar Boz for being the source of joy in my life. I would like to thank Ece Zıraman, Nermin Uğur, Onur Demir, and Tilbe Mutluay for their wonderful friendship. I want to thank Aylin Kömez, Beliz Bediz, and Neşe Erdem for their support and friendship.

There are no words to express how much I owe to my dearest friend Armağan Hergüner for his endless support.

I cannot express my heartfelt thanks to my sweetheart sisters Berna User and Rana User-Smits together with Kerem Göçen and Kenny Smits. They were, are, and will always be there to support me. I also would like to thank my beloved parents, who loved and supported me unconditionally throughout my life. I owe them everything I have.

Finally, I would like to thank TUBITAK for supporting this study through 212T031 and 114Z243 projects. I also express my gratitude to METU BAP for supporting this work through BAP-08-11-2015-019.

TABLE OF CONTENTS

ABSTRACT.....	v
ÖZ	vii
ACKNOWLEDGEMENTS	ix
TABLE OF CONTENTS.....	xi
LIST OF TABLES	xiv
LIST OF FIGURES	xvi
CHAPTERS	
1. INTRODUCTION	1
1.1. Breast Cancer	1
1.1.1. Breast Cancer Cell Lines	2
1.1.2. Estrogen Signaling in Breast Cancer	2
1.1.2.1. Features of Estrogen Receptors	2
1.1.2.2. Features of 17 β -Estradiol	4
1.1.2.3. E2-ER α Signaling.....	5
1.2. Methylation and Its Relation to Breast Cancer	6
1.2.1. Methylation in Breast Cancer	9
1.3. Aim of the Study	10
2. MATERIALS AND METHODS.....	11
2.1. Cell Lines and Treatments	11
2.1.1. Treatments	11
2.2. Transfection.....	12

2.2.1.	Transient Transfection	12
2.2.2.	Generation of Stable Cell Lines.....	12
2.3.	Western Blot	13
2.3.1.	Total Protein Isolation	13
2.3.2.	Western Blot.....	13
2.4.	Growth Assay.....	14
2.5.	Immunocytochemistry	14
2.6.	Dual Luciferase Reporter Assay	15
2.7.	Expression Analysis.....	16
2.7.1.	Primer Design	16
2.7.2.	Total RNA Isolation	16
2.7.2.1.	Genomic DNA Contamination Control	17
2.7.3.	cDNA Synthesis	17
2.7.4.	Real Time-Quantitative Polymerase Chain Reaction (RT-qPCR)	18
2.8.	Cell Cycle Distribution	19
2.8.1.	Preparation of Samples.....	19
2.8.2.	Analysis of Samples	19
2.9.	Methylation and Transcriptomic Analysis.....	20
3.	RESULTS AND DISCUSSION	21
3.1.	Generation of an ER-Negative Cell Model That Synthesizes Human ER α Introduced Exogenously	21
3.1.1.	Expression of ER α in Stably Transfected MDAMB231 Cells.....	21
3.1.2.	The Effects of E2 on Cellular Proliferation of Candidate Monoclonal	23
3.2.	Functional Screening of MDA-ER α 5 Stable Monoclonal as the Cell Model.....	24

3.2.1.	Western Blot Analysis of MDA-ER α 5 Stable Monoclonal.....	24
3.2.2.	Immunocytochemistry of MDA-ER α 5 Stable Monoclonal.....	25
3.2.3.	Dual-Luciferase Reporter Assay.....	28
3.2.4.	Expression Analyses of Endogenous Estrogen Responsive Genes	29
3.2.5.	Cell Cycle Distribution in Response to E2	35
3.3.	Repression of Cellular Proliferation in the MDA-ER α 5 Stable Monoclonal in Response to E2.....	37
3.4.	Genome-Wide Methylation Profile Analysis.....	39
3.5.	Whole-Genome Transcriptomic Profile Analysis.....	55
4.	CONCLUSION AND FUTURE DIRECTIONS	59
	BIBLIOGRAPHY	61
APPENDICES		
A.	DEXTRAN COATED CHARCOAL STRIPPED FETAL BOVINE SERUM	67
B.	BUFFERS.....	69
C.	MIQE GUIDELINES	71
D.	PRIMERS.....	75
E.	GENOMIC DNA CONTAMINATION CONTROL	77
F.	PERFORMANCE OF RT-qPCR REACTIONS	79
G.	KINETIC ANALYSIS OF CELL CYCLE HISTOGRAMS	81
H.	TOP 100 SIGNIFICANT GENOMIC REGIONS IN METHYLOME ANALYSES.....	85
I.	LINKS FOR METHYLATION TRACKS.....	131
J.	GENES SHOWING SIGNIFICANT CHANGES IN TRANSCRIPTOMIC ANALYSES.....	133

LIST OF TABLES

Table 1. Reaction Conditions and Product Size Information.....	18
Table 2. Whole Transcriptomic Profile Analyses for Subset of Genes in MDA-ER α 5 ethanol vs E2 treatment.....	55
Table 3. Whole Transcriptomic Profile Analyses for Subset of Genes in MCF7 ethanol vs E2 treatment.....	56
Table C 1. MIQE Checklist.....	71
Table D 1. Primer List.....	75
Table H 1. Top 100 Hypermethylated Genomic Regions in MDA-ER α 5 Cells After 6h E2 Treatment.....	85
Table H 2. Top 100 Hypomethylated Genomic Regions in MDA-ER α 5 Cells After 6h E2 Treatment.....	90
Table H 3. Top 100 Hypermethylated Genomic Regions in MCF7 Cells After 6h E2 Treatment.....	95
Table H 4. Top 100 Hypomethylated Genomic Regions in MCF7 Cells After 6h E2 Treatment.....	100
Table H 5. Top 100 Hypermethylated Genomic Regions in MDA-ER α 5 and MCF7 Cells After 6h OH Treatment.....	105
Table H 6. Top 100 Hypomethylated Genomic Regions in MDA-ER α 5 and MCF7 Cells After 6h OH Treatment.....	110
Table H 7. Top 100 Hypermethylated Genomic Regions in MDA-ER α 5 and MCF7 Cells After 6h E2 Treatment.....	117

Table H 8. Top 100 Hypomethylated Genomic Regions in MDA-ER α 5 and MCF7 Cells After 6h E2 Treatment.....	124
Table J 1. Genes Showing Significant Changes in Transcriptomic Analysis of MDA-ER α 5 Monoclone After 6h E2 Treatment Compared to Ethanol Group.....	133
Table J 2. Genes Showing Significant Changes in Transcriptomic Analysis of MCF7 Cells After 6h E2 Treatment Compared to Ethanol Group.....	135

LIST OF FIGURES

Figure 1. Schematic representation of domains of ER α and ER β proteins and their distribution.....	3
Figure 2. Schematic representation of ERE-dependent (A) and ERE-independent (B) genomic E2-ER α signaling.....	6
Figure 3. Schematic representation of cytosine methylation and demethylation.....	7
Figure 4. Bisulfite-induced oxidative deamination of methylated cytosine residues	8
Figure 5. Western Blot analysis of stable monoclonal cell lines (A and B).....	22
Figure 6. E2 effects on cellular growth of stable monoclonal cell lines.....	24
Figure 7. Western Blot analysis of MDA-ER α 5 Stable Monoclonal Cell Line.....	25
Figure 8. Immunocytochemistry for nuclear localization of ER α protein with ER α HC-20x antibody.....	26
Figure 9. Immunocytochemistry for nuclear localization of ER α protein with Flag M2 antibody.....	27
Figure 10. Dual-Luciferase reporter assay of the candidate monoclonal cell line.....	29
Figure 11. <i>YPEL2</i> mRNA Expression Analysis.....	31
Figure 12. <i>YPEL3</i> mRNA Expression Analysis.....	32
Figure 13. <i>CTGF</i> mRNA Expression Analysis.....	33
Figure 14. <i>TFF1/pS2</i> (A) and <i>CCNA1</i> (B) mRNA Expression Analyses.....	34
Figure 15. Cell cycle phase distributions upon E2 treatment.....	37
Figure 16. Growth of monoclonal MDA-ER α 5 (A), MCF7 (B), and MDA-EV2 (C)	39
Figure 17. A representative image for genomic DNA integrity.....	40

Figure 18. Differential methylation status of MDA-ER α 5 monoclonal cells.....	41
Figure 19. Differential methylation status of MCF7 cells.....	42
Figure 20. Differential methylation statuses of MDA-ER α 5 monoclonal cells and MCF7 cells.....	43
Figure 21. Differential methylation status of <i>YPEL2</i> in ethanol vs E2 treated MDA-ER α 5 cells.....	45
Figure 22. Differential methylation status of <i>YPEL2</i> in ethanol vs E2 treated MCF7 cells.....	45
Figure 23. Differential methylation status of <i>YPEL3</i> in ethanol vs E2 treated MDA-ER α 5 cells.....	46
Figure 24. Differential methylation status of <i>YPEL3</i> in ethanol vs E2 treated MCF7 cells.....	46
Figure 25. Differential methylation status of <i>CTGF</i> in ethanol vs E2 treated MDA-ER α 5 cells.....	47
Figure 26. Differential methylation status of <i>CTGF</i> in ethanol vs E2 treated MCF7 cells.....	47
Figure 27. Differential methylation status of <i>TFF1/pS2</i> in ethanol vs E2 treated MDA-ER α 5 cells.....	48
Figure 28. Differential methylation status of <i>TFF1/pS2</i> in ethanol vs E2 treated MCF7 cells.....	48
Figure 29. Differential methylation status of <i>CCNA1</i> in ethanol vs E2 treated MDA-ER α 5 cells.....	49
Figure 30. Differential methylation status of <i>CCNA1</i> in ethanol vs E2 treated MCF7 cells.....	49
Figure 31. Differential methylation status of <i>YPEL2</i> in ethanol treated MDA-ER α 5 vs MCF7 cells	50
Figure 32. Differential methylation status of <i>YPEL3</i> in ethanol treated MDA-ER α 5 vs MCF7 cells.....	50

Figure 33. Differential methylation status of <i>CTGF</i> in ethanol treated MDA-ER α 5 vs MCF7 cells.....	51
Figure 34. Differential methylation status of <i>TFF1/pS2</i> in ethanol treated MDA-ER α 5 vs MCF7 cells.....	51
Figure 35. Differential methylation status of <i>CCNA1</i> in ethanol treated MDA-ER α 5 vs MCF7 cells.....	52
Figure 36. Differential methylation status of <i>YPEL2</i> in E2 treated MDA-ER α 5 vs MCF7 cells.....	52
Figure 37. Differential methylation status of <i>YPEL3</i> in E2 treated MDA-ER α 5 vs MCF7 cells.....	53
Figure 38. Differential methylation status of <i>CTGF</i> in E2 treated MDA-ER α 5 vs MCF7 cells.....	53
Figure 39. Differential methylation status of <i>TFF1/pS2</i> in E2 treated MDA-ER α 5 vs MCF7 cells.....	54
Figure 40. Differential methylation status of <i>CCNA1</i> in E2 treated MDA-ER α 5 vs MCF7 cells.....	54
Figure 41. Biological function clustering of genes showing significant changes in ethanol vs E2 treated MCF7 cells with RNA-seq.....	57
Figure E 1. Genomic DNA control PCR.....	77
Figure G 1. Cell cycle kinetics of MDA-ER α 5 monoclonal.....	81
Figure G 2. Cell cycle kinetics of MCF7 cells.....	82
Figure G 3. Cell cycle kinetics of MDA-EV2 monoclonal.....	83

CHAPTER 1

INTRODUCTION

1.1. Breast Cancer

Breast cancer is the most common cancer among women worldwide and incidences in men are also present. By the end of 2016, 246,600 women are expected to be diagnosed with breast cancer and estimated death is 40,000 in the United States of America [1]. Breast cancer is also the leading cancer type among women of Turkey, with an average incidence rate of 40.7/100,000 in 2013 and is the eighth most common death cause among women, with a ratio of 2.1% [2].

Breast cancer is a formidable disease due to its heterogeneity in terms of molecular and clinical subtypes. As of 2013, breast cancer classification consists of histopathological and molecular traits [3]. The histopathological classification is based on morphological (i.e. tumor size, location, grade and whether there is axillary lymph node metastasis or not) and immunohistochemical analyses of tissue samples in terms of estrogen receptor (ER), progesterone receptor (PR) and human epithelial growth factor receptor 2 (HER2) synthesis. On the other hand, molecular classification is based on differential gene expression pattern of subtypes, which provides more detailed picture about the heterogeneity of the carcinoma [3]. A better understanding of underlying mechanism involved in the initiation and progression of breast cancer and the advent of technologies are enabling the development of various platforms for subtype classifications with the potential of patient-targeted therapies.

1.1.1. Breast Cancer Cell Lines

In order to study various fundamental characteristics of breast cancer subtypes, immortalized cell lines or cell lines derived from primary tumors have been used for decades. Two breast cancer models used in this study are MCF7 and MDAMB231 cell lines. MCF7 cell line was derived from a pleural effusion surgically removed from a 69-year-old patient with metastatic breast cancer [4]. MCF7 cells endogenously express ER α and PR but not HER2; a combination which allows MCF7 cells to be used as a model for hormone-sensitive breast cancer [5]. MDAMB231 cell line was derived from a pleural effusion surgically removed from a 51-year-old patient having an inner quadrant tumor [6]. Unlike MCF7 cells, MDAMB231 cells are classified as triple negative in terms of ER, PR and HER2 expression. This cell line has been used as a model for triple-negative breast cancer, which displays an aggressive profile both in diagnosis, treatment and reoccurrence [7].

1.1.2. Estrogen Signaling in Breast Cancer

Estrogen signaling in breast cancer is important for both disease initiation and progression. To better understand the molecular mechanism, features of estrogen receptors and 17 β -estradiol is explained in the following sections.

1.1.2.1. Features of Estrogen Receptors

In mammals, 17 β -estradiol (E2) transmits the signal through its receptors; estrogen receptor α (ER α) and ER β , which are transcription factors [8], [9]. ER α is synthesized from *ESR1* found on the 6q25.1 locus; whereas ER β is the product of *ESR2* gene found on 14q23-24.1 genomic locus [9]. Estrogen receptors are type I nuclear receptors [10] and they are expressed at different levels in various tissues [11]. Upon translation, they form the ER α or ER β homodimer as well as the ER α / β heterodimer when co-synthesized [8]. ER dimers translocate primarily to nucleus independently from E2 binding [8]. In breast tissue, ER α is the primary ER subtype to convey E2 signaling that regulates cellular proliferation, motility, and death [11].

ER α and ER β have common structural properties with six structural domains contributing to their similar functions [11]. The A/B region of ERs having 17% amino acid identity between ERs is the N-terminal ligand-independent transactivation domain and it involves in protein-protein interactions responsible for activation of target gene transcriptions [8], [9], [12]. C region comprises the DNA-binding domain (DBD), and it is important for DNA binding ability of ERs as well as for their dimerization (albeit weakly). This domain is highly conserved between ERs and share 97% amino-acid identity [9]. D domain which is also known as the hinge region shows high divergence between ER α and ER β with a shared 30% amino acid identity [9]. The hinge region contains nuclear localization signal (NLS) and also numbers of motifs for post-translational modifications including acetylation and sumoylation [9]. In addition, the D domain connects the C and E/F domains [8]. The highly conserved (56% amino acid identity) E/F region is located at the C-terminus of the receptors and it possesses ligand-binding domain (LBD), dimerization domain and ligand-dependent transactivation function (AF-2) (Figure 1) [9]. The binding of E2 induces conformational changes in the carboxyl terminus of ER α that results in a more stable receptor homodimer and a binding surface for cofactors. This conformational change allows the formation of a transcriptionally active E2-ER α complex to regulate the expression of E2-responsive genes [8].

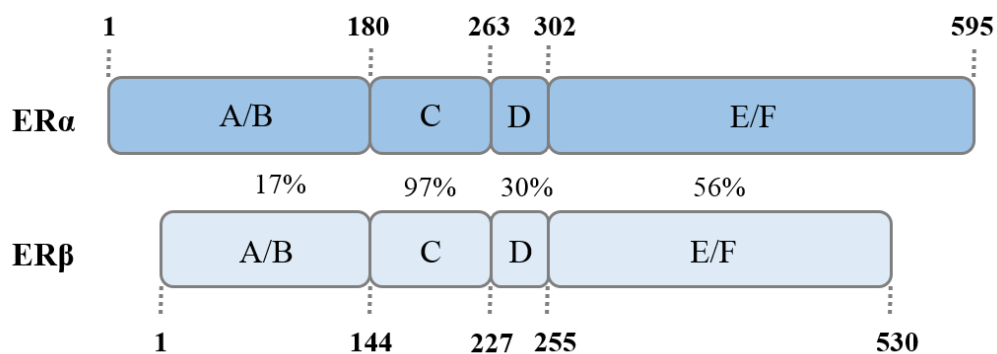


Figure 1. Schematic representation of domains of ER α and ER β proteins and their distribution. Numbers at the end of dashed lines show amino acid length of regions. Percent values show amino acid identity between corresponding domains of ER proteins. Figure depicts proteins from N-terminus to C-terminus.

1.1.2.2. Features of 17 β -Estradiol

Estrogens are steroid hormones acting on estrogen receptors to induce signaling cascade. Estrogens are synthesized from cholesterol primarily in the ovaries. Although minor amounts of estrone (E1) and estriol (E2) are present, the most potent estrogen hormone in the circulation is 17 β -estradiol (E2) [11]. E2 is involved in various physiological functions including development and maintenance of reproductive organs, regulation of cardiovascular, musculoskeletal, immune, and central nervous system homeostasis [13], [14]. In addition, E2 also contributes to the initiation and development of target tissue malignancies [13], [14].

E2 is considered as a proliferative agent. Studies with E2 withdrawals or E2 antagonists clearly show that E2 is required for proliferation of ER α -positive cell lines, including MCF7 cells [15]. To study the structural and functional features of ER α in breast cancer, many groups attempted to exogenously express ER α by transfections [15]–[19] or viral infection [20] in an effort to generate a model that emulates endogenously ER α expressing breast cancer cells. However, the paradoxical observation was that in ER α synthesizing cells introduced exogenously, the cellular proliferation is repressed in response to E2 in contrast to cells that synthesize ER α endogenously. Jiang and Jordan (1991), Garcia *et al.* (1992), and Lazennec and Katzenellenbogen (1993) attempted to enable hormonal responsiveness of ER α -negative MDAMB231 breast cancer cells by using stable transfection of ER α [17], [21] or viral infection [20], and they independently observed that E2 represses proliferation. This was also the case in which E2 effectively repressed the proliferation of MDAMB468 cells stably transfected with ER α cDNA [22]. Zajchowski *et al.* (1993) studied different E2 response pathways in between normal human mammary epithelial cells and 21T breast cancer cells by using stable transfection and obtained similar results [15]. In addition, observations indicate that gene expressions involved in cellular proliferation in response to E2-ER α are differentially altered in cell lines expressing ER α endogenously *vs* exogenously [23]. Although these pioneering studies provided a model system to study structural/functional features of ER α , the mechanism by which ER α in response to E2 differentially regulate cellular proliferation remains unknown.

1.1.2.3. E2-ER α Signaling

Newly synthesized ER α dimerizes and the dimer translocates to the nucleus independently from E2 binding while a small portion (nearly 5%) of ER remains outside of nucleus and locates to membrane, cytoplasm and mitochondria [12], [24]. Different intracellular localizations of ER allow E2 signaling to occur from various locations. Although extranuclear ER contributes, the long-lasting phenotypic effects of E2 on cells rely on the nuclear ER [11].

The E2-ER α complex regulates gene expression through either Estrogen Responsive Element (ERE)-dependent or ERE-independent genomic signaling pathway (Figure 2). EREs are palindromic sequences (GGTCAnnnTGACC, 'n' denotes for any nucleotide) found on the regulatory regions of E2-responsive genes [9], [25]. It was shown that the E2-ER α complex can bind to the consensus ERE sequences having only one nucleotide change in the core sequence but can tolerate up to three nucleotide changes when surrounding sequences of the core contains a cytosine and/or adenosine residue [25]. Unliganded ER α is also capable of binding to ERE with oscillation; however this interaction is inefficient and binding of E2 to ER α increases the stability of ER α dimer and affinity for co-regulatory proteins as well as ERE interaction period [26].

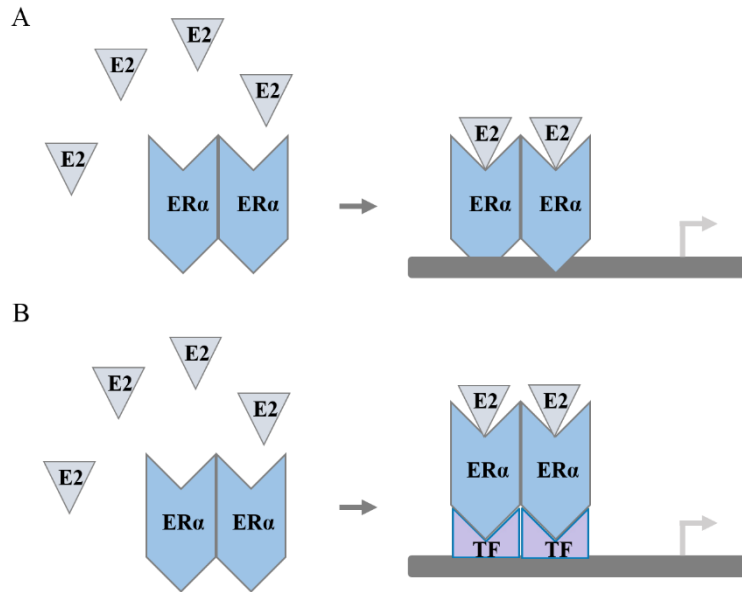


Figure 2. Schematic representation of ERE-dependent (A) and ERE-independent (B) genomic E2-ER α signaling.

When E2-ER α directly binds to ERE sequences on regulatory elements on the genome, it is called the ERE-dependent E2-ER α signaling pathway. However, the E2-ER α complex has also ability to interact with other transcription factors such as AP1, Sp1 which are already in contact with their respective response elements on the genome in regulating downstream gene expressions [12]. In this situation, there is not a direct interaction between responsive element and the E2-ER α complex, the signaling pathway is hence called as the ERE-independent E2-ER α signaling pathway. Both nuclear pathways are critical for the transcriptional regulation of estrogen responsive genes involved in the cellular proliferation, differentiation, migration and death.

1.2. Methylation and Its Relation to Breast Cancer

Methylation of DNA at cytosine (C) nucleotides is an important epigenetic alteration that results in differential gene expressions [27], [28]. Different methylation statuses of the same regions on the genome in different tissues act as a mark for tissue-specific gene expression profiles. Accordingly, it is suggested that differences in gene

expressions caused by DNA methylation are necessary for embryonic development, genomic imprinting and X-chromosome inactivation, silencing of transposable elements, stem cell differentiation, and inflammation [27]–[30].

In eukaryotes, C residues of specific regions, namely CpG dinucleotides with ‘p’ denoting the phosphate group between cytosine and guanine (G) nucleotides, are methylated, and these methylated regions could define transcriptionally active, inactive, or unaffected regions [30], [31]. In addition, it was reported that CHG residues (also shown as CpHpG) with ‘H’ denoting any of the adenine (A), thymine (T) and C nucleotides are also methylated [31]. DNA methylation is mediated by DNA methyltransferases (DNMT) having conserved catalytic domains. DNMTs enable the transfer of a methyl group from *S*-adenosyl-methionine (SAM) to the 5-position of the cytosine ring (Figure 3), resulting in methylated CpG dinucleotides, and the methylation status is maintained by DNMT1, DNMT3A, and DNMT3B proteins [28], [29].

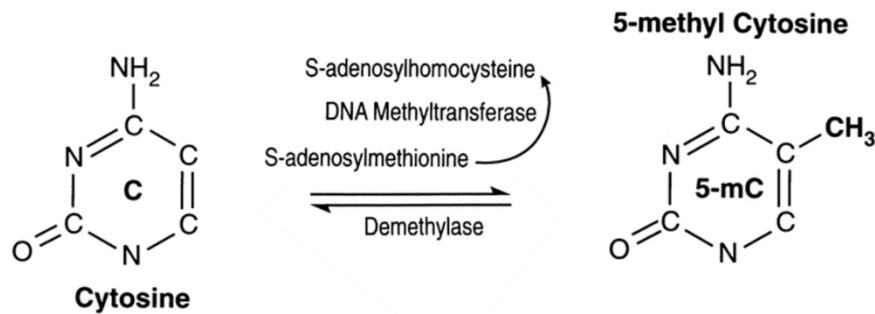


Figure 3. Schematic representation of cytosine methylation and demethylation. Figure was adapted from the article [28].

Continuous improvements in molecular biology techniques are enabling the exploration of whole genome methylation pattern of a given system in a single-base-pair resolution [31]. Most commonly used technique in methylation studies is the conversion of cytosine to uracil residue after bisulfite-induced oxidative deamination on the genome. In this approach, methylated cytosines are protected from the conversion to uracil, which allows the use of direct sequencing to determine the locations of unmethylated cytosines (Figure 4) [28].

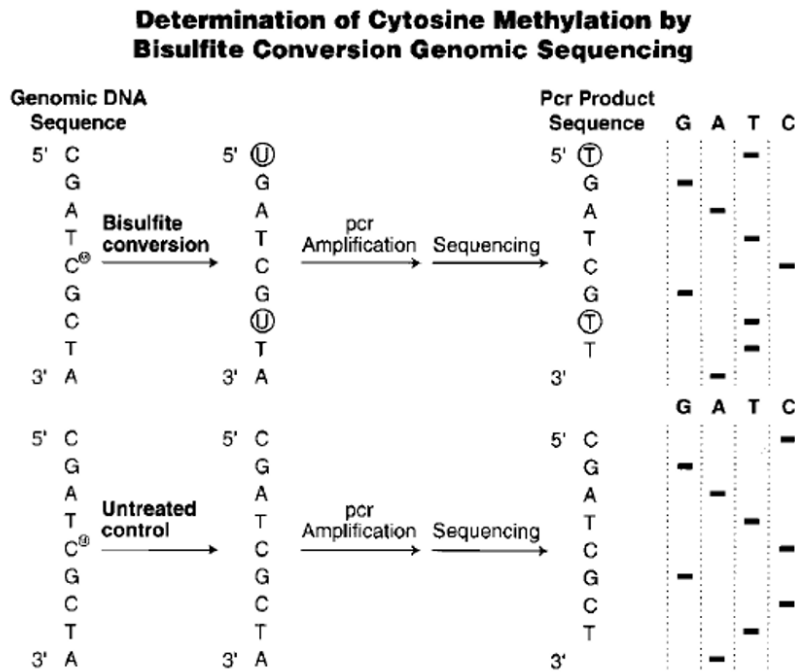


Figure 4. Bisulfite-induced oxidative deamination of methylated cytosine residues. Image was taken from the article [28].

DNA methylation and demethylation processes are highly dynamic processes and balanced events. The physical accessibility of methylation-prone regions to methylation machinery on the chromatin during these dynamic events is an important factor in gene regulations. Accordingly, there are different mechanisms for transcriptional regulation caused by methylation. It was suggested that the methylation of DNA facilitates recruitment of methylated DNA binding proteins such as methyl-CpG-binding protein 1 and 2 (MeCP1 and MeCP2, respectively) which further recruit co-repressors and histone deacetylases (HDAC) together with histone methyltransferases resulting in a less accessible chromatin conformation for transcription machinery [28]–[30]. Another suggested mechanism for methylation of cytosine to repress downstream gene expression is the prevention of binding of transcription factors by occupying their corresponding binding region(s) on the regulatory regions of genome [28], [30]. In addition, emphasizing the importance of dynamic harmony between methylation of chromatin and chromatin structure, due to

chemical structure and charge of the methyl groups added, chromatin becomes inaccessible to transcription machinery [27]–[29]. However, although methylation events close to promoter and/or regulatory regions of genes are considered to reflect the repressed state of transcription, it was also suggested that methylation in the gene body regions facilitates a prolonged transcription rather than transcription prevention [30].

1.2.1. Methylation in Breast Cancer

Various studies suggested that local hypermethylation of tumor-suppressor genes and general hypomethylation of proliferation-related genes play critical roles in carcinogenesis [27]–[29]. According to Szyf *et al.* (2004), stage-specific DNA methylation could be used as signatures for staging primary breast cancer and also for breast cancer subtypes [29].

The absence of ER α expression in some breast cancers is shown to be due to the hypermethylation of the ER α gene locus [29], [30]. Studies including DNA methyltransferase inhibitors (e.g. nucleoside analogue 5-aza-deoxy-cytidine, 5-aza-CdR) and antisense oligonucleotides against *DNMT1* transcript showed that methylated genes in cancer cells can be reactivated [29]. In MDAMB231 cells, the expression of ER α was activated upon 5-aza-CdR treatment [32].

DNA methylation profiles of primary breast cancer and metastatic breast cancer show distinct gene expression patterns [29]. Together with improvements on experimental approaches, there are number of studies focusing on the relationship between breast cancer and genome-wide DNA methylation. Corroborating findings from tumor samples with ER α -positive or ER α -negative statuses, experimental studies using hierarchical clustering analyses showed that methylation patterns differ among endogenously ER α expressing cells and ER α -negative cells [33]–[35]. In order to identify localization-specific methylation patterns, immunoprecipitation against methylated DNA approach was used by Ruike *et al.* and samples were sequenced [36]. Similarly, Ung *et al.* (2014) studied the relationship between ER α binding sites and the methylation pattern *in silico* [30]. In their study, they suggested that ER α binding to ERE sites dramatically altered by methylation patterns in genome level.

They also uncovered that methylated CpGs, highly correlated with gene expressions, are enriched in regions 1kb or more downstream of transcription start sites, suggesting significant regulatory roles for CpGs distal to gene transcription start sites [30].

1.3. Aim of the Study

E2 is considered as a proliferative agent. However, pioneering studies assessing the action of mechanism of ER α revealed a paradoxical phenomenon: E2 represses cellular proliferation of breast cancer cells expressing ER α introduced exogenously [15]–[19] as a result of repression of genes involved in proliferation [23].

Since distinct DNA methylation patterns contribute to altered gene expression signatures that result in the manifestation of breast cancer subtypes [28]–[30], [32], we suggest that differences in genome-wide methylation statuses of cell lines expressing ER α endogenously *vs* exogenously could underlie differential gene expressions, and hence the polarity in the direction of cellular proliferation as well.

CHAPTER 2

MATERIALS AND METHODS

2.1. Cell Lines and Treatments

MDAMB231 and MCF7 cells were kind gifts of Dr. A. Elif Erson Bensan from Middle East Technical University, Ankara, Turkey. Both cell lines were maintained in high glucose Dulbecco's modified eagle medium (DMEM) without phenol red (Lonza, Belgium, BE-12-917F) supplemented by 8% fetal bovine serum (FBS, Biochrom AG, Germany, S0115), 1% penicillin streptomycin (P/S, Lonza, Belgium, DE17-602E) and 0.5% L-Glutamine (Lonza, Belgium, BE17-605E) (DMEM/FBS).

MDAMB231-Flag-ER α (MDA-ER α 5) and MDAMB231-EV (MDA-EV) stable cell lines were maintained in DMEM without phenol red supplemented with 8% dextran coated charcoal (Sigma Aldrich, Germany, C6241) stripped fetal bovine serum (CD-FBS), 1% P/S, 0.5% L-Glutamine and 0.750 mg/mL G-418 solution (Roche, Germany, 04727894001) (CD-FBS/DMEM, Appendix A).

All cells were grown as monolayers in 95% humidified incubator at 37°C with 5% CO₂, and maintained for six-week maximum.

2.1.1. Treatments

For treatments, cells were seeded in phenol red-free DMEM supplemented with 8% CD-FBS, 1% P/S and 0.5% L-Glutamine and grown for 48 hours for hormone depletion. Whenever it was appropriate, various treatment groups for different durations were used. These treatment groups included 1) physiological concentrations (10^{-9} M) of the steroid hormone 17 β -estradiol (E2, Sigma Aldrich, Germany, E2257), 2) 10^{-7} M of complete ER α antagonist Imperial Chemical

Industries 182,780 (ICI, Tocris Biosciences, MN, USA), 3) a combination of E2 (10^{-9} M) and ICI (10^{-7} M) and 4) 0.01% of molecular grade ethanol as vehicle control.

2.2. Transfection

Transfection of mammalian cells with suitable vectors is a useful approach in molecular biology. In our study, we performed two types of transfections as explained in the following sections.

2.2.1. Transient Transfection

The transfection complex for transient transfections for one well of a six-well plate was prepared as follows; two μ g DNA was added into 200 μ L of phenol red-free DMEM. Four μ L of TurboFect Transfection Reagent (Life Technologies, USA, R0531) (2 μ L/ μ g DNA) was added and after a brief vortex, mixture was incubated at room temperature for 30 minutes for transfection complex formation. Medium in the wells was refreshed and the transfection complex was added into wells dropwise. Four hours after transfection, medium in the wells was refreshed. Appropriate experiments were done subsequently.

2.2.2. Generation of Stable Cell Lines

MDAMB231 cells were seeded into a six-well plate as 75×10^3 cells/well in 8% CD-FBS/DMEM. 48 hours later, cells were transfected with one μ g of 1) pcDNA3.1(-)-Flag-ER α or 2) pcDNA3.1 (-) as empty vector (EV) control plasmid. Transfection was performed as described in 2.2.1. Three days after transfection, medium was changed to CD-FBS/DMEM medium containing 1.5 mg/mL of G-418 solution for selection of positive colonies. Medium was changed in every three days until colony formation was observed in pcDNA3.1(-)-Flag-ER α and -EV wells. Individual colonies (named as MDA-ER α # with '#' denoting the colony number or MDA-EV for -EV control) were selected with one mL pipette tip and transferred into separate wells of a 48-well plate. G-418 concentration was kept as 1.5 mg/mL until colonies were frozen as stocks. For maintenance of the cells, G-418 concentration in the media was used at 0.750 mg/mL.

Clones were screened with Western Blot analysis for Flag-ER α protein synthesis.

2.3. Western Blot

Western Blot analysis is used to detect proteins in gels by appropriate antibodies. In the following sections, steps of Western Blot are explained in detail.

2.3.1. Total Protein Isolation

Cells were seeded into six-well plates as 15×10^4 /well in CD-FBS/DMEM. 48 hours later, cells were collected by trypsinization (Lonza, Belgium, BE17-161E) and centrifuged at 600 g for six minutes. Cell pellets were washed twice with 1X Phosphate Buffered Saline (PBS, Lonza, Belgium, 17-516). Cell pellets were lysed with 250 μ L/well M-PER Mammalian Protein Extraction Reagent (Thermo Scientific, USA, 78501) containing 1X cOmplete, EDTA-free protease inhibitor (Roche, Germany, 11873580001) for 20 minutes at room temperature with intermittent vortex agitation. Cell lysates were centrifuged at 14,000 g for 20 minutes at 4°C. Supernatants were collected without disturbing the pellets and protein concentrations were determined by Quick Start Bradford Protein Assay (Bio-Rad, USA, 5000201). Proteins were stored at -80°C.

2.3.2. Western Blot

Proteins as 50 μ g/sample were loaded into wells of a 8% SDS-PAGE with 5% stacking gel as follows; volumes of samples containing 50 μ g of total protein were equalized by adding distilled water and samples were denatured in 6X Laemmli Buffer (Appendix B) at 95°C for six minutes. Equal volumes of samples were loaded into wells. Gel was subjected to electrophoresis for approximately two hours at 100 V. Gel was then transferred onto a PVDF membrane (Roche, Germany, 3010040001) using wet transfer system for 60 minutes at 100 V. Membrane was blocked with buffer containing 5% skim milk (Bio-Rad, USA, 170-6404) in 0.05% Tris Buffered Saline-Tween (TBS-T) for ER α (HC-20) antibody (Santa Cruz Biotechnology Inc., USA, sc-543) for one hour at room temperature. The ER α HC-20 antibody was diluted to 1:500 in the blocking buffer and the membrane was incubated for one hour

at room temperature. After incubation, membrane was washed three times with 0.05% TBS-T. An HRP-conjugated secondary antibody (Santa Cruz Biotechnology, USA, sc-2004) was prepared as 1:2500 dilution in the blocking buffer and the membrane was incubated for one hour at room temperature. After three times washing with 0.05% TBS-T, the membrane was incubated for five minutes with enhanced chemiluminescence (ECL, Bio-Rad, USA, 1705061) in 1:3 luminol-enhancer reagent:peroxide reagent ratio. Visualization was done with ChemiDoc™ MP system (Bio-Rad, USA, 1708280) and images were analyzed with Image Lab™ software (Bio-Rad, USA). PageRuler™ Plus Prestained Protein Ladder (Life Technologies, USA, 26619) was used as molecular weight marker.

2.4. Growth Assay

Cells were seeded as 1250 cells/well to each well of a 48-well plate in 8% CD-FBS/DMEM. 48 hours later, cells were treated either with 10^{-9} M of E2 or ethanol (0.01%) as vehicle control. Treatment was renewed after three days and cells were counted with hemocytometer on the third and sixth days of treatment. Assay was done for three independent times performed in duplicate. Results are shown as percent change of three biological replicate \pm SEM. Unpaired, two-tailed t-test with 95% confidence interval was used for statistical analysis.

2.5. Immunocytochemistry

For immunocytochemistry (ICC), MDA-ER α 5 and MDA-EV stable cell lines were used. As a positive control of the ER α HC-20x (Santa Cruz Biotechnology Inc., USA, sc-543x) antibody, wild type MCF7 cells, and MDAMB231 cells which were transiently transfected with pcDNA3.1(-)-Flag-ER α were used. For a positive control of Flag M2 (Sigma Aldrich, Germany, F1804) antibody, transiently pcDNA3.1(-)-Flag-ER α transfected MDAMB231 cells were used. Sterile cover slips in ethanol bath were put into each well of a 12-well plate and incubated in laminar flow hood until ethanol evaporated completely. Then, plates were subjected to UV sterilization for at least 30 minutes. Cells were seeded as 12500/well in 8% CD-FBS/DMEM.

After 48 hours, MDAMB231 cells were transfected as described in 2.2.1. and medium was also changed for other wells. 48 hours after transfection, cells were washed three times with PBS. Fixation was done by incubating with freshly prepared 2% cold paraformaldehyde in PBS for one hour at room temperature. Cells were washed with PBS for three times, permeabilized with 0.4% Triton-X 100 prepared in PBS for 10 minutes at room temperature and washed with PBS three times again. Fixed cells were blocked for one hour at room temperature with 10% Normal Goat Serum (NGS, Sigma Aldrich, Germany, G9023) for ER α HC-20x antibody or with 10% Bovine Serum Albumin (BSA, Roche, Germany, 10735078001) for Flag M2 antibody prepared in PBS. ER α HC-20x antibody was used at 1:500 dilution prepared in 2% NGS and Flag M2 antibody was used at 1:250 dilution prepared in 3% BSA. For primary antibodies, cells were incubated for two hours at room temperature. Then, cells were washed three times with PBS and incubated with secondary antibodies for 30 minutes at room temperature in the dark. For ER α HC-20x antibody, an Alexa Fluor[®] 488 conjugated goat anti-rabbit (Abcam, USA, ab150077) antibody was diluted at 1:1000 in 2% NGS, or for Flag M2 antibody, an Alexa Fluor[®] 488 conjugated goat anti-mouse (Abcam, USA, ab150113) antibody diluted at 1:1000 in 3% BSA was used. After three subsequent washes with PBS, coverslips were placed onto glass slides with a drop of Fluoroshield Mounting Medium with DAPI (Abcam, USA, ab104139) and edges of coverslips were sealed with nail polish, and were kept in +4°C until visualization. Slides were visualized under fluorescent microscope (Nikon Eclipse 50i) having Nikon camera (DS-Fi1) in the laboratory of Dr. Rengül Çetin Atalay (METU, Ankara, Turkey). Blue filter (X340-380, DM400) is used and for DAPI, and green filter (X465-495, DM50) was used for ER α signal.

2.6. Dual Luciferase Reporter Assay

For dual luciferase reporter assays, two vectors were used; 1) a pGL3 vector containing *Firefly Luciferase* (pGL3-2ERE) gene driven by TATA promoter bearing two consensus ERE sequences upstream of the TATA box, and 2) a pGL3 vector containing *Renilla Luciferase* (pRL) gene driven by SV40 promoter. pGL3-2ERE and pRL were used as 125 ng/well and 0.250 ng/well, respectively. 4×10^4 cells were

seeded into 48-well plate in CD-FBS/DMEM. 48 hours after seeding, cells were co-transfected with expression vectors. Four hours after transfection, media were replaced with without or with ligands as described in Section 2.1.1. 24 hours after treatment, cells were gently washed with PBS for three times and lysed with 50 μ L/well of 1X Passive Lysis Buffer from Dual-Luciferase[®] Reporter Assay kit (Promega, USA, 017319) at room temperature on medium-speed rocker for 15-20 minutes. After observing white, clump-like cell lysates, plates were wrapped with parafilm and stored at -80°C until analysis.

For luciferase analysis, Dual-Luciferase[®] Reporter Assays (Promega, USA, 017319) was used according to manufacturer's instructions. Samples were analyzed with Modulus Microplate Luminometer (Turner Biosystems, USA) in the Dr. A. Elif Erson Bensan's laboratory at METU, Ankara, Turkey. The luminescence signal from *Firefly Luciferase* (pGL3-2ERE) was normalized to luminescence signal from *Renilla Luciferase* (pRL). Assay was done as three independent experiments performed in triplicate. Results are shown as relative luciferase activity of three biological replicate \pm SEM. Unpaired, two-tailed t-test with 95% confidence interval was used for statistical analysis.

2.7. Expression Analysis

In expression analysis, MIQE Guidelines [37] were followed in terms of RNA isolation, cDNA synthesis, and quantification of the data. MIQE Guidelines check list is available in Appendix C.

2.7.1. Primer Design

Primers were designed specific to each gene; specificity was ensured by NCBI Primer Blast. Complete list of all primers used in this study is given in Appendix D.

2.7.2. Total RNA Isolation

Cells were seeded as 2×10^5 cells/well into each well of a six-well plate in CD-FBS/DMEM. 48 hours later, cells were treated either with 10^{-9} M of E2 or (0.01%) ethanol as vehicle control. Six hours after treatment, cells were collected with

trypsinization and washed twice with PBS. Cell pellets were kept at -80°C until isolation. Quick-RNA™ MiniPrep kit (Zymo Research, USA, R1055) including on-column DNaseI digestion was used for total RNA isolation according to instructions of manufacturer. Concentration of RNA samples were measured with NanoDrop 2000 (Thermo Scientific, USA).

2.7.2.1. Genomic DNA Contamination Control

In order to control efficiency of on-column genomic DNA digestion, 600 ng of total RNA isolates were subjected to PCR with glyceraldehyde 3-phosphate dehydrogenase (GAPDH) primers. Final reaction mixture consisted of 1U of Taq polymerase (Thermo Scientific, USA, EP0402), 1X Taq Buffer with KCl, two mM of MgCl₂, 200 μM of dNTP mix, 0.5 μM of forward and reverse primer each, and molecular grade water to 20 μL reaction volume. Reaction conditions were as follows; initial denaturation at 95°C for three minutes, denaturation at 95°C for 30 seconds, annealing at 65°C for 30 seconds, extension at 72°C for 30 seconds. Denaturation, annealing and extension steps were repeated for 40 cycles with a final extension at 72°C for 10 minutes, infinite hold at 4°C. As positive control, 100 ng of genomic DNA was used in the same set of experimental PCR. In case of genomic DNA contamination, RNA isolation protocol was repeated until samples were free from contamination. Figure E.1. in Appendix E shows a representative PCR result.

2.7.3. cDNA Synthesis

cDNA library was carried out with 300 ng total RNA isolates using RevertAid First Strand cDNA Synthesis Kit (Thermo Scientific, USA, K1621) according to manufacturer's instructions. Briefly, initial mixture was prepared by following contents; 300 ng RNA template, one μL of 100 μM Oligo(dT)₁₈ primer, and molecular grade water to complete reaction volume to 12 μL. Reaction mixture was incubated at 65°C for five minutes in T100™ Thermal Cycler (Bio-Rad, USA) with the heated lid function off, and samples were chilled on ice subsequently. Remaining components of cDNA synthesis were prepared as master mix as follows: 1X Reaction Buffer, one mM final concentration of dNTP mix, one U/μL final concentration of RiboLock™ RNase Inhibitor, and 10 U/μL final concentration of RevertAid™ M-MuLV Reverse Transcriptase. Master mix was allocated as eight μL/RNA sample

and total 20 μ L of reaction mixture was incubated at 42°C for one hour and reaction was stopped at 70°C for five minutes. cDNA samples were stored at -80°C.

2.7.4. Real Time-Quantitative Polymerase Chain Reaction (RT-qPCR)

For expression analysis, SsoAdvanced™ Universal SYBR® Green Supermix (Bio-Rad, USA, 172-5272) was used together with 0.3 μ M final concentration of each primer and 1:10 cDNA dilutions. Total reaction volume was 20 μ L and CFX Connect™ Real-Time PCR Detection System (Bio-Rad, USA) was used. MIQE Checklist is available in Appendix C.

Fold changes of target genes were normalized to the Pumilio Homolog 1 (*PUM1*) gene and as a positive control of the treatments, trefoil factor 1 (*TFF1/pS2*) gene was used. Reaction conditions for all gene primers used in this study is given in Table 1.

Table 1. Reaction conditions and product size information.

	Steps / Gene						
	Names	<i>PUM1</i>	<i>TFF1/pS2</i>	<i>YPEL2</i>	<i>YPEL3</i>	<i>CCNA1</i>	<i>CTGF</i>
Cycles	Polymerase Activation and DNA Denaturation	95°C for 10 minutes					
	Denaturation	94°C for 30 sec					
	Annealing	60°C	55°C	65°C	65°C	55°C	55°C
	Extension + Plate Read	72°C for 30 sec					
	Rapid Heating	95°C for 10 sec					
	Melt Curve Generation	55°C to 99°C, increment 1.0°C, 5.0 sec					
	Product Size (bp)	111	209	138	115	146	139

All gene expression experiments consist of three technical repeats of three biological replicates. E2, ICI, and ICI+E2 treatments were compared to ethanol treatment, which was set to one for each gene expression profile. For the statistical analysis,

one-tailed paired t-test with 95% confidence interval was performed by using GraphPad Prism v.5 for Windows (San Diego California, USA).

2.8. Cell Cycle Distribution

Since previous studies suggested that E2 is an anti-proliferative agent for ER α -negative cells synthesizing ER α introduced exogenously, cell cycle distribution is also assessed to examine the effects of E2 on these model cells.

2.8.1. Preparation of Samples

Cells were seeded onto six-well plates as 5×10^4 /well in CD-FBS/DMEM. 48 hours later, cells were treated with 10^{-9} M of E2 or ethanol (0.01%) as vehicle control. Cells were collected with trypsinization and washed once with PBS at room temperature 48 hours after treatment. Cells were gently re-suspended in 100 μ L of PBS and immediately fixed with ice-cold 70% ethanol diluted in distilled water. For fixation, falcon tubes were placed onto a vortex with the minimum speed and four ml of ethanol was added dropwise to prevent clumping of cells. Fixed cells were stored at -20°C until analysis.

2.8.2. Analysis of Samples

Samples were centrifuged at 600 g for six minutes at room temperature and supernatants were discarded. Pellets were re-suspended with PBS and samples were transferred into Eppendorf tubes. Samples were centrifuged at same conditions and pellets were re-suspended with 200 μ L of staining buffer prepared in PBS containing propidium iodide (PI, Sigma Aldrich, Germany, P4710) with 0.02 mg/mL final concentration, RNase A (Thermo Scientific, USA, EN0531) with 200 μ g/mL final concentration, and Triton[®] X-100 (AppliChem, Germany, A4975) with 0.1% (v/v) final concentration. Cell cycle analysis was done with BD Accuri[™] C6 Cytometer (BD Biosciences). Assay was done as three independent experiments, and cell percentages in cell cycle phases were used in statistical analyses. Results are shown as percent change of three biological replicate \pm SEM. Unpaired, two-tailed t-test with 95% confidence interval was used for statistical analysis.

2.9. Methylation and Transcriptomic Analysis

MDA-ER α 5 and MCF7 cells were seeded as 2.5×10^6 into each T75 cm² tissue culture flasks in CD-FBS/DMEM. 48 hours later, cells were treated with 10^{-9} M of E2 or ethanol (0.01%) as vehicle control. Six hours after treatment, cells were trypsinized and washed with PBS twice. Pellets were divided into three tubes and stored at -80°C to be used in genome-wide methylation and transcriptomic analyses. All experiments were repeated three independent times with three technical replicates.

One of the pellets were used for genomic DNA isolation. Quick-gDNA™ MiniPrep kit (Zymo Research, USA, D3024) was used according to manufacturer's instructions. Samples were shipped at -80°C conditions as genomic DNA to Zymo Research Corporation, Epigenetic Services (USA) for Methylation Mini-Seq full service sequencing.

One of the pellets from each sample was shipped at -80°C conditions to University of Rochester, Genomics Research Center (USA) for whole-genome transcriptomic analysis.

CHAPTER 3

RESULTS AND DISCUSSION

3.1. Generation of an ER-Negative Cell Model That Synthesizes Human ER α Introduced Exogenously

Previous studies showed that E2 enhances cellular proliferations in cell models that synthesize ER α endogenously while it represses cellular growth in ER-negative cells that synthesize ER α introduced exogenously as a result of polar directions in gene expressions playing critical roles in cellular proliferations. Since methylation is a critical component of transcription, we hypothesized that differences in genome-wide methylation statuses of cell models underlie the polar direction of model cell proliferations. To test this prediction, we aimed to generate a cell line that synthesizes ER α introduced exogenously using ER α -negative MDAMB231 cells derived from a mammary adenocarcinoma. In order to assess the functionality of model cell line, various approaches were used to show that ER α protein is capable of regulating gene expressions and cellular proliferation through changes in cell cycle phases.

3.1.1. Expression of ER α in Stably Transfected MDAMB231 Cells

To generate MDAMB231 cells synthesizing ER α stably, cells were transfected with the pcDNA3.1(-)-Flag-ER α mammalian expression vector or with an empty vector (EV control) as described in 2.2.2. During stable monoclonal generation, 24 candidate monoclonal cells were selected initially. In the course of maintenance, one candidate monoclonal cell (MDA-ER α 24) did not survive. In order to show that stably transfected ER α protein is expressed in selected monoclonal cells, protein isolation and Western Blot analysis were carried out as described in 2.3. For initial analyses, candidate monoclonal cells were selected based on the level of ER α synthesis compared to

endogenously ER α expressing MCF7 cells. Western Blot assay accomplished by using an ER α -specific antibody (Figure 5) revealed that monoclonal synthesized ER α at varying levels.

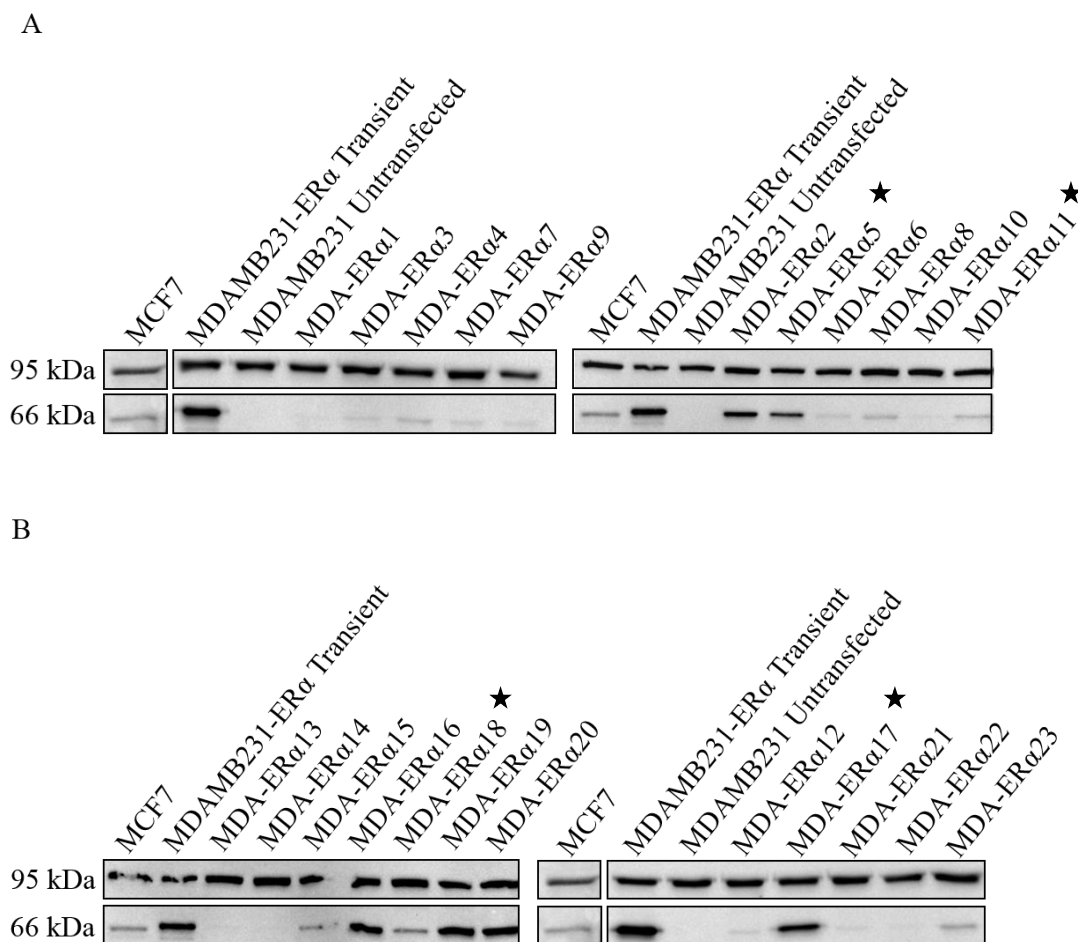


Figure 5. Western Blot analysis of stable monoclonal cell lines (A and B). MDAMB231 cells were stably transfected as described in 2.2.2. with pcDNA3.1(-) bearing ER α cDNA or no insert as the empty vector (EV). 50 μ g total protein was loaded into 8% SDS-PAGE. Total protein isolated from MCF7 cells was used as positive control for the HC-20 ER α antibody (Santa Cruz Biotechnology Inc., USA, sc-543). A non-specific band at 95 kDa detected by the antibody was used as the loading control. Two independent Western Blot experiments resulted in similar findings. Images were taken after 90 seconds of exposure.

Based on these results, MDA-ER α 5, 11, 17, and 23 monoclonal synthesizing ER α at levels comparable to those observed in MCF7 cells were selected (indicated by asterisks). In addition, MDA-EV2 and MDA-EV3 monoclonal, stably transfected with a pcDNA3.1(-) empty vector (EV), were selected as control cell lines based on

their similar morphological features to those of untransfected MDAMB231 cells for further functional analyses.

3.1.2. The Effects of E2 on Cellular Proliferation of Candidate Monoclonal

E2 represses cellular proliferation in breast cancer cell models that synthesize ER α introduced exogenously [15]–[19]. To assess the effects of E2 and consequently the functionality of ER α on proliferation of monoclonal cells, cell counting was performed initially. Monoclonal cells MDA-ER α 5, 11, 17, and 23 as well as MDA-EV2 and MDA-EV3 were subjected to growth assay in the absence or presence of 10^{-9} M E2. Cells grown in 48-well plates were collected and counted on the sixth day with hemocytometer. Counting showed that of the monoclonal cells, E2 treatment repressed the proliferation of only MDA-ER α 5 cells while the E2 treatment had no significant effect on the growth of the untransfected MDAMB231 cells, which were used as negative control (Figure 6). In contrast, and expectedly, E2 significantly enhanced the growth of MCF7 cells. Based on these initial observations, MDA-ER α 5 monoclonal cell was selected as the cell model, which would allow us to comparatively assess the directional ability of E2 to modulate cellular proliferation in comparison with MCF7 cells. MDA-EV2 was also selected as negative control.

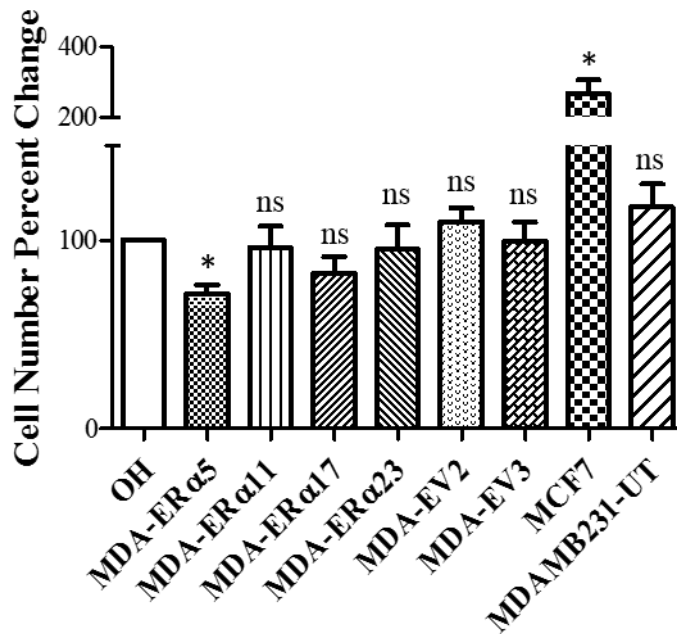


Figure 6. E2 effects on cellular growth of stable monoclonal cells. Cells were seeded as 1250 cells/well to each well of a 48-well plate in 8% CD-FBS/DMEM. 48 hours later, cells were treated either with 10^{-9} M E2 or ethanol (0.01%; OH) as vehicle control. Treatment was renewed after three days and cells were counted with hemocytometer on the sixth day of treatment. Results are shown as percent change of E2 treatment compared to the ethanol vehicle replicated three independent times with duplicate well/treatment \pm SEM. Unpaired, two-tailed t-test with 95% confidence interval was used for statistical analysis (*; significant $p < 0.05$, **; very significant $p < 0.01$, ***; extremely significant $p < 0.001$, ns; nonsignificant $p > 0.05$).

3.2. Functional Screening of MDA-ERα5 Stable Monoclonal as the Cell Model

In the initial screening of MDAMB231 monoclonal cells stably transfected with ERα cDNA, only MDA-ERα5 showed responsiveness to E2 in terms of modulation of cellular proliferation. To ensure that this E2 responsiveness of MDA-ERα cells is due to a functional ERα synthesis, MDA-ERα5 cells in comparison with MDA-EV2 and MCF7 cells were subjected to Western blot (WB), immunocytochemistry (ICC), Luciferase reporter assay as well as cell cycle distribution and proliferation assays.

3.2.1. Western Blot Analysis of MDA-ERα5 Stable Monoclonal

To assess the ERα protein expression and its levels compared to endogenously expressing MCF7 cells, Western Blot assay was used for MDA-ERα5 stable monoclonal cells.

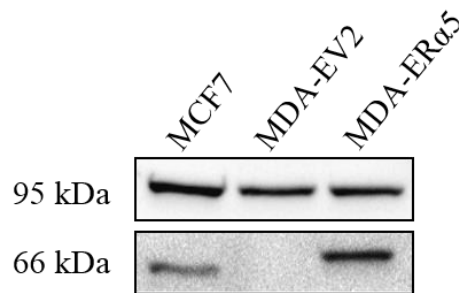


Figure 7. Western Blot analysis of MDA-ER α 5 stable monoclonal. 50 μ g total protein was loaded into 8% SDS-PAGE. Total protein isolated from MCF7 cells was used as positive control for the ER α HC-20 antibody. Non-specific bands at 95 kDa were used as loading control. Two independent Western Blot experiments gave similar results. Images were taken after 120 seconds of exposure.

Western Blot analysis (Figure 7) showed that the MDA-ER α 5, but not MDA-EV2, monoclonal synthesizes ER α protein approximately 2.5 fold more, estimated with Bio-Rad ImageLab Software (USA), than that observed in MCF7 cells.

3.2.2. Immunocytochemistry of MDA-ER α 5 Stable Monoclonal

ER α protein localizes to nucleus independent from E2 binding in ER-positive cell lines [38]. To show that ER α synthesized in MDA-ER α 5 is located in the nucleus as in endogenously ER α synthesizing MCF7 cells, immunocytochemistry (ICC) was performed. To confirm that the Flag tag present in the amino-terminus of ER α did not affect ER α localization, both the ER α HC-20x antibody (Figure 8) and Flag M2 antibody (Figure 9) were used in ICC experiments. Images were acquired with the same exposure time with 40x objective. Experiments were repeated for three independent times with similar results. Results showed that ER α is localized in the nucleus of MDA-ER α 5, whereas, as expected, there was no synthesis of the receptor in MDA-EV2.

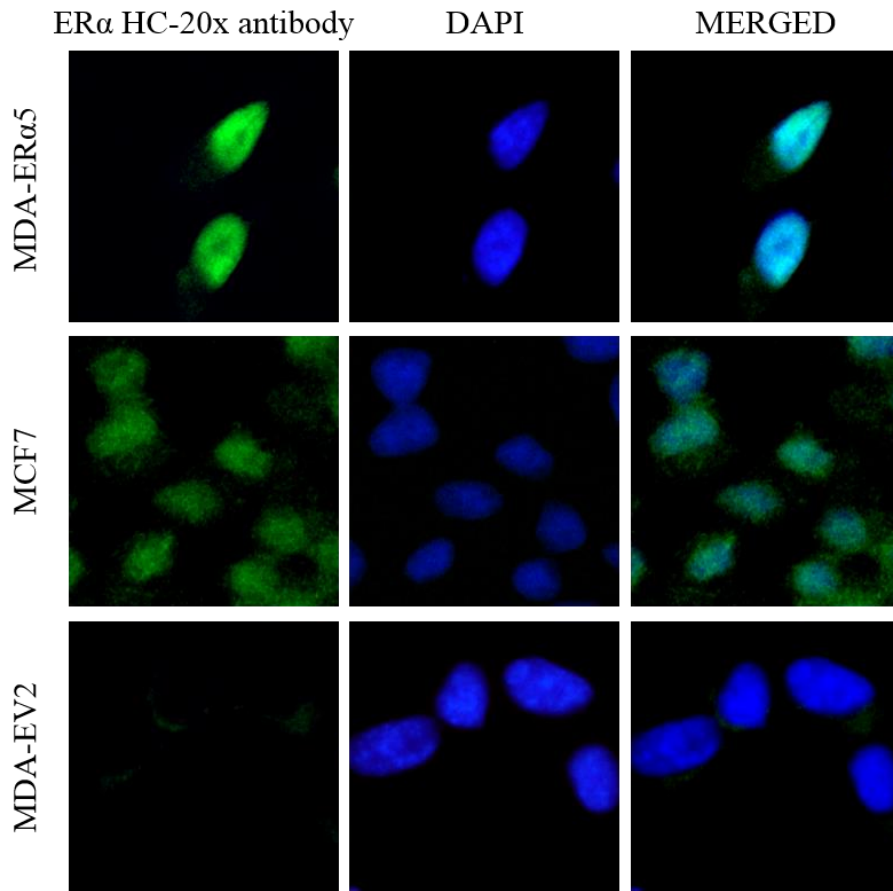


Figure 8. Immunocytochemistry for nuclear localization of ER α protein with the ER α HC-20x antibody. Cells were seeded as 12500 cells/well to each well of a 12-well plate containing coverslips in 8% CD-FBS/DMEM. For positive control of the ER α HC-20x antibody, MCF7 cells were used. Cells were fixed by 2% paraformaldehyde, and permeabilized with 0.4% Triton-X 100. Fixed cells were blocked with 10% Normal Goat Serum. The ER α HC-20x antibody was used at 1:500 dilution followed by an Alexa Fluor® 488 conjugated goat anti-rabbit (1:1000). DAPI was used to stain nuclei. Similar results were obtained in two independent experiments.

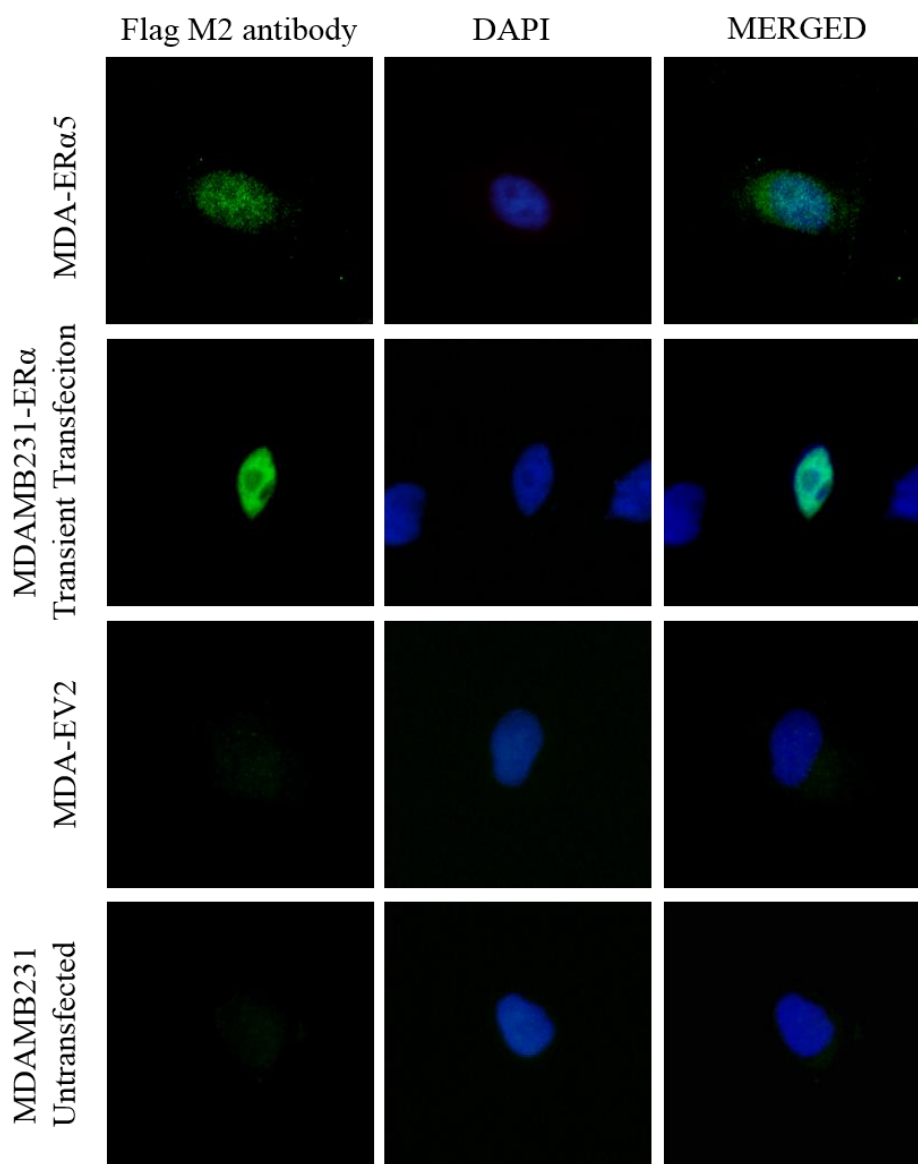


Figure 9. Immunocytochemistry for nuclear localization of ER α protein with Flag M2 antibody. Cells were seeded as 12500 cells/well to each well of a 12-well plate containing coverslips in 8% CD-FBS/DMEM. For positive control of the Flag M2 antibody, MDAMB231 cells were transfected with two μ g of pcDNA3.1(-)-Flag-ER α vector. Cells were fixed by 2% paraformaldehyde, and permeabilized with 0.4% Triton-X 100. Fixed cells were blocked with 10% Bovine Serum Albumin. The Flag M2 antibody was used at 1:250 dilution followed by an Alexa Fluor® 488 conjugated goat anti-mouse (1:1000). DAPI was used to stain nuclei. Similar results were obtained in two independent experiments.

3.2.3. Dual-Luciferase Reporter Assay

To initially assess that ER α synthesized in MDA-ER α 5 is capable of regulating the expression of an estrogen responsive gene in response to E2 as a reflection of functionality of the receptor, Dual-Luciferase Reporter Assay was used as described in 2.6. The same assay was also performed in MCF7 cells as a positive control (Figure 10B). pGL3-2ERE was used as the reporter vector driving the expression of *Firefly Luciferase* cDNA. The reporter vector promoter is consisted of a TATA box promoter with two ERE sites in tandem (2xERE-Luc), placed upstream of the promoter to provide responsiveness to E2-ER α complex. Together with pGL3-2ERE, cells were co-transfected with pRL, a reporter vector expressing the *Renilla Luciferase* cDNA for transfection efficiency. After transient transfections, cells were treated without or with 10^{-9} M of E2 for 24h. To show that changes in the *Firefly Luciferase* activity is the result of E2 binding to ER α , cells were also treated with 10^{-7} M ICI 182,780 (ICI), a complete antagonist of ER α , in the absence (%0.01, ethanol, OH) or the presence of 10^{-9} M E2.

In MDA-ER α 5, E2 enhanced the *Firefly Luciferase* enzyme activity compared to ethanol control. ICI treatment, on the other hand, repressed both basal and E2 induced *Firefly Luciferase* activity (Figure 10A). The results suggest that transcriptional responses are ER α -specific. Although the extent of enzyme activity was higher in comparison with those observed in MDA-ER α 5 cells, E2 treatment also enhanced, whereas ICI repressed, the reporter enzyme activity in MCF7 cells, as expected (Figure 10B). On the other hand, ER ligands had no effect on enzyme activity in MDA-EV2 cells (Figure 10C).

Thus, these results indicate that ER α localized in the nucleus of MDA-ER α 5 cells is capable of inducing transcription in response to E2.

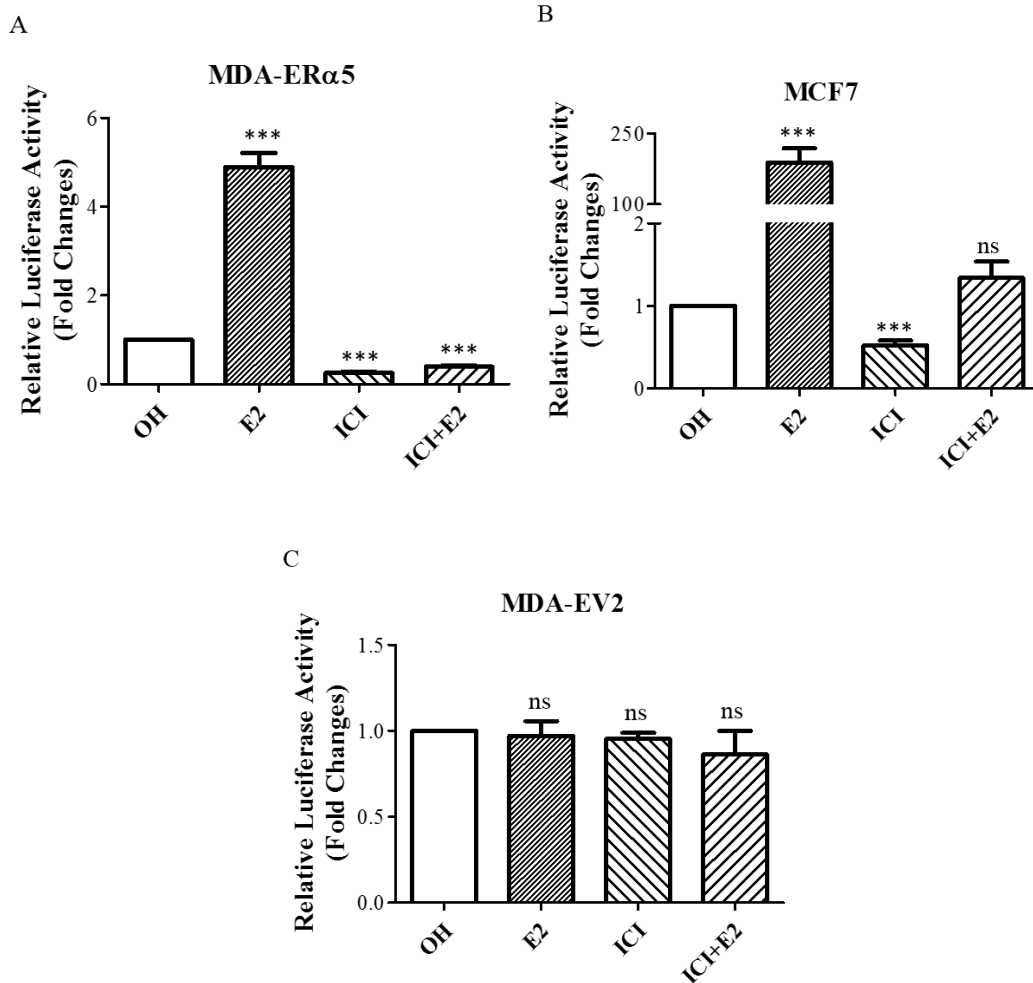


Figure 10. Dual-Luciferase reporter assay of the candidate monoclonal. Cells were seeded as 4×10^4 cells/well into each well of a 48-well plate in 8% CD-FBS/DMEM. 48 hours after seeding, cells were co-transfected with two vectors; 1) a pGL3 vector containing Firefly Luciferase (pGL3-2ERE) gene (125 ng/well), and 2) a pGL3 vector containing Renilla Luciferase (pRL) gene (0.250 ng/well). Four hours after transfection, media were replaced with fresh medium without (0.01% ethanol, OH) or with 10^{-9} M of E2, and/or 10^{-7} M of ICI. 24 hours after treatment, cells were lysed and subjected to Dual-Luciferase® Reporter Assay. Results are shown as the mean \pm SEM of three independent experiments with three technical repeats/experiment. For the statistical analysis, one-tailed paired t-test with 95% confidence interval was performed (*; significant $p < 0.05$, **; very significant $p < 0.01$, ***; extremely significant $p < 0.001$, ns; non-significant $p > 0.05$).

3.2.4. Expression Analyses of Endogenous Estrogen Responsive Genes

To ensure that ER α synthesized MDA-ER α 5 cells is also capable of regulating endogenous estrogen responsive genes in response to E2, the expression profiles of *YPCL2*, *YPCL3*, *CTGF*, *TFF1/pS2*, and *CCNA1* genes as estrogen responsive gene models [12], [23] were assessed.

Yippee-like 2 (*YPEL2*) and *YPEL3* are two of the five, highly conserved *YPEL* gene family members (*YPEL1* through *YPEL5*). Ypel proteins are highly conserved gene products which share remarkably high amino acid identity (55-85%) [39]. Although Ypel3 was suggested to be a DNA damage response related protein [40], a function is yet to be assigned to Ypel2. However, the aberrations at the chromosomal loci of *YPEL2* (17q23) is found to be frequently associated with breast cancer [41], an indication that *YPEL2* could be a critical gene in the initiation and progression of the disease. In a microarray study conducted in Muyan's laboratory, *YPEL2* and *YPEL3* genes were found to be E2 responsive [12].

Connective tissue growth factor (*CTGF*) is a member of Connective Tissue Growth Factor (CTGF), Cystein rich protein (Cyr61), and Nephroblastoma overexpressed gene (*CCN*) gene family and it is expressed in high levels in the early development of the embryo as well as in scar tissue [42]. It is shown that CTGF is regulated with E2 [43] and in the microarray study conducted in Muyan's laboratory, *CTGF* was shown to be downregulated after E2 treatment [12].

The trefoil factor 1, (*TFF1*; or *pS2*) gene is a well-studied estrogen responsive gene. Although function is unclear, TFF1 protein is thought to play a role in healing of the epithelium [44].

Cyclin A1 (*CCNA1*) is a member of mammalian A-type cyclin family [45]. Cyclin A1 is expressed in testis and brain, as well as in cell lines, and is suggested to be important for entry into metaphase of meiosis [46]. In addition, *CCNA1* is necessary for proceeding from S phase to G2 phase in cell cycle [47]. *CCNA1* is a known E2-regulated gene [47].

For mRNA expression analyses, cells grown in six-well tissue culture plates in the absence of E2 for 48h were treated with 10^{-9} M E2 for 6h, a duration anticipated to induce changes in the transcription of immediate/early estrogen-responsive genes [12], [48]. The isolated total RNA was processed for and subjected to real time quantitative PCR (RT-qPCR) for gene expression analyses as described in 2.7. In RT-qPCR, MIQE Guidelines (Appendix C) were followed [37]. For each reaction,

melt curve was generated (Appendix F). Fold changes of target genes were normalized to Pumilio Homolog 1 (*PUM1*) gene.

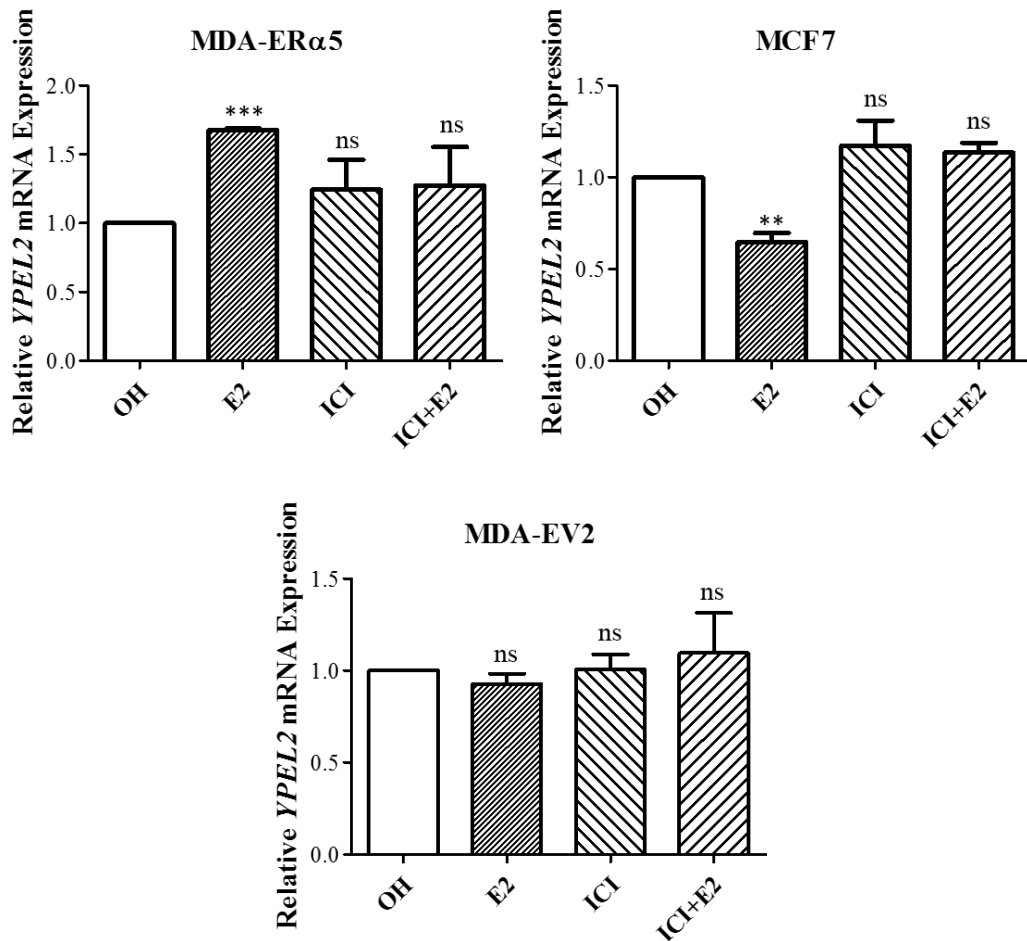


Figure 11. *YPEL2* mRNA Expression Analysis. Cells were seeded as 2×10^5 cells/well into each well of a six-well plate in 8% CD-FBS/DMEM. 48 hours later, cells were treated without (0.01% ethanol, OH) or with 10^{-9} M of E2, and/or 10^{-7} M of ICI. Six hours after treatment, cells were collected and subjected to total RNA isolation and RT-qPCR. mRNA expression levels were normalized to *PUM1* expression. E2, ICI, and ICI+E2 treatments were compared to ethanol treatment, which was set to one for each gene expression profile. Results are shown as the mean \pm SEM of three independent experiments with three technical repeats. For the statistical analysis, one-tailed paired t-test with 95% confidence interval was performed by using GraphPad Prism v.5 for Windows (San Diego California, USA) (*; significant $p < 0.05$, **; very significant $p < 0.01$, ***; extremely significant $p < 0.001$, ns; non-significant $p > 0.05$).

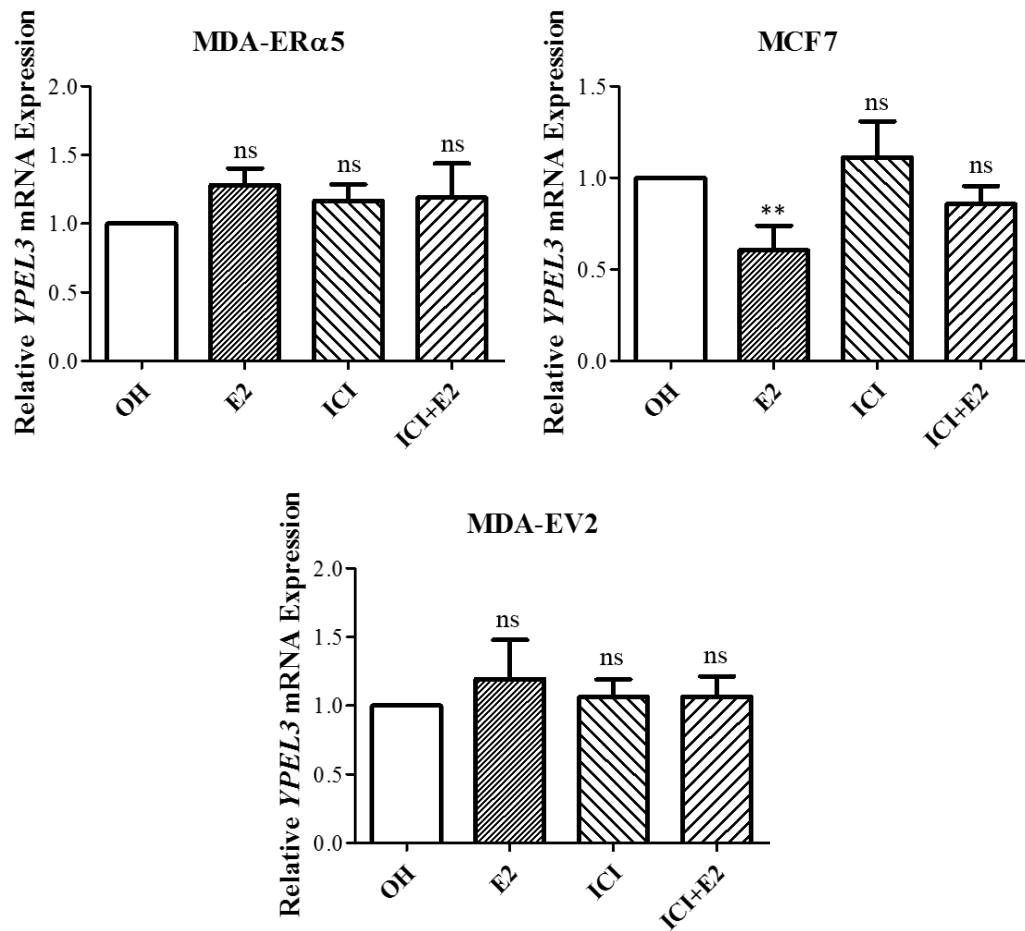


Figure 12. YPEL3 mRNA Expression Analysis. Cells were seeded as 2×10^5 cells/well into each well of a six-well plate in 8% CD-FBS/DMEM. 48 hours later, cells were treated without (0.01% ethanol, OH) or with 10^{-9} M of E2, and/or 10^{-7} M of ICI. Six hours after treatment, cells were collected and subjected to total RNA isolation and RT-qPCR. mRNA expression levels were normalized to *PUM1* expression. E2, ICI, and ICI+E2 treatments were compared to ethanol treatment, which was set to one for each gene expression profile. Results are shown as the mean \pm SEM of three independent experiments with three technical repeats. For the statistical analysis, one-tailed paired t-test with 95% confidence interval was performed by using GraphPad Prism v.5 for Windows (San Diego California, USA) (*; significant $p < 0.05$, **; very significant $p < 0.01$, ***; extremely significant $p < 0.001$, ns; non-significant $p > 0.05$).

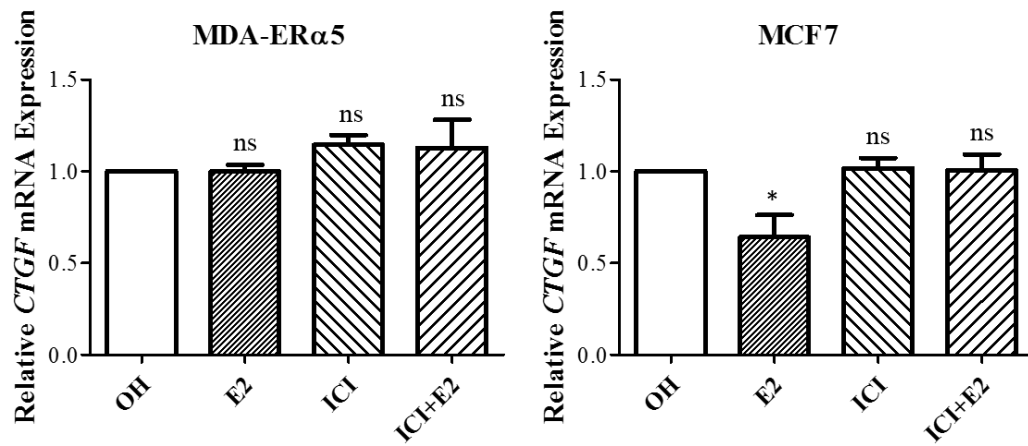
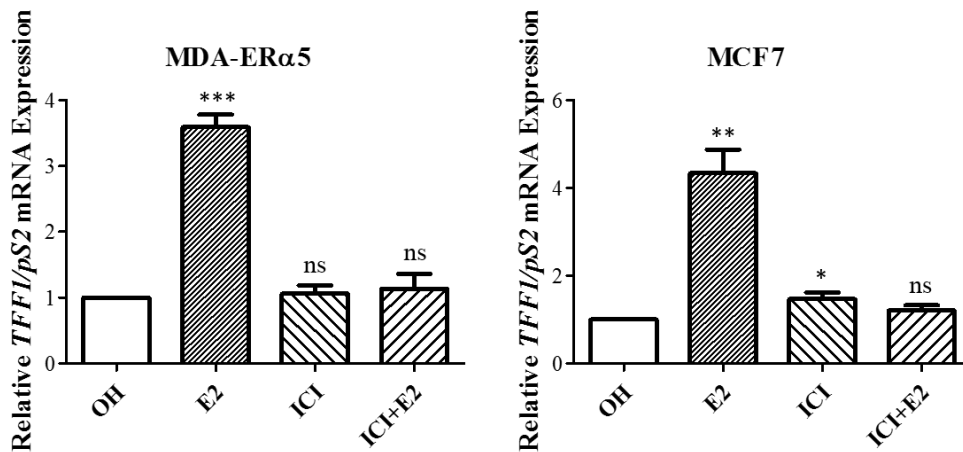


Figure 13. CTGF mRNA Expression Analysis. Cells were seeded as 2×10^5 cells/well into each well of a six-well plate in 8% CD-FBS/DMEM. 48 hours later, cells were treated without (0.01% ethanol, OH) or with 10^{-9} M of E2, and/or 10^{-7} M of ICI. Six hours after treatment, cells were collected and subjected to total RNA isolation and RT-qPCR. mRNA expression levels were normalized to *PUM1* expression. E2, ICI, and ICI+E2 treatments were compared to ethanol treatment, which was set to one for each gene expression profile. MDA-EV2 cells did not give significant results, hence data are not shown for simplicity. Results are shown as the mean \pm SEM of three independent experiments with three technical repeats. For the statistical analysis, one-tailed paired t-test with 95% confidence interval was performed by using GraphPad Prism v.5 for Windows (San Diego California, USA) (*; significant $p < 0.05$, **; very significant $p < 0.01$, ***; extremely significant $p < 0.001$, ns; non-significant $p > 0.05$).

A



B

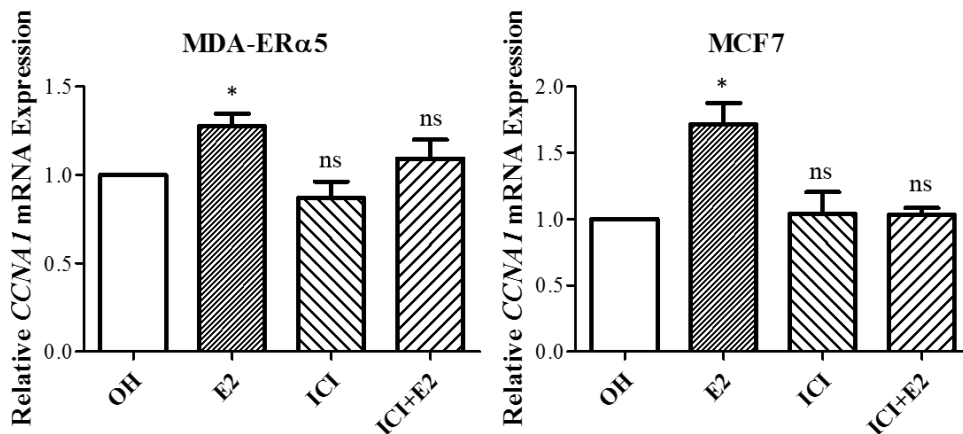


Figure 14. *TFF1/pS2* (A) and *CCNA1* (B) mRNA Expression Analyses. Cells were seeded as 2×10^5 cells/well into each well of a six-well plate in 8% CD-FBS/DMEM. 48 hours later, cells were treated without (0.01% ethanol, OH) or with 10^{-9} M of E2, and/or 10^{-7} M of ICI. Six hours after treatment, cells were collected and subjected to total RNA isolation and RT-qPCR. mRNA expression levels were normalized to *PUM1* expression. E2, ICI, and ICI+E2 treatments were compared to ethanol treatment, which was set to one for each gene expression profile. MDA-EV2 cells did not give significant results, hence data are not shown for simplicity. Results are shown as the mean \pm SEM of three independent experiments with three technical repeats. For the statistical analysis, one-tailed paired t-test with 95% confidence interval was performed by using GraphPad Prism v.5 for Windows (San Diego California, USA) (*; significant $p < 0.05$, **; very significant $p < 0.01$, ***; extremely significant $p < 0.001$, ns; non-significant $p > 0.05$).

Observations showed that ligands had no effect on the expression of any gene tested in the MDA-EV2 monoclonal cell line. On the other hand, E2 enhanced *YPEL2* gene expression in the MDA-ER α 5 monoclonal cell line in an ER α -specific manner as ICI alone

had no effect on the expression of the gene, but it prevented E2 mediated transcriptional augmentation. E2, however, effectively repressed the expression of *YPEL2* in endogenously ER α expressing MCF7 cells. In contrast, E2 treatment had no effect on *YPEL3* gene expression in MDA-ER α 5 cells while E2 increased the *YPEL3* gene expression in MCF7 cells. In both cell models, E2 effectively increased *TFF1/pS2* gene expression. Recapitulating previous observations derived from this and other laboratories, these results indicate that E2 can modulate endogenous gene expressions with patterns that are in 1) polar directions (*YPEL2*; Figure 11), 2) the same directions (*TFF1/pS2* and *CCNA1*; Figure 14A-B) or 3) cell-type specific manner (*YPEL3* and *CTGF*; Figure 12-13) in cells that synthesize ER α endogenously or introduced exogenously.

3.2.5. Cell Cycle Distribution in Response to E2

In the initial cellular proliferation assays, it was found that the treatment of MDA-ER α 5 cells with 10^{-9} M E2 repressed cellular proliferation on the sixth day of the treatment compared to ethanol (OH, 0.01%) control whereas E2 enhanced the growth of MCF7 cells at the same time-point. On the other hand, E2 had no effect on the proliferation of MDA-EV2 cells as expected. To assess whether E2-mediated cellular proliferation in polar direction is also reflected in differential distribution of cell populations in cell cycle phases, cell cycle analysis was carried out. MDA-ER α 5 and MCF7 cells were grown in the absence of E2 for 48h, and were treated without or with 10^{-9} M E2 and maintained for 48h. Cells were then collected and subjected to flow cytometer BD Accuri™ C6 Cytometer (BD Biosciences) as described in 2.8. Changes in cell populations upon E2 treatment were normalized to the ethanol treatment (0.01%) group for each cell cycle phase.

Kinetic analysis of cell cycle histograms, for which gating strategy was shown in Appendix G, revealed that E2 increased the cell population in G1 phase with a decrease in S phase in MDA-ER α 5 cells. In contrast, in MCF7 cells, G1 phase population decreased and S phase population increased significantly upon E2 treatment (Figure 15). For MDA-EV2 cells, no significant change was observed.

Thus, E2-mediated directional polarity of the proliferation of MDA-ER α and MCF7 cells is a reflection in alterations in cell cycle phases.

These functional assays suggest that the MDA-ER α 5 monoclonal can be used as a model cell line in comparison with MCF7 cells to test the initial hypothesis that polar directions in cellular proliferation in response to E2 are due to distinct methylation profiles of cell lines.

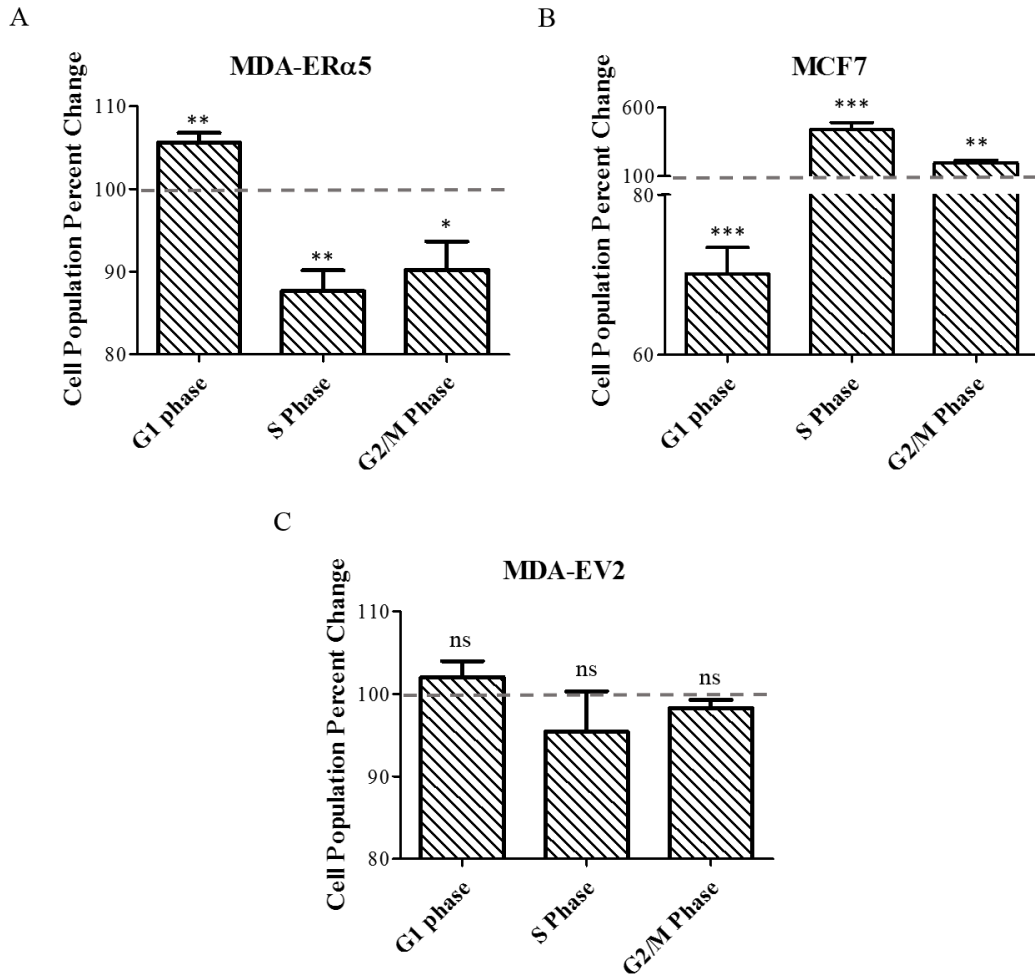


Figure 15. Cell cycle phase distributions upon E2 treatment. Cells were seeded onto six-well plates as 5×10^4 /well in 8% CD-FBS/DMEM. 48 hours later, cells were treated either with 10^{-9} M of E2 or ethanol (0.01%) as vehicle control. Samples were collected 48 hours after treatment, and immediately fixed with ice-cold 70% ethanol. For analysis, samples were stained with a staining buffer containing 0.02 mg/mL propidium iodide. Cell population changes normalized to cell population in each cell cycle phase in ethanol treatment group. Dashed line represents the 100% border. Results are shown as percent change of three biological replicate \pm SEM. Unpaired, two-tailed t-test with 95% confidence interval was used for statistical analysis (*; significant $p < 0.05$, **; very significant $p < 0.01$, ***; extremely significant $p < 0.001$, ns; non-significant $p > 0.05$).

3.3. Repression of Cellular Proliferation in the MDA-ER α 5 Stable Monoclonal in Response to E2

Functional examination of the MDA-ER α 5 stable monoclonal showed that ER α introduced exogenously is functional. ER α localized in the nucleus, regulated estrogen responsive gene expressions, and altered cell cycle distribution in response to E2. This enabled us to assess changes in cellular proliferation of the MDA-ER α 5

monoclonal in response to E2 treatment. MCF7 cells were used as the positive control of the E2 treatment since E2 is a proliferative agent in these cells.

In Figure 16, proliferation results were shown as percent change in the cell number after three and six days of E2 treatment. There is a significant increase in cellular proliferation of MCF7 cells while E2 repressed the proliferation of the MDA-ER α 5 monoclonal. MDA-EV2 monoclonals were not responsive to E2, as expected.

Thus, our results showed that E2 exerts an anti-proliferative effect on MDA-ER α 5 cells synthesizing ER α introduced exogenously.

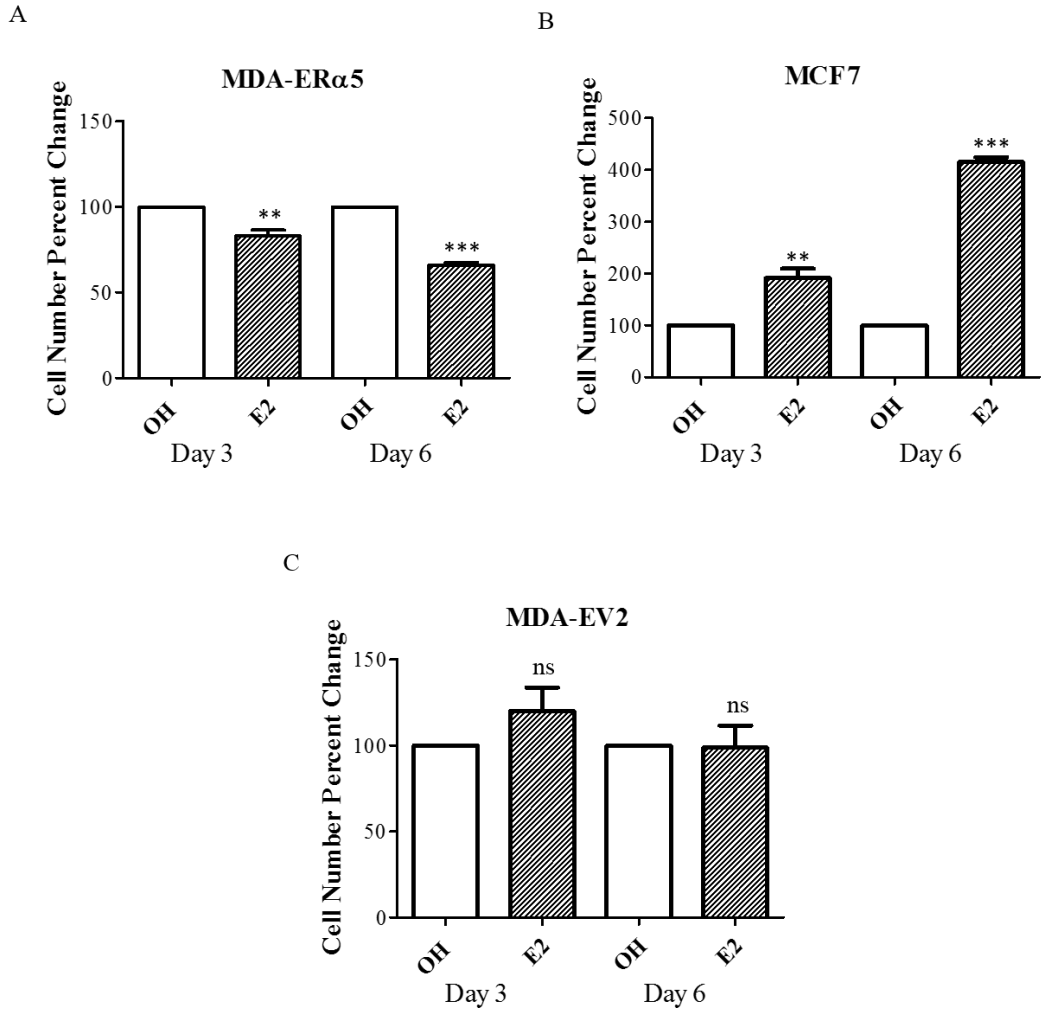


Figure 16. Growth of monoclonal MDA-ER α 5 (A), MCF7 (B), and MDA-EV2 (C). Cells were seeded as 1250 cells/well to each well of a 48-well plate in 8% CD-FBS/DMEM. 48 hours later, cells were treated either with 10^{-9} M E2 or ethanol (0.01%; OH) as vehicle control. Treatment was renewed after three days and cells were counted with hemocytometer on the third and sixth days of treatment. Results shown as percent change compared to ethanol control are the mean \pm SEM of three biological replicate with duplicate wells/treatment. Unpaired, two-tailed t-test with 95% confidence interval was used for statistical analysis (*; significant $p < 0.05$, **; very significant $p < 0.01$, ***; extremely significant $p < 0.001$, ns; non-significant $p > 0.05$).

3.4. Genome-Wide Methylation Profile Analysis

Our results collectively indicate that we have established a cell model that recapitulates the previous observations that E2 is an anti-mitotic agent in ER-negative cells synthesizing ER α introduced exogenously in contrast to ER-positive cells wherein E2 acts as an effective proliferative hormone.

The establishment of the MDA-ER α 5 cell model allowed us to test our hypothesis that directional effect of E2 on cellular proliferation is due to differences in the transcriptomic profiles of the cell models as results of differences in genome-wide methylation status.

To examine this prediction, we employed genome-wide methylome and transcriptome analyses. For both analyses, the samples were generated from the same experiments. Cells grown in 8% CD-FBS/DMEM, and treated with 10⁻⁹ M of E2 or ethanol (0.01%) as vehicle control for 48 hours. Six hours after treatment, cells were collected, washed and divided into three aliquots.

For methylome analysis, genomic DNA isolation was carried out using one of the pellets (detailed in 2.9) and integrity of genomic DNA was assessed by running samples in agarose gel electrophoresis (Figure 17). Samples were stored in -80°C and shipped in same conditions to Zymo Research Corporation, Epigenetic Services (USA).

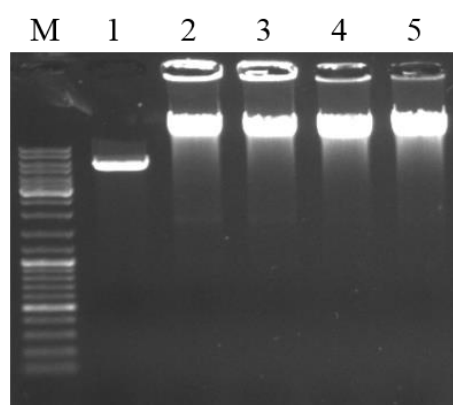


Figure 17. A representative image for genomic DNA integrity. Genomic DNA isolation was done by using Quick-gDNA™ MiniPrep kit (Zymo Research, USA, D3024). Genomic DNA quality was examined by running 500 ng of each samples in 0.7% agarose gel for 30 minutes at 100 V. 250 ng of pcDNA3.1(-) plasmid linearized with BamHI restriction enzyme (5428 bp) was used for positive control. GeneRuler DNA Ladder Mix (Thermo Scientific, USA, SM0331) was used as marker (M). Same results were obtained for all technical replicates. Lane 1: Linearized pcDNA3.1(-) plasmid. Lane 2: MDA-ER α 5 6h ethanol treatment. Lane 3: MDA-ER α 5 6h E2 treatment. Lane 4: MCF7 6h ethanol treatment. Lane 5: MCF7 6h E2 treatment.

Methylation Mini-Seq full service sequencing results were provided by Zymo Research Corporation (USA). For each cell line (MDA-ER α 5 monoclonal and MCF7

cells), 6h E2 treated samples were compared to 6h OH treated samples (Figure 18-19). In addition, 6h E2 treated MDA-ER α 5 vs 6h E2 treated MCF7 comparisons were made (Figure 20). List of genomic regions in each heat map is provided in Appendix H. Heat maps show differentially methylated regions in terms of their p-value order. Yellow color represents highly methylated DNA regions while red color represents poorly methylated DNA regions, and orange color represents intermediate of methylation regions.

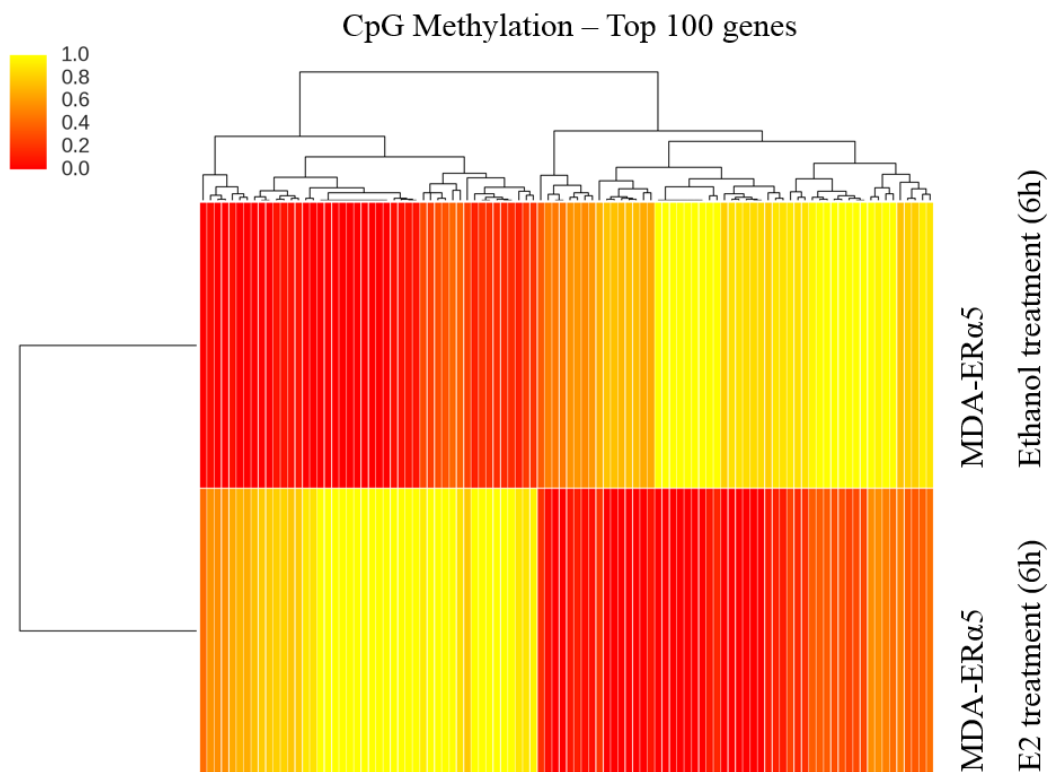


Figure 18. Differential methylation status of the MDA-ER α 5 monoclonal cell line. Shown is the comparative analysis of methylation status of highly divergent 100 gene loci in the absence or presence of E2. Cells were seeded as 2.5×10^6 into each T75 cm² tissue culture flasks in 8% CD-FBS/DMEM. 48 hours later, cells were treated either with 10^{-9} M of E2 or ethanol (0.01%) as vehicle control. Six hours after treatment, cells were trypsinized and washed with PBS twice. All experiments were repeated three independent times with three technical replicates. Quick-gDNA™ MiniPrep kit (Zymo Research, USA, D3024) was used according to manufacturer’s instructions for genomic DNA isolation. Samples were shipped at -80°C conditions as genomic DNA to Zymo Research Corporation, Epigenetic Services (USA) for Methylation Mini-Seq full service sequencing.

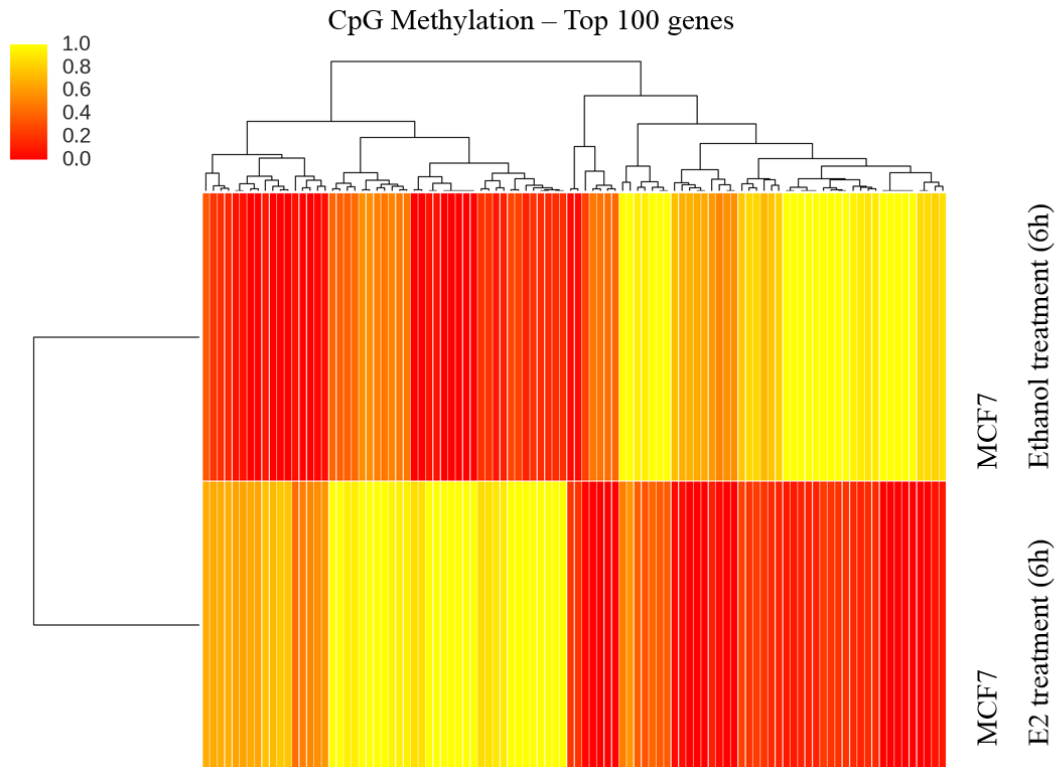


Figure 19. Differential methylation status of MCF7 cells. Shown is the comparative analysis of methylation status of highly divergent 100 gene loci in the absence or presence of E2. Cells were seeded as 2.5×10^6 into each T75 cm² tissue culture flasks in 8% CD-FBS/DMEM. 48 hours later, cells were treated either with 10^{-9} M of E2 or ethanol (0.01%) as vehicle control. Six hours after treatment, cells were trypsinized and washed with PBS twice. All experiments were repeated three independent times with three technical replicates. Quick-gDNA™ MiniPrep kit (Zymo Research, USA, D3024) was used according to manufacturer's instructions for genomic DNA isolation. Samples were shipped at -80°C conditions as genomic DNA to Zymo Research Corporation, Epigenetic Services (USA) for Methylation Mini-Seq full service sequencing.

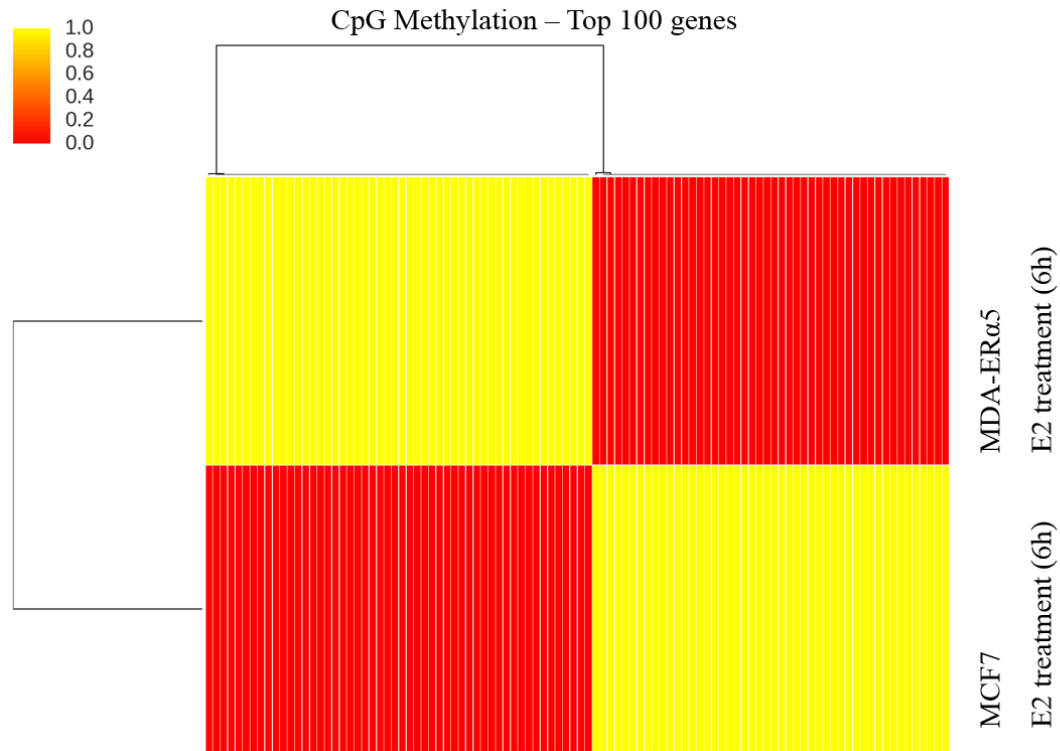


Figure 20. Differential methylation status of MDA-ER α 5 monoclonal and MCF7 cells. Shown is the comparative analysis of methylation status of highly divergent 100 gene loci in the absence or presence of E2. Cells were seeded as 2.5×10^6 into each T75 cm² tissue culture flasks in 8% CD-FBS/DMEM. 48 hours later, cells were treated either with 10^{-9} M of E2 or ethanol (0.01%) as vehicle control. Six hours after treatment, cells were trypsinized and washed with PBS twice. All experiments were repeated three independent times with three technical replicates. Quick-gDNA™ MiniPrep kit (Zymo Research, USA, D3024) was used according to manufacturer's instructions for genomic DNA isolation. Samples were shipped at -80°C conditions as genomic DNA to Zymo Research Corporation, Epigenetic Services (USA) for Methylation Mini-Seq full service sequencing.

Although analyses of methylation and transcriptomic results in depth are in progress, initial observations suggested that E2 treatment changes methylation statuses of the genome of both MDA-ER α 5 monoclonal and MCF7 cells. Additionally, in comparison of 6h E2 treatment samples of MDA-ER α 5 and MCF7 cells, it was found that there is a dramatic difference in methylation statuses of same genomic regions. These observations support the initial hypothesis that differences in genome-wide methylation statuses of cell lines expressing ER α endogenously vs exogenously could underlie differential gene expressions, and hence polarity in cellular proliferation.

To ensure that RT-qPCR results of selected genes (Section 3.2.4) showing expression changes correlate with directions in methylation profiles of their gene locus, methylation tracks were uploaded to USCS Genome Browser [49] and chromosomal location of genes and methylation statuses were visualized. URLs of methylation tracks were provided in APPENDIX I.

Methylation patterns of *YPEL2*, *YPEL3*, *CTGF*, *TFF1/pS2*, and *CCNA1* genes, which were responsive to E2, were assessed in three different groups: 1) ethanol vs E2 comparison of each cell line, 2) methylation pattern of same genomic regions of ethanol treated samples of MDA-ER α 5 and MCF7 were compared to each other, and 3) methylation pattern of same genomic region of E2 treated samples of MDA-ER α 5 and MCF7 were compared to each other.

In group one, we observed that E2 changes methylation pattern of same region compared to ethanol treatment group of both MDA-ER α 5 and MCF7 cells (Figure 21-30). In figures, each gene (*YPEL2*, *YPEL3*, *CTGF*, *TFF1/pS2*, and *CCNA1*) was shown for ethanol vs E2 treated MDA-ER α 5 cells first, and then for ethanol vs E2 treated MCF7 cells. For each of these genes, a distinct methylation pattern was discernable for both MDA-ER α 5 and MCF7 cells. This suggests that E2 treatment induces changes in the methylation profiles of these E2 responsive genes in MDA-ER α 5 or MCF7 cells. Expectedly, comparisons of only ethanol treatments of MDA-ER α 5 and MCF7 cells to each other (group two) showed that these two cell lines have unique methylation patterns for these genes (Figure 31-35). For the third group, methylation profiles of the same genomic region of the both cell lines in the presence of E2 were compared to each other (Figure 32-40). Results suggest that E2 mediated changes in methylation profiles also differ in cell lines.

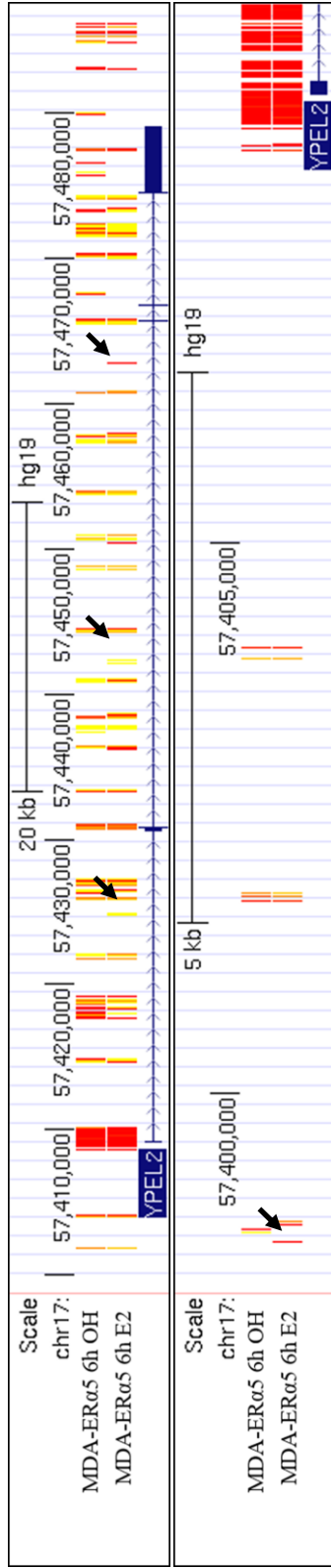


Figure 21. Differential methylation status of *YPEL2* in ethanol vs E2 treated MDA-ERα5 cells. Figure on the top shows the methylation pattern of the gene locus while figure at the bottom shows methylation pattern of upstream of the gene. Yellow lines represent higher level of methylation and red lines represent lower levels of methylation. Some of the differentially methylated regions were indicated with black arrows.

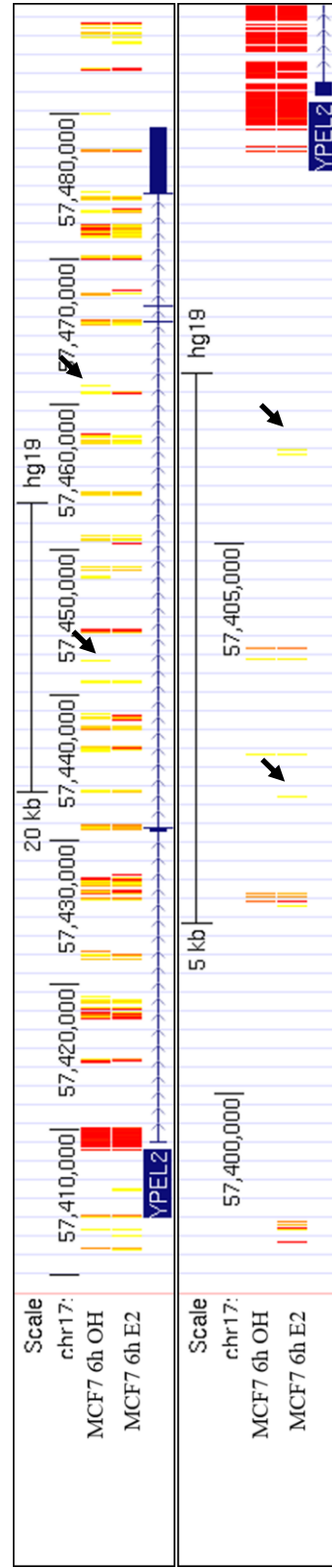


Figure 22. Differential methylation status of *YPEL2* in ethanol vs E2 treated MCF7 cells. Figure on the top shows the methylation pattern of the gene locus while figure at the bottom shows methylation pattern of upstream of the gene. Yellow lines represent higher level of methylation and red lines represent lower levels of methylation. Some of the differentially methylated regions were indicated with black arrows.

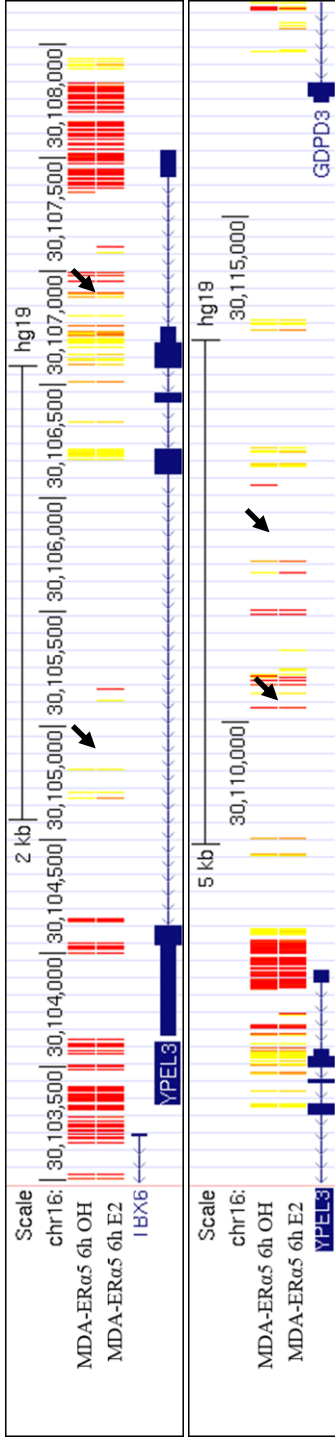


Figure 23. Differential methylation status of *YPEL3* in ethanol vs E2 treated MDA-ER α 5 cells. Figure on the top shows the methylation pattern of the gene locus while figure at the bottom shows methylation pattern of upstream of the gene. Yellow lines represent higher level of methylation and red lines represent lower levels of methylation. Some of the differentially methylated regions were indicated with black arrows.

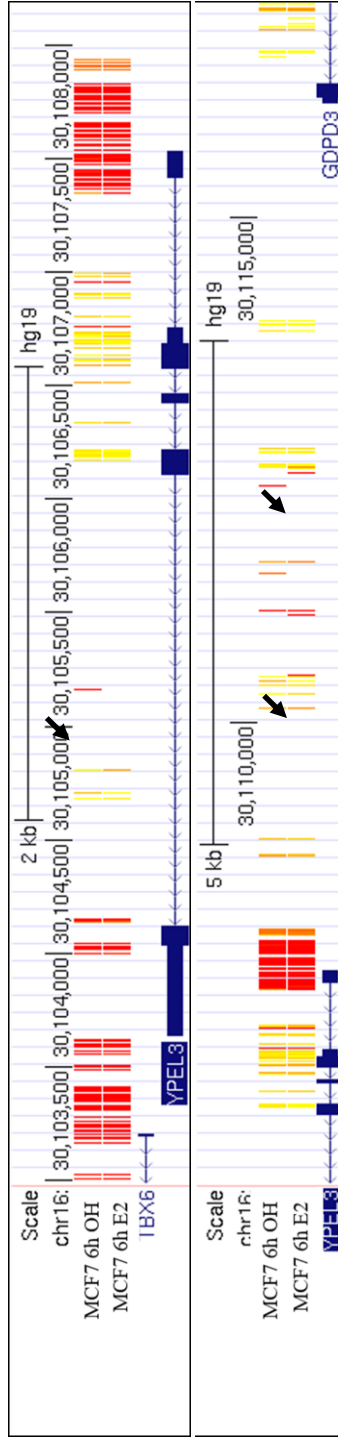


Figure 24. Differential methylation status of *YPEL3* in ethanol vs E2 treated MCF7 cells. Figure on the top shows the methylation pattern of the gene locus while figure at the bottom shows methylation pattern of upstream of the gene. Yellow lines represent higher level of methylation and red lines represent lower levels of methylation. Some of the differentially methylated regions were indicated with black arrows.

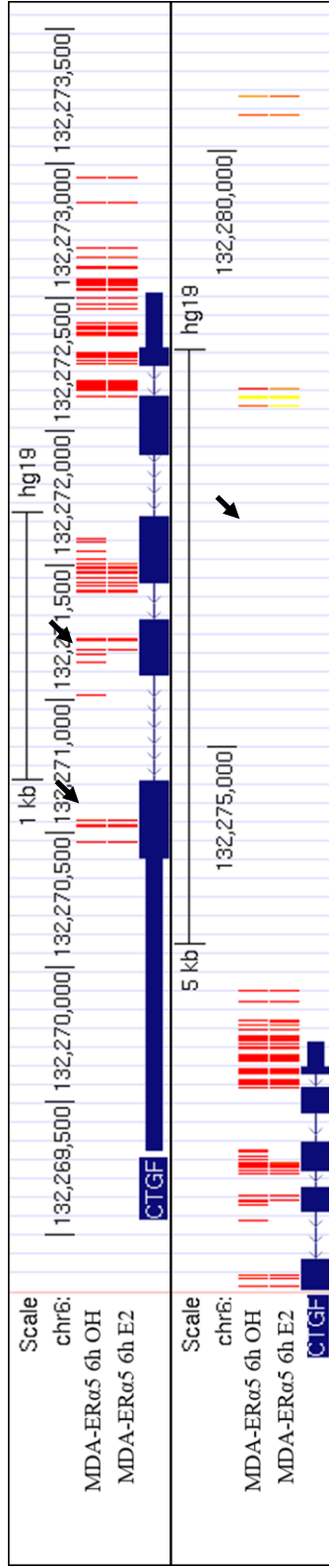


Figure 25. Differential methylation status of *CTGF* in ethanol vs E2 treated MDA-ERα5 cells. Figure on the top shows the methylation pattern of the gene locus while figure at the bottom shows methylation pattern of upstream of the gene. Yellow lines represent higher level of methylation and red lines represent lower levels of methylation. Some of the differentially methylated regions were indicated with black arrows.

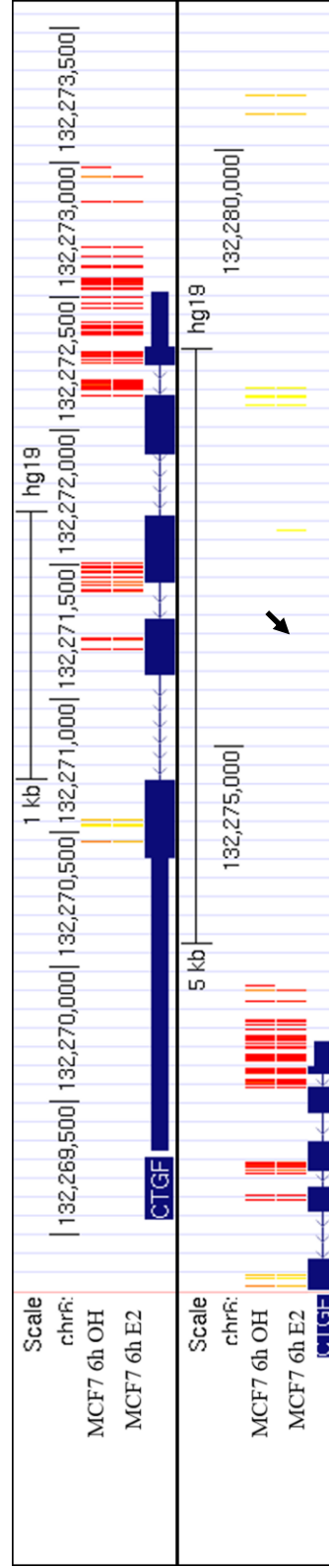


Figure 26. Differential methylation status of *CTGF* in ethanol vs E2 treated MCF7 cells. Figure on the top shows the methylation pattern of the gene locus while figure at the bottom shows methylation pattern of upstream of the gene. Yellow lines represent higher level of methylation and red lines represent lower levels of methylation. Some of the differentially methylated regions were indicated with black arrows.

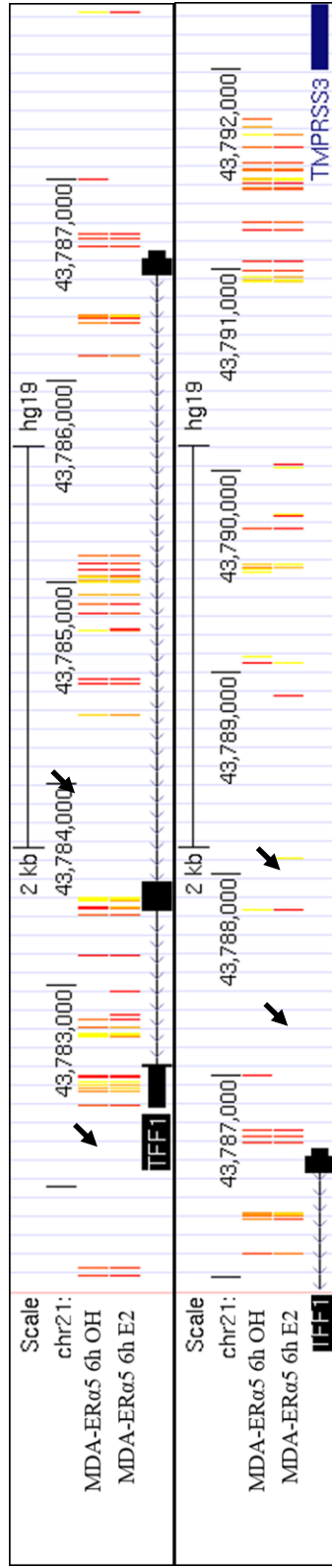


Figure 27. Differential methylation status of *TFF1/pS2* in ethanol vs E2 treated MDA-ER α 5 cells. Figure on the top shows the methylation pattern of the gene locus while figure at the bottom shows methylation pattern of upstream of the gene. Yellow lines represent higher level of methylation and red lines represent lower levels of methylation. Some of the differentially methylated regions were indicated with black arrows.

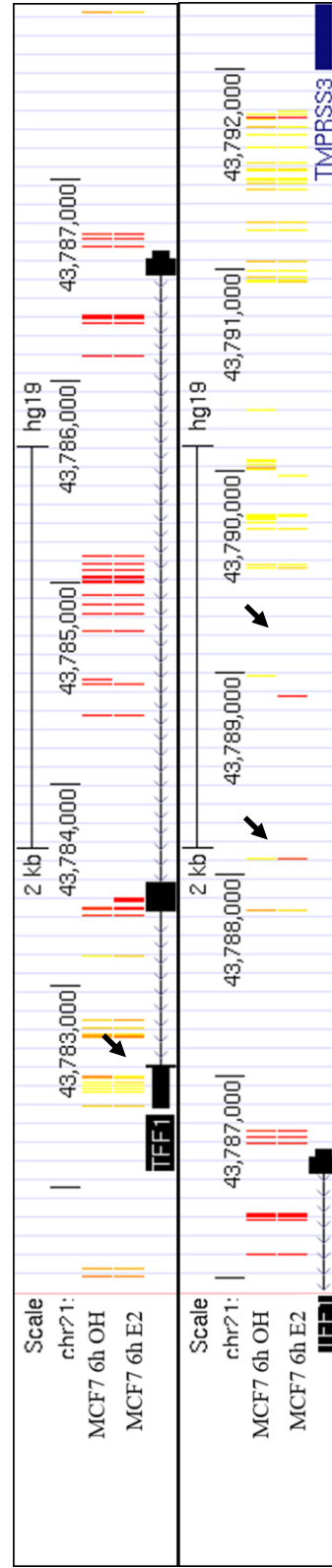


Figure 28. Differential methylation status of *TFF1/pS2* in ethanol vs E2 treated MCF7 cells. Figure on the top shows the methylation pattern of the gene locus while figure at the bottom shows methylation pattern of upstream of the gene. Yellow lines represent higher level of methylation and red lines represent lower levels of methylation. Some of the differentially methylated regions were indicated with black arrows.

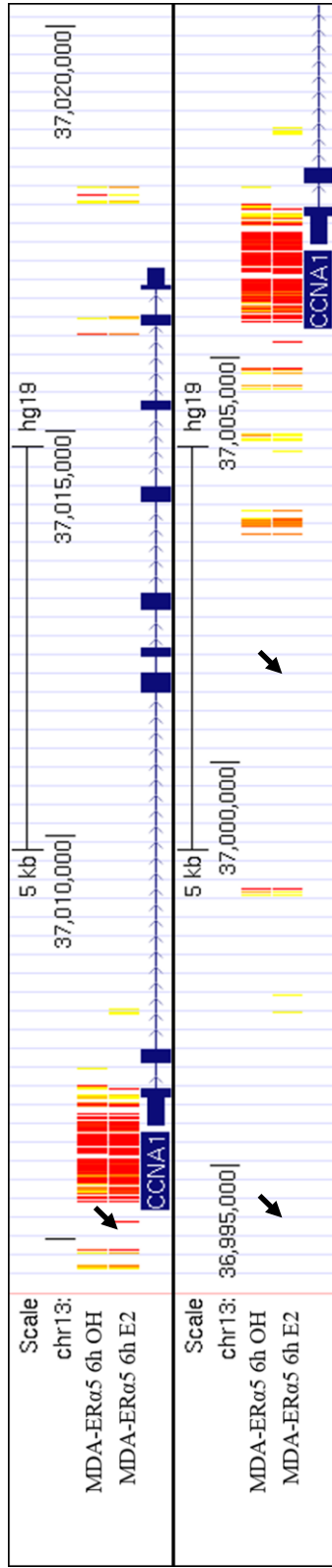


Figure 29. Differential methylation status of *CCNA1* in ethanol vs E2 treated MDA-ER α 5 cells. Figure on the top shows the methylation pattern of the gene locus while figure at the bottom shows methylation pattern of upstream of the gene. Yellow lines represent higher level of methylation and red lines represent lower levels of methylation. Some of the differentially methylated regions were indicated with black arrows.

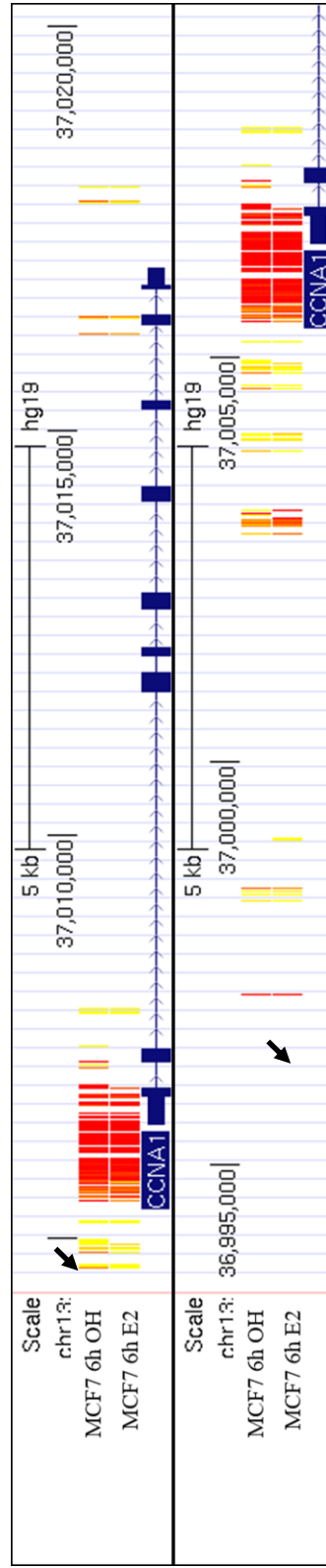


Figure 30. Differential methylation status of *CCNA1* in ethanol vs E2 treated MCF7 cells. Figure on the top shows the methylation pattern of the gene locus while figure at the bottom shows methylation pattern of upstream of the gene. Yellow lines represent higher level of methylation and red lines represent lower levels of methylation. Some of the differentially methylated regions were indicated with black arrows.

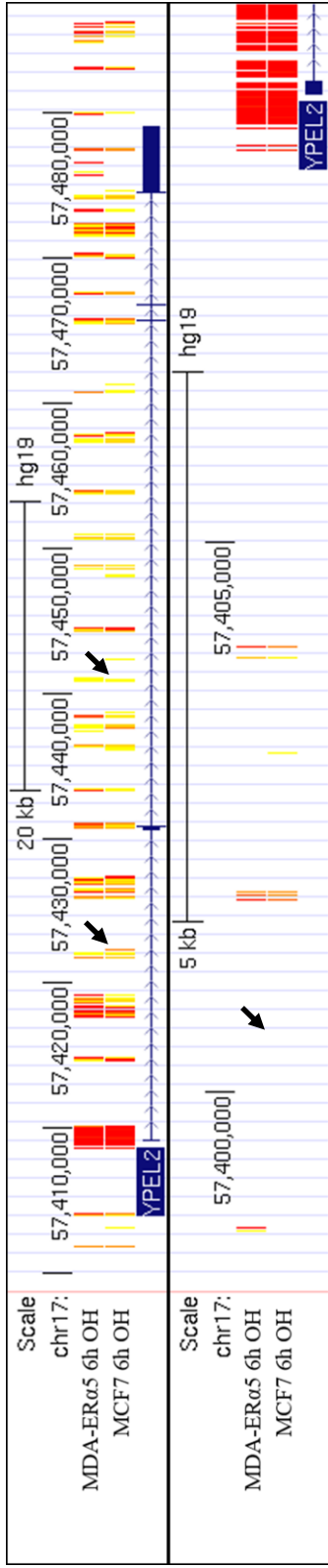


Figure 31. Differential methylation status of *YPEL2* in ethanol treated MDA-ER α 5 vs MCF7 cells. Figure on the top shows the methylation pattern of the gene locus while figure at the bottom shows methylation pattern of upstream of the gene. Yellow lines represent higher level of methylation and red lines represent lower levels of methylation. Some of the differentially methylated regions were indicated with black arrows.

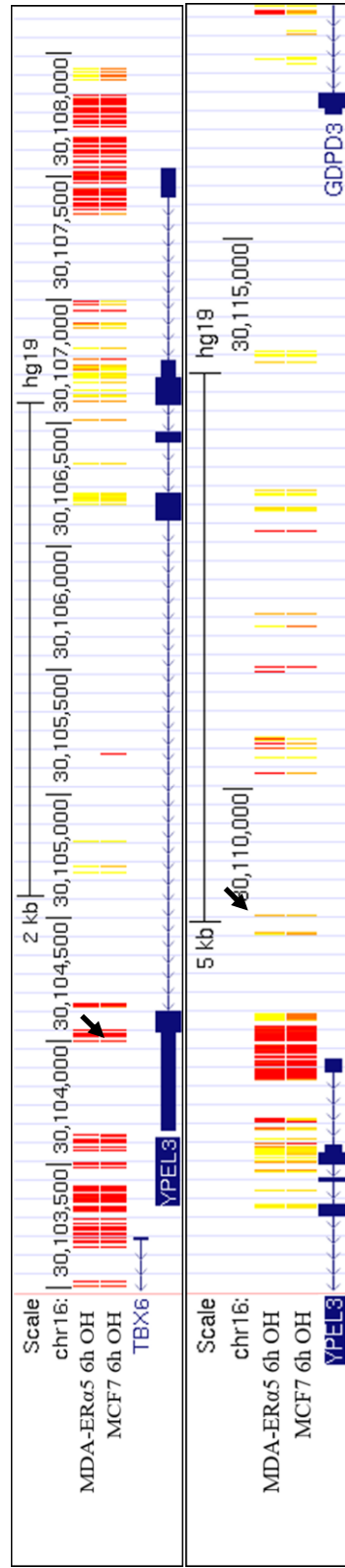


Figure 32. Differential methylation status of *YPEL3* in ethanol treated MDA-ER α 5 vs MCF7 cells. Figure on the top shows the methylation pattern of the gene locus while figure at the bottom shows methylation pattern of upstream of the gene. Yellow lines represent higher level of methylation and red lines represent lower levels of methylation. Some of the differentially methylated regions were indicated with black arrows.

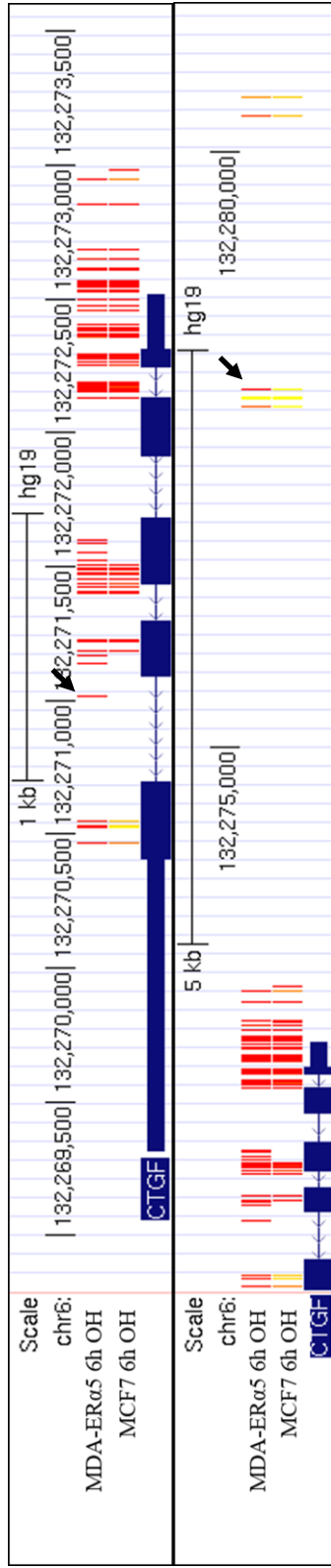


Figure 33. Differential methylation status of *CTGF* in ethanol treated MDA-ER α 5 vs MCF7 cells. Figure on the top shows the methylation pattern of the gene locus while figure at the bottom shows methylation pattern of upstream of the gene. Yellow lines represent higher level of methylation and red lines represent lower levels of methylation. Some of the differentially methylated regions were indicated with black arrows.

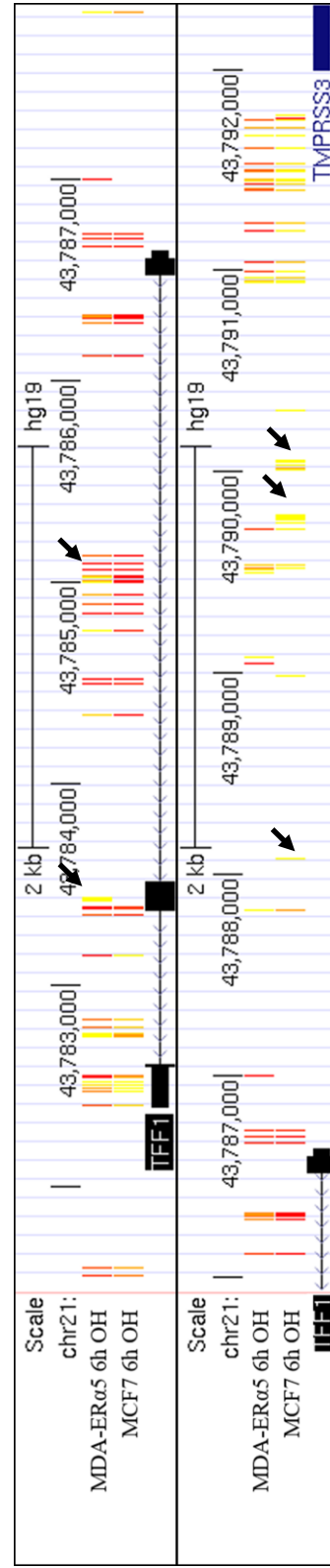


Figure 34. Differential methylation status of *TFF1/pS2* in ethanol treated MDA-ER α 5 vs MCF7 cells. Figure on the top shows the methylation pattern of the gene locus while figure at the bottom shows methylation pattern of upstream of the gene. Yellow lines represent higher level of methylation and red lines represent lower levels of methylation. Some of the differentially methylated regions were indicated with black arrows.

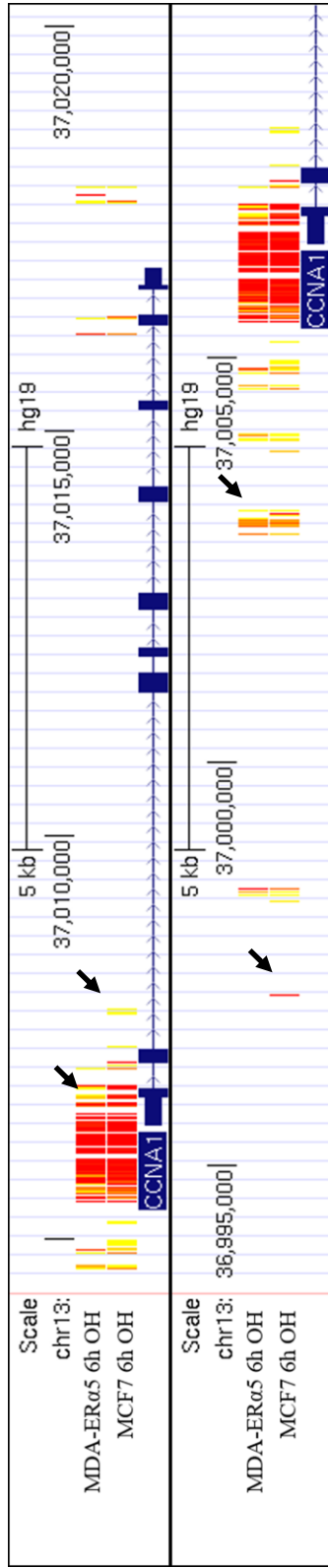


Figure 35. Differential methylation statuses of *CCNA1* in ethanol treated MDA-ER α 5 vs MCF7 cells. Figure on the top shows the methylation pattern of the gene locus while figure at the bottom shows methylation pattern of upstream of the gene. Yellow lines represent higher level of methylation and red lines represent lower levels of methylation. Some of the differentially methylated regions were indicated with black arrows.

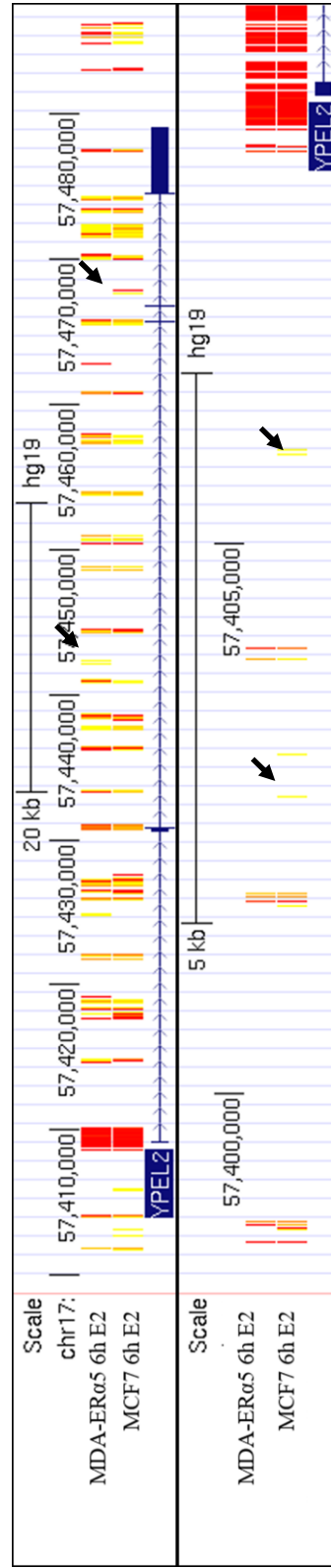


Figure 36. Differential methylation statuses of *YPEL2* in E2 treated MDA-ER α 5 vs MCF7 cells. Figure on the top shows the methylation pattern of the gene locus while figure at the bottom shows methylation pattern of upstream of the gene. Yellow lines represent higher level of methylation and red lines represent lower levels of methylation. Some of the differentially methylated regions were indicated with black arrows.

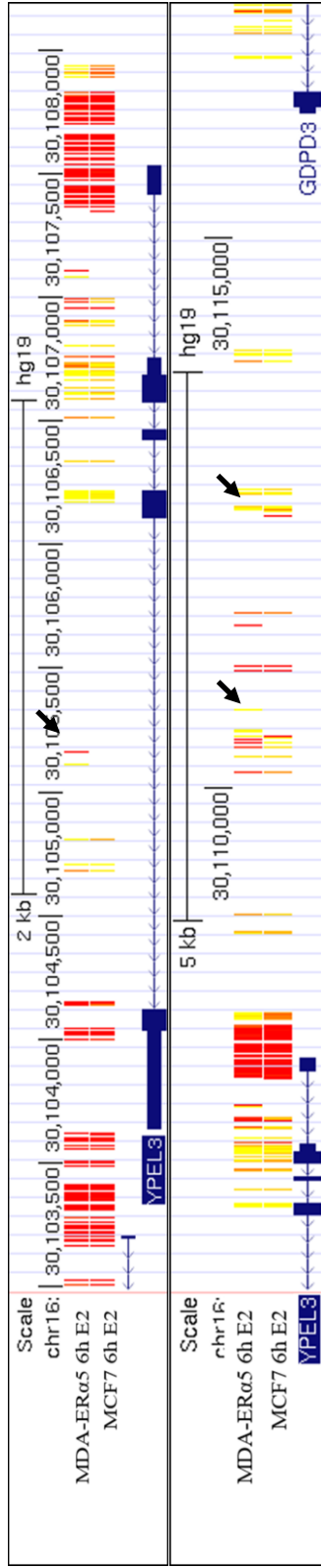


Figure 37. Differential methylation status of *YPEL3* in E2 treated *MDA-ERα5* vs *MCF7* cells. Figure on the top shows the methylation pattern of the gene locus while figure at the bottom shows methylation pattern of upstream of the gene. Yellow lines represent higher level of methylation and red lines represent lower levels of methylation. Some of the differentially methylated regions were indicated with black arrows.

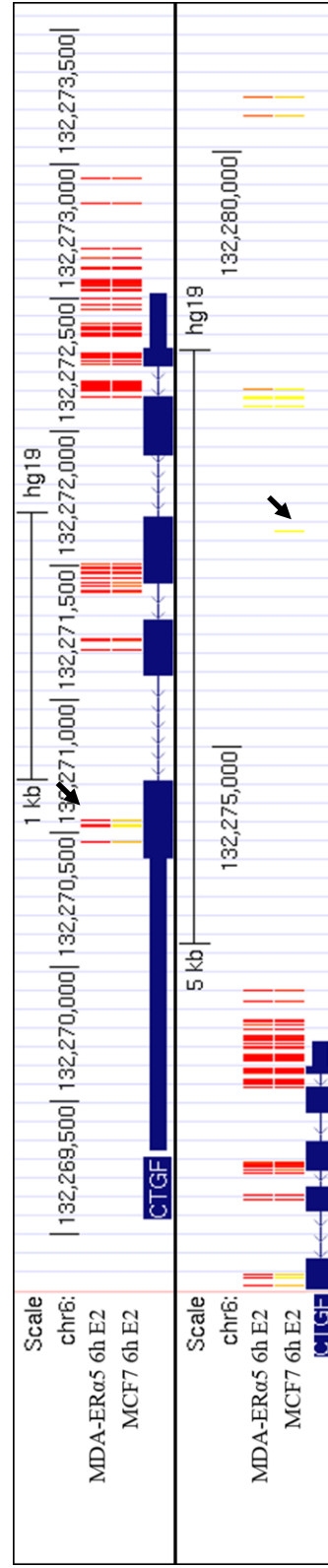


Figure 38. Differential methylation status of *CTGF* in E2 treated *MDA-ERα5* vs *MCF7* cells. Figure on the top shows the methylation pattern of the gene locus while figure at the bottom shows methylation pattern of upstream of the gene. Yellow lines represent higher level of methylation and red lines represent lower levels of methylation. Some of the differentially methylated regions were indicated with black arrows.

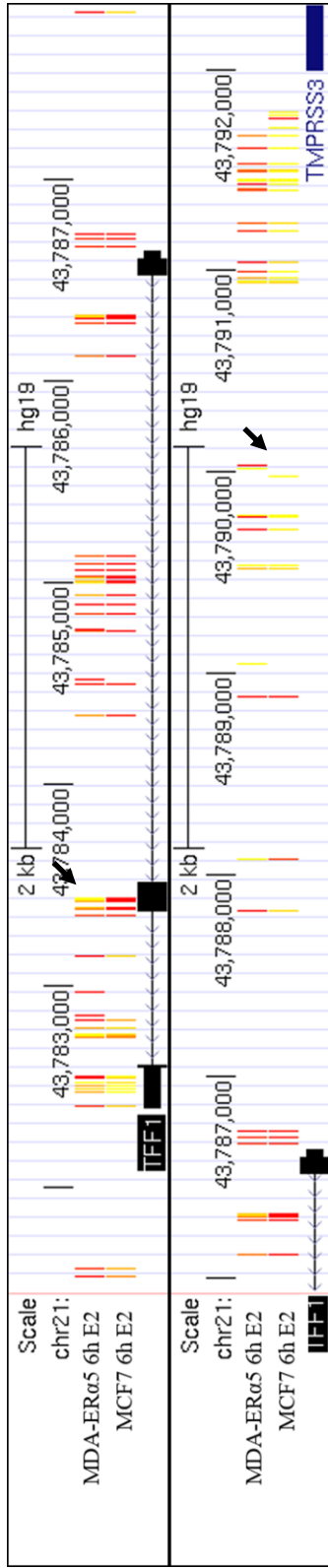


Figure 39. Differential methylation status of *TFF1/pS2* in E2 treated MDA-ER α 5 vs MCF7 cells. Figure on the top shows the methylation pattern of the gene locus while figure at the bottom shows methylation pattern of upstream of the gene. Yellow lines represent higher level of methylation and red lines represent lower levels of methylation. Some of the differentially methylated regions were indicated with black arrows.

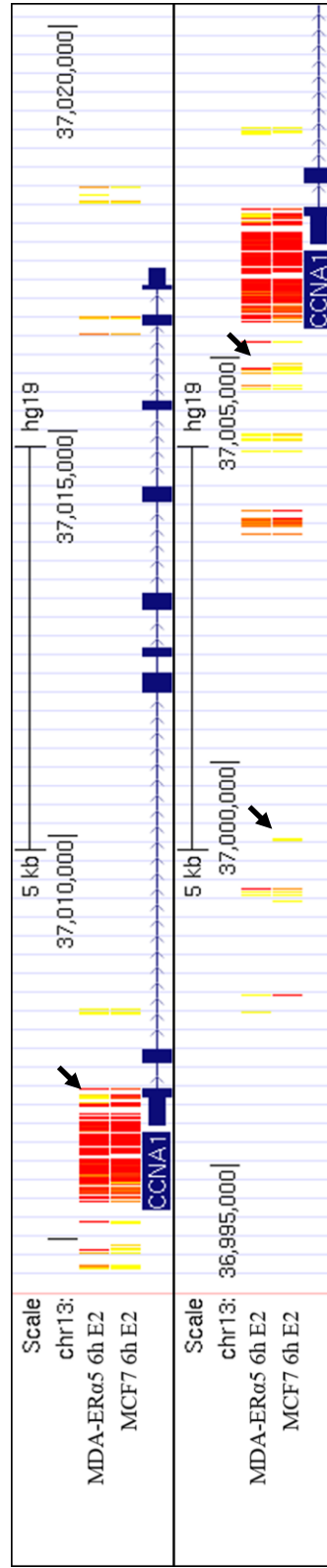


Figure 40. Differential methylation status of *CCNA1* in E2 treated MDA-ER α 5 vs MCF7 cells. Figure on the top shows the methylation pattern of the gene locus while figure at the bottom shows methylation pattern of upstream of the gene. Yellow lines represent higher level of methylation and red lines represent lower levels of methylation. Some of the differentially methylated regions were indicated with black arrows.

3.5. Whole-Genome Transcriptomic Profile Analysis

One of the cell pellets prepared from the same biological samples for methylation analysis was subjected to whole-genome transcriptomic profiling to assess whether methylation status of cell lines correlate with gene expression pattern. Genome-wide transcriptome analysis revealed remarkably small number of genes responded to E2 in contrast to previous findings of this and other laboratories, which report hundreds of transcripts. We observed that E2 treatment of MDA-ER α 5 cells for six hours resulted in significant changes in the expression of only 23 transcripts (Appendix J). E2, on the other hand, regulated the expression of 140 transcripts in MCF7 cells (Appendix J).

Table 2. Whole Transcriptomic Profile Analyses for Subset of Genes in MDA-ER α 5 ethanol vs E2 treatment.

Gene ID	Gene Symbol	Locus	p-Value
ENSG00000175155.8	<i>YPEL2</i>	chr17:59331688-59403303	0,443547
ENSG00000090238.11	<i>YPEL3</i>	chr16:30092313-30104116	0,718572
ENSG00000118523.5	<i>CTGF</i>	chr6:131948175-132077393	0,267299
ENSG00000160182.2	<i>TFF1</i>	chr21:42362281-42366594	0,000341
ENSG00000133101.9	<i>CCNA1</i>	chr13:36431519-36442882	0,054373

Table 3. Whole Transcriptomic Profile Analyses for Subset of Genes in MCF7 ethanol vs E2 treatment.

Gene ID	Gene Symbol	Locus	p-Value
ENSG00000175155.8	<i>YPEL2</i>	chr17:59331688-59403303	0,143355
ENSG00000090238.11	<i>YPEL3</i>	chr16:30092313-30104116	0,0260659
ENSG00000118523.5	<i>CTGF</i>	chr6:131948175-132077393	6,67E-05
ENSG00000160182.2	<i>TFF1</i>	chr21:42362281-42366594	1,11E-05
ENSG00000133101.9	<i>CCNA1</i>	chr13:36431519-36442882	0,00746204

Bioinformatics analyses of both genome-wide methylation and whole transcriptomic profile results are currently being studied. Although we have a small list for genes that are differentially modulated by E2 in transcriptome profiling, we still used DAVID Bioinformatics Database [50] to functionally cluster genes from the initial RNA-seq analysis. In ethanol vs E2 treated MCF7 cells, 140 significant genes with the clustering of biological functions are shown in Figure 41. Enrichment scores, indicated on the left side of the figure, define abundance of biological processes as clusters in the gene list, which show, as expected, that E2 is involved in various biological processes. On the other hand, the DAVID Bioinformatics Database was not able to cluster these genes into biologically relevant groups due to small samples size (23 genes) of MDA-ER α 5 cells.

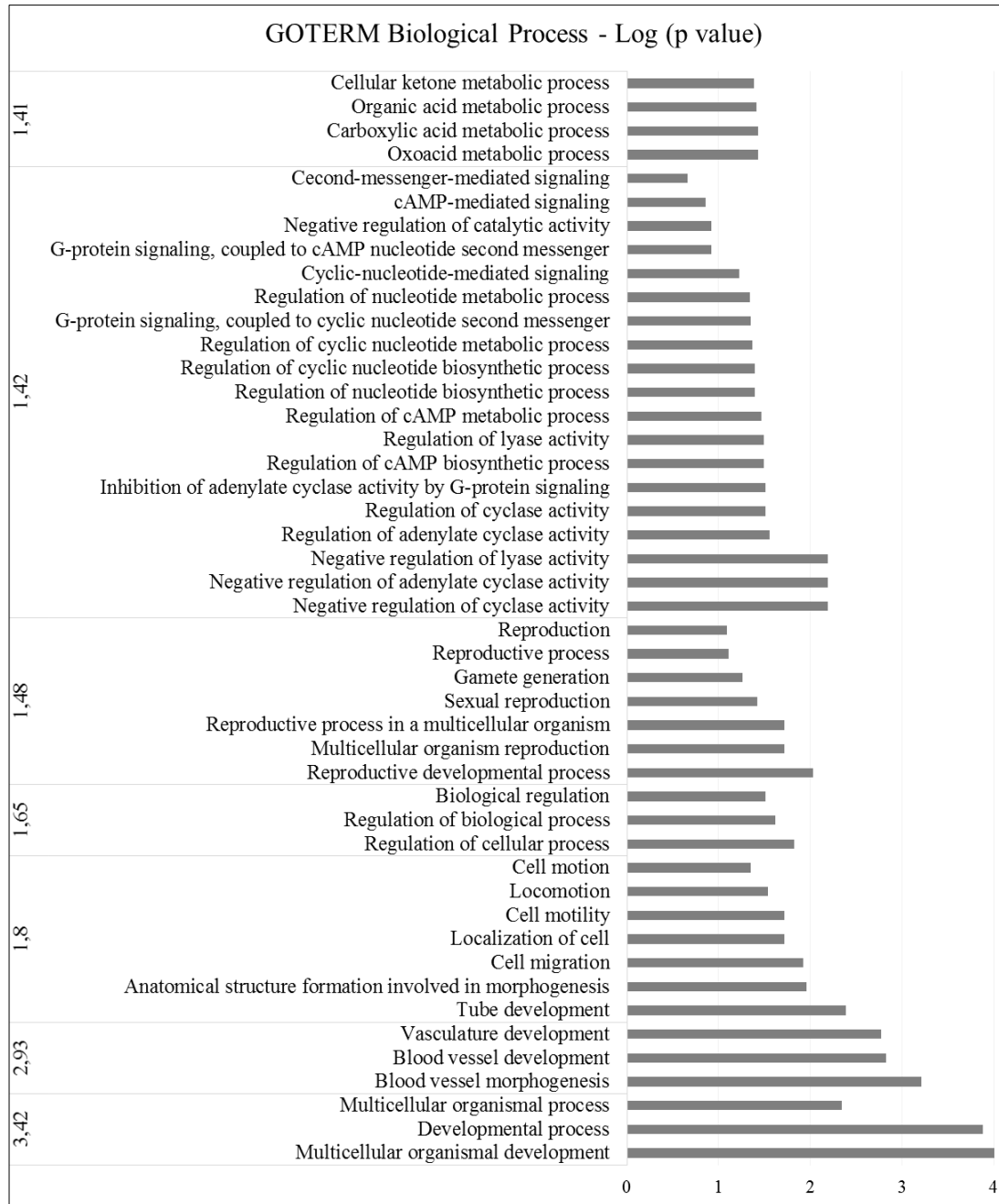


Figure 41. Biological function clustering of genes showing significant changes in ethanol vs E2 treated MCF7 cells with RNA-seq. Genes are clustered according to their biological function and numbers on the left side indicate the enrichment score. Numbers at the bottom indicate log (p-value).

Although for every set of experiment, the expression of the *TFF1/pS2* gene was used as the positive control to E2 treatment before an experiment was deemed to be a biological replicate for whole-genome methylome and transcriptome analyses, this unexpectedly small number of genes regulated differentially in response to E2

suggests that there are significant variations among biological replicates adversely affecting the p-value. Indeed, glancing into the results of biological replicates including our selected genes implies this may be the case. This rendered the correlation of methylation status to transcriptome profiling difficult to perform. For example, in RT-qPCR assays, we observed that E2 effectively induces changes in the expression of *YPEL2*, *YPEL3* or *CTGF* in a cell-type dependent manner; however, transcriptome analysis showed no significant change in *YPEL2*, *YPEL3* or *CTGF* in MDA-ER α 5 cells (Table 2). E2 exerted no effect on *YPEL2* or *YPEL3* in MCF7 cells, while significantly altering the expression of *CTGF* (Table 3).

These results suggest that our results may yet be unreliable to generate a correlation between methylation status and gene expressions. A possible solution could involve the inclusion of more samples in analyses.

CHAPTER 4

CONCLUSION AND FUTURE DIRECTIONS

For testing our initial hypothesis that differential methylation pattern of regulatory regions of genes could underlie the proliferative vs anti-proliferative effect, hence, the differential expression of genes, of E2 in cells synthesizing ER α endogenously or introduced exogenously, we have generated a cell model. In our functional assays, we were able to show that ER α synthesized in the MDA-ER α 5 monoclonal functions expectedly in terms of intracellular localization, E2 binding, regulating estrogen responsive gene expressions as well as modulating cell cycle distribution. Based on these findings, we have tested the responses of MDA-ER α 5 in comparison to MCF7 cells synthesizing ER α endogenously to E2. In keeping with previous observations from this and other laboratories, our results showed that E2 is an anti-proliferative in MDA-ER α 5 in contrast to MCF7 cells wherein E2 is proliferative hormone.

In summary;

1. The MDA-ER α 5 monoclonal synthesizes ER α (Section 3.2.1.) that localizes in the nucleus as in MCF7 cells (Section 3.2.2.).
2. ER α in MDA-ER α 5 cells is capable of regulating responsive gene expressions (Section 3.2.3. & Section 3.2.4.).
3. ER α in response to E2 alters cell cycle phases: E2-ER α represses G1-S phase transition in MDA-ER α 5 cells in contrast to MCF7 cells wherein E2 augments cell population entering to S phase (Section 3.2.5.).
4. E2 effects on cellular proliferation show polar directions: E2 effectively decreased the proliferation of MDA-ER α 5 cells in clear contrast to the increased proliferation of MCF7 cells by E2 (Section 3.3.).

5. Genome-wide methylation profiling clearly indicate that these model cell lines have distinct methylation patterns, as assessed by ethanol treated group, for the same genomic region (Section 3.4.).
 6. E2 also affected genome-wide methylation status and transcription profiles of both MDA-ER α 5 and MCF7 cells (Section 3.4. & Section 3.5.).
- ❖ These observations indicate that the MDA-ER α 5 monoclonal cell line generated by stable transfection of an expression vector containing ER α cDNA could be used for the understanding of underlying mechanism of the paradoxical bi-potential effect of E2 on cellular proliferation in cells that synthesize the ER α receptor endogenously or introduced exogenously.

However, discrepancies in between the expression of some of endogenous genes assessed by RT-qPCR and RNA-Seq analyses also suggest that the results of transcriptomic profiling, of at least for MDA-ER α 5 cells, are yet unreliable. Although the underlying reason(s) is unclear, apparent variations among biological replicates of RNA-Seq results necessitate the re-evaluation of sample sizes that we have used in analysis. Since samples for genome-wide methylome and transcriptome analyses derived from the same set of experimental groups, our results also suggest a cautious approach to methylome results as well. Consequently, at the moment, this prevents us to propose a correlation between methylation and transcriptomic profiles of cell models in response to E2. One likely solution to this apparent problem could involve an increase in sample size for both analyses.

In addition, results of both methylome and transcriptome analyses are to be verified by various approaches including targeted methylation specific polymerase chain reaction (MSP) [51] and RT-qPCR to ensure that these exploratory approaches indeed produce biologically meaningful findings.

BIBLIOGRAPHY

- [1] American Cancer Society, “Cancer facts & figures 2016,” 2016.
- [2] T. C. S. Bakanlığı, “Türkiye’de Kanser Kayıtlılığı,” *Daire Faaliyetleri*, 2013. [Online]. Available: <http://kanser.gov.tr/daire-faaliyetleri/kanser-kayitciligi/108-Türkiyede-kanserkayitcigi>. [Accessed: 01-Jan-2016].
- [3] S. J. Dawson, O. M. Rueda, S. Aparicio, and C. Caldas, “A new genome-driven integrated classification of breast cancer and its implications,” *EMBO J.*, vol. 32, no. 5, pp. 617–628, 2013.
- [4] H. D. Soule, J. Vazquez, A. Long, S. Albert, and M. Brennan, “A Human Cell Line From a Pleural Effusion Derived From a Breast Carcinoma,” *J Natl Cancer Inst*, vol. 51, no. 5, pp. 1409–1416, 1973.
- [5] A. Zheng, A. Kallio, and P. Härkönen, “Tamoxifen-Induced Rapid Death of MCF-7 Breast Cancer Cells Is Mediated via Extracellularly Signal-Regulated Kinase Signaling and Can Be Abrogated by Estrogen,” *Endocrinology*, vol. 148, no. 6, pp. 2764–2777, 2007.
- [6] B. R. Brinkley, P. T. Beall, L. J. Wible, M. L. Mace, D. S. Turner, and R. M. Cailleau, “Variations in Cell Form and Cytoskeleton in Human Breast Carcinoma Cells in Vitro,” *Cancer Res.*, vol. 40, no. 9, pp. 3118–3129, 1980.
- [7] A. Prat and C. M. Perou, “Deconstructing the molecular portraits of breast cancer.,” *Mol. Oncol.*, vol. 5, no. 1, pp. 5–23, Mar. 2011.
- [8] J. Huang, X. Li, T. Qiao, R. A. Bambara, R. Hilf, and M. Muyan, “A tale of two estrogen receptors (ERs): how differential ER-estrogen responsive element interactions contribute to subtype-specific transcriptional responses,” *Nucl. Recept. Signal.*, vol. 4, pp. 1–4, 2006.
- [9] P. Ascenzi, A. Bocedi, and M. Marino, “Structure-function relationship of estrogen receptor alpha and beta: Impact on human health,” *Mol. Aspects Med.*, vol. 27, no. 4, pp. 299–402, Aug. 2006.
- [10] M. J. Linja, K. P. Porkka, Z. Kang, K. J. Savinainen, and O. A. Ja, “Expression of Androgen Receptor Coregulators in Prostate Cancer Expression of Androgen Receptor Coregulators in Prostate Cancer,” vol. 10, pp. 1032–1040, 2004.

- [11] Y. Huang, X. Li, and M. Muyan, "Estrogen receptors similarly mediate the effects of 17 β -estradiol on cellular responses but differ in their potencies," *Endocrine*, vol. 39, no. 1, pp. 48–61, Feb. 2011.
- [12] S. L. Nott, Y. Huang, X. Li, B. R. Fluharty, X. Qiu, W. V. Welshons, S. Y. Yeh, and M. Muyan, "Genomic Responses from the Estrogen-responsive Element-dependent Signaling Pathway Mediated by Estrogen Receptor α Are Required to Elicit Cellular Alterations," *J. Biol. Chem.*, vol. 284, no. 22, pp. 15277–15288, 2009.
- [13] L. R. Nelson and S. E. Bulun, "Estrogen production and action," *J. Am. Acad. Dermatol.*, vol. 45, no. 3, pp. 116–124, 2001.
- [14] C. J. Gruber, W. Tschugguel, C. Schneeberger, and J. Huber, "Production and Actions of Estrogens," *N. Engl. J. Med.*, vol. 346, no. 5, pp. 340–352, 2002.
- [15] D. A. Zajchowski, R. Sager, and L. Webster, "Estrogen Inhibits the Growth of Estrogen Receptor-negative, but not Estrogen Receptor-positive, Human Mammary Epithelial Cells Expressing a Recombinant Estrogen Receptor," *CANCER Res.*, vol. 53, pp. 5004–5011, 1993.
- [16] J. C. Reese and B. S. Katzenellenbogen, "Differential DNA-binding abilities of estrogen receptor occupied with two classes of antiestrogens: studies using human estrogen receptor overexpressed in mammalian cells," *Nucleic Acids Res*, vol. 19, no. 23, pp. 6595–6602, 1991.
- [17] M. Garcia, D. Derocq, G. Freiss, and H. Rochefort, "Activation of estrogen receptor transfected into a receptor-negative breast cancer cell line decreases the metastatic and invasive potential of the cells," *Proc. Natl. Acad. Sci. U. S. A.*, vol. 89, no. 23, pp. 11538–11542, 1992.
- [18] F. Pakdel, P. Le Goff, and B. S. Katzenellenbogen, "An Assessment of the Role of Domain F and Pest Wequences in Estrogen Receptor Half-Life and Bioactivity," *J. Steroid Biochem. Mol. Biol.*, vol. 46, no. 6, pp. 663–672, 1993.
- [19] A. S. Levenson, B. D. Gehm, S. T. Pearce, J. Horiguchi, L. A. Simons, J. E. Ward, J. L. Jameson, and V. C. Jordan, "Resveratrol Acts as an Rstrogen Receptor (ER) Agonist in Breast Cancer Cells Stably Transfected with ER α ," *Int. J. Cancer*, vol. 104, no. 5, pp. 587–596, 2003.
- [20] G. Lazennec and B. S. Katzenellenbogen, "Expression of human estrogen receptor using an efficient adenoviral gene delivery system is able to restore hormone-dependent features to estrogen receptor-negative breast carcinoma cells," *Mol. Cell. Endocrinol.*, vol. 149, no. 1–2, pp. 93–105, 1999.
- [21] S. Jiang and V. C. Jordan, "Growth Regulation of Estrogen Receptor-Negative Breast Cancer Cells Transfected With Complementary DNAs for Estrogen Receptor," *J. Natl. Cancer Inst.*, vol. 84, no. 8, pp. 580–591, 1991.

- [22] W. Wang, R. Smith, R. Burghardt, and S. H. Safe, "17 beta-Estradiol-mediated growth inhibition of MDA-MB-468 cells stably transfected with the estrogen receptor: cell cycle effects," *Mol. Cell. Endocrinol.*, vol. 133, no. 1, pp. 49–62, 1997.
- [23] B. K. Lundholt, P. Briand, and A. E. Lykkesfeldt, "Growth inhibition and growth stimulation by estradiol of estrogen receptor transfected human breast epithelial cell lines involve different pathways," *Breast Cancer Res. Treat.*, vol. 67, no. 3, pp. 199–214, 2001.
- [24] S. R. Hammes and E. R. Levin, "Extranuclear steroid receptors: nature and actions.," *Endocr. Rev.*, vol. 28, no. 7, pp. 726–41, Dec. 2007.
- [25] P. Yi, S. Bhagat, R. Hilf, R. A. Bambara, and M. Muyan, "Differences in the Abilities of Estrogen Receptors to Integrate Activation Functions Are Critical for Subtype-Specific Transcriptional Responses," *Mol. Endocrinol.*, vol. 16, no. 8, pp. 1810–27, 2002.
- [26] M. Muyan, L. M. Callahan, Y. Huang, and A. J. Lee, "The ligand-mediated nuclear mobility and interaction with estrogen-responsive elements of estrogen receptors are subtype specific," *J. Mol. Endocrinol.*, vol. 49, no. 3, pp. 249–266, 2012.
- [27] M. Weber, J. J. Davies, D. Wittig, E. J. Oakeley, M. Haase, W. L. Lam, and D. Schübeler, "Chromosome-wide and promoter-specific analyses identify sites of differential DNA methylation in normal and transformed human cells," *Nat. Genet.*, vol. 37, no. 8, pp. 853–862, 2005.
- [28] R. Singal and G. D. Ginder, "DNA Methylation," *Blood*, vol. 93, no. 12, pp. 4059–4070, 1999.
- [29] M. Szyf, P. Pakneshan, and S. A. Rabbani, "DNA methylation and breast cancer," *Biochem. Pharmacol.*, vol. 68, no. 6, pp. 1187–1197, 2004.
- [30] M. Ung, X. Ma, K. C. Johnson, B. C. Christensen, and C. Cheng, "Effect of estrogen receptor α binding on functional DNA methylation in breast cancer," *Epigenetics*, vol. 9, no. 4, pp. 523–532, 2014.
- [31] P. W. Laird, "Principles and challenges of genome-wide DNA methylation analysis," *Nat. Rev. Genet.*, vol. 11, no. 3, pp. 191–203, 2010.
- [32] Q. Yang, L. Shan, G. Yoshimura, M. Nakamura, Y. Nakamura, T. Suzuma, T. Umemura, I. Mori, T. Sakurai, and K. Kakudo, "5-Aza-2'-Deoxycytidine Induces Retinoic Acid Receptor Beta 2 Demethylation, Cell Cycle Arrest and Growth Inhibition in Breast Carcinoma Cells," vol. 22, no. 5, pp. 2753–6., 2002.
- [33] M. J. Fackler, C. Umbricht, D. Williams, P. Argani, L. A. Cruz, V. F. Merino, W. W. Teo, Z. Zhang, P. Huang, K. Visvanathan, J. Marks, S. Ethier, J. W.

- Gray, A. C. Wolff, L. M. Cope, and S. Sukumar, "Genome-wide Methylation Analysis Identifies Genes Specific to Breast Cancer Hormone Receptor Status and Risk of Recurrence," vol. 71, no. 19, pp. 6195–6207, 2012.
- [34] L. Li, K. M. Lee, W. Han, J. Y. Choi, J. Y. Lee, G. H. Kang, S. K. Park, D. Y. Noh, K. Y. Yoo, and D. Kang, "Estrogen and progesterone receptor status affect genome-wide DNA methylation profile in breast cancer," *Hum. Mol. Genet.*, vol. 19, no. 21, pp. 4273–4277, 2010.
- [35] M. Widschwendter, K. D. Siegmund, H. M. Müller, H. M. Mu, H. Fiegl, C. Marth, E. Mu, P. A. Jones, and P. W. Laird, "Association of Breast Cancer DNA Methylation Profiles with Hormone Receptor Status and Response to Tamoxifen Association of Breast Cancer DNA Methylation Profiles with Hormone Receptor Status and Response to Tamoxifen," no. 16, pp. 3807–3813, 2004.
- [36] Y. Ruike, Y. Imanaka, F. Sato, K. Shimizu, and G. Tsujimoto, "Genome-wide analysis of aberrant methylation in human breast cancer cells using methyl-DNA immunoprecipitation combined with high-throughput sequencing," *BMC Genomics*, vol. 11, p. 137, 2010.
- [37] S. A. Bustin, V. Benes, J. A. Garson, J. Hellemans, J. Huggett, M. Kubista, R. Mueller, T. Nolan, M. W. Pfaffl, G. L. Shipley, J. Vandesompele, and C. T. Wittwer, "The MIQE guidelines: minimum information for publication of quantitative real-time PCR experiments.," *Clin. Chem.*, vol. 55, no. 4, pp. 611–22, Apr. 2009.
- [38] J. Huang, X. Li, R. Hilf, R. A. Bambara, and M. Muyan, "Molecular basis of therapeutic strategies for breast cancer.," *Curr. Drug Targets. Immune. Endocr. Metabol. Disord.*, vol. 5, no. 4, pp. 379–396, 2005.
- [39] K. Hosono, T. Sasaki, S. Minoshima, and N. Shimizu, "Identification and characterization of a novel gene family YPEL in a wide spectrum of eukaryotic species.," *Gene*, vol. 340, no. 1, pp. 31–43, Sep. 2004.
- [40] K. D. Kelley, K. R. Miller, A. Todd, A. R. Kelley, R. Tuttle, and S. J. Berberich, "YPEL3, a p53-regulated gene that induces cellular senescence.," *Cancer Res.*, vol. 70, no. 9, pp. 3566–75, May 2010.
- [41] J. Pärssinen, T. Kuukasjärvi, R. Karhu, and a Kallioniemi, "High-level amplification at 17q23 leads to coordinated overexpression of multiple adjacent genes in breast cancer.," *Br. J. Cancer*, vol. 96, no. 8, pp. 1258–64, Apr. 2007.
- [42] R. Lu and G. Serrero, "Mediation of estrogen mitogenic effect in human breast cancer MCF-7 cells by PC-cell-derived growth factor (PCDGF/granulin precursor).," *Proc. Natl. Acad. Sci. U. S. A.*, vol. 98, no. 1, pp. 142–147, 2001.
- [43] Z. Wang, B. C. Liu, G. T. Lin, C. S. Lin, T. F. Lue, E. Willingham, and L. S.

- Baskin, "Up-Regulation of Estrogen Responsive Genes in Hypospadias: Microarray Analysis," *J. Urol.*, vol. 177, no. 5, pp. 1939–1946, 2007.
- [44] M. D. Corte, F. Tamargo, A. Alvarez, J. C. Rodriguez, J. Vazquez, R. Sanchez, M. L. Lamelas, L. O. Gonzalez, M. T. Allende, J. L. Garcia-Muniz, A. Fueyo, and F. Vizoso, "Cytosolic levels of TFF1/pS2 in breast cancer: Their relationship with clinical-pathological parameters and their prognostic significance," *Breast Cancer Res. Treat.*, vol. 96, no. 1, pp. 63–72, 2006.
- [45] D. Liu, M. M. Matzuk, W. K. Sung, Q. Guo, P. Wang, and D. J. Wolgemuth, "Cyclin A1 is required for meiosis in the male mouse.," *Nat. Genet.*, vol. 20, no. 4, pp. 377–80, 1998.
- [46] C. Sweeney, M. Murphy, M. Kubelka, S. E. Ravnik, C. F. Hawkins, D. J. Wolgemuth, and M. Carrington, "A distinct cyclin A is expressed in germ cells in the mouse.," *Development*, vol. 122, pp. 53–64, 1996.
- [47] Y. F. Wong, T. H. Cheung, K. W. K. Lo, S. F. Yim, N. S. S. Siu, S. C. S. Chan, T. W. F. Ho, K. W. Y. Wong, M. Y. Yu, V. W. Wang, C. Li, G. J. Gardner, T. Bonome, W. B. Johnson, D. I. Smith, T. K. H. Chung, and M. J. Birrer, "Identification of molecular markers and signaling pathway in endometrial cancer in Hong Kong Chinese women by genome-wide gene expression profiling.," *Oncogene*, vol. 26, no. 13, pp. 1971–82, 2007.
- [48] J. Frasor, J. M. Danes, B. Komm, K. C. N. Chang, C. Richard Lyttle, and B. S. Katzenellenbogen, "Profiling of estrogen up- and down-regulated gene expression in human breast cancer cells: Insights into gene networks and pathways underlying estrogenic control of proliferation and cell phenotype," *Endocrinology*, vol. 144, no. 10, pp. 4562–4574, 2003.
- [49] W. J. Kent, C. W. Sugnet, T. S. Furey, K. M. Roskin, T. H. Pringle, A. M. Zahler, and A. D. Haussler, "The Human Genome Browser at UCSC," *Genome Res.*, vol. 12, no. 6, pp. 996–1006, 2002.
- [50] D. W. Huang, R. A. Lempicki, and B. T. Sherman, "Systematic and integrative analysis of large gene lists using DAVID bioinformatics resources.," *Nat. Protoc.*, vol. 4, no. 1, pp. 44–57, 2009.
- [51] J. G. Herman, J. R. Graff, S. Myohanen, B. D. Nelkin, and S. B. Baylin, "Methylation-specific PCR: a novel PCR assay for methylation status of CpG islands.," *Proc. Natl. Acad. Sci.*, vol. 93, no. 18, pp. 9821–9826, 1996.

APPENDIX A

DEXTRAN COATED CHARCOAL STRIPPED FETAL BOVINE SERUM

10 g dextran coated charcoal (Sigma Aldrich, Germany, C6241) was added into 500 ml fetal bovine serum (FBS, Biochrom AG, Germany, S0115) in its own bottle. An autoclaved magnetic fish was used for stirring of the FBS at a medium speed to ensure that the charcoal is not broken into fine particles and incubation was performed at +4°C for overnight. After the incubation, the mixed FBS with charcoal was divided as equally weighted into two sterile Nalgene bottles and centrifuged at 10800 g (8000 rpm for Sorvall SLA-3000 rotor) for 30 minutes at +4°C. Both of the supernatants were transferred into a 0.45 µM sterile filter unit (Sarstedt, Germany, 83.1823) and filtered. For the second round of the treatment, again 10 g dextran coated charcoal was added and stirred with a sterile magnetic fish for 4-6 hours at +4°C. After the incubation, the mixture was divided into two equally weighted sterile Nalgene bottles and centrifuged at 10800 g for 30 minutes at +4°C. The supernatants were transferred into a 0.45 µM sterile filter unit and filtered in the biological safety cabinet. Finally, charcoal dextran treated fetal bovine serum (CD-FBS) was aliquoted as 40 mL aliquotes into 50 mL sterile falcon tubes and stored at -20°C.

APPENDIX B

BUFFERS

6X Laemmli Buffer (10 mL)

Tris-base 3,75 mL (1M Tris, pH 6.8)

SDS 1.2 g

Glycerol 6 mL (100%)

Bromophenol Blue 1.2 mg

❖ β -mercaptoethanol is added freshly (Final concentration is 30%)

APPENDIX C

MIQE GUIDELINES

Table C 1. MIQE checklist.

ITEM TO CHECK	IMPORTANCE	CHECKLIST
EXPERIMENTAL DESIGN		
Definition of experimental and control groups	E	YES
Number within each group	E	YES
Assay carried out by core lab or investigator's lab?	D	YES
Acknowledgement of authors' contributions	D	N/A
SAMPLE		
Description	E	N/A
Volume/mass of sample processed	D	N/A
Microdissection or macrodissection	E	N/A
Processing procedure	E	N/A
If frozen - how and how quickly?	E	N/A
If fixed - with what, how quickly?	E	N/A
Sample storage conditions and duration (especially for FFPE samples)	E	N/A
NUCLEIC ACID EXTRACTION		
Procedure and/or instrumentation	E	YES
Name of kit and details of any modifications	E	YES
Source of additional reagents used	D	N/A
Details of DNase or RNase treatment	E	YES
Contamination assessment (DNA or RNA)	E	YES
Nucleic acid quantification	E	YES
Instrument and method	E	YES
Purity (A260/A280)	D	NO

Table C 1. (continued)

Yield	D	NO
REVERSE TRANSCRIPTION		
Complete reaction conditions	E	YES
Amount of RNA and reaction volume	E	YES
Priming oligonucleotide and concentration	E	YES
Reverse transcriptase and concentration	E	YES
Temperature and time	E	YES
Manufacturer of reagents and catalogue numbers	D	YES
Cqs with and without RT	D	NO
Storage conditions of cDNA	D	YES
qPCR TARGET INFORMATION		
If multiplex, efficiency and LOD of each assay.	E	N/A
Sequence accession number	E	YES
Location of amplicon	D	YES
Amplicon length	E	NO
<i>In silico</i> specificity screen (BLAST, etc)	E	NO
Pseudogenes, retropseudogenes or other homologs?	D	YES
Sequence alignment	D	YES
Secondary structure analysis of amplicon	D	NO
Location of each primer by exon or intron (if applicable)	E	YES
What splice variants are targeted?	E	YES
qPCR OLIGONUCLEOTIDES		
Primer sequences	E	YES
RTPrimerDB Identification Number	D	N/A
Probe sequences	D	N/A
Location and identity of any modifications	E	N/A
Manufacturer of oligonucleotides	D	NO
Purification method	D	NO
qPCR PROTOCOL		
Complete reaction conditions	E	YES
Reaction volume and amount of cDNA/DNA	E	YES
Primer, (probe), Mg ⁺⁺ and dNTP concentrations	E	N/A

Table C 1. (continued)

Polymerase identity and concentration	E	N/A
Buffer/kit identity and manufacturer	E	YES
Exact chemical constitution of the buffer	D	N/A
Additives (SYBR Green I, DMSO, etc.)	E	YES
Manufacturer of plates/tubes and catalog number	D	NO
Complete thermocycling parameters	E	YES
Reaction setup (manual/robotic)	D	YES
Manufacturer of qPCR instrument	E	YES
qPCR VALIDATION		
Evidence of optimization (from gradients)	D	NO
Specificity (gel, sequence, melt, or digest)	E	YES
For SYBR Green I, C _q of the NTC	E	YES
Standard curves with slope and y-intercept	E	YES
PCR efficiency calculated from slope	E	YES
Confidence interval for PCR efficiency or standard error	D	NO
r ² of standard curve	E	YES
Linear dynamic range	E	YES
C _q variation at lower limit	E	YES
Confidence intervals throughout range	D	N/A
Evidence for limit of detection	E	NO
If multiplex, efficiency and LOD of each assay.	E	N/A
DATA ANALYSIS		
qPCR analysis program (source, version)	E	YES
C _q method determination	E	YES
Outlier identification and disposition	E	N/A
Results of NTCs	E	YES
Justification of number and choice of reference genes	E	YES

E: essential information, D: desirable information, N/A: not applicable

APPENDIX D

PRIMERS

Table D 1. Primer list.

Primer Name	Sequence (5' to 3')
PUM1_FP	AGTGGGGGACTAGGCGTTAG
PUM1_REP	GTTTTTCATCACTGTCTGCATCC
TFF1/pS2_FP	TTGTGGTTTTTCCTGGTGTCA
TFF1/pS2_REP	CCGAGCTCTGGGACTAATCA
CCNA1_FP	GTGTATGAAGTAGACACCGG
CCNA1_REP	GTCACATTTATCACATCTGTGC
CTGF_FP	GGTTACCAATGACAACGCCTC
CTGF_REP	GATAGGCTTGGAGATTTTGGG
YPEL2_FP	CAGCATCTACCCAACCCAGTGTCC
YPEL2_REP	GATGGCGTCAGGGTGGGAGG
YPEL3_FP	GCATGCACTGTGACCTTGGG
YPEL3_REP	CTATAGGGCAGGTGGGGCAGG
GAPDH_FP	GGGAGCCAAAAGGGTCATCA
GAPDH_REP	TTTCTAGACGGCAGGTCAGGT

APPENDIX E

GENOMIC DNA CONTAMINATION CONTROL

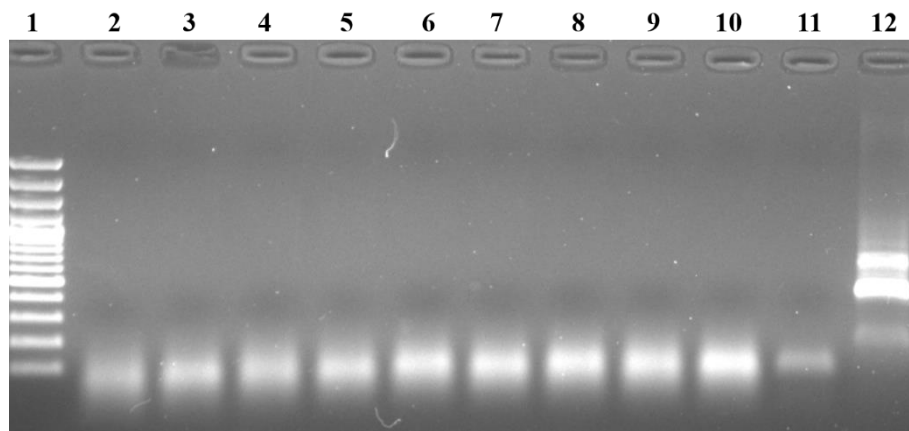
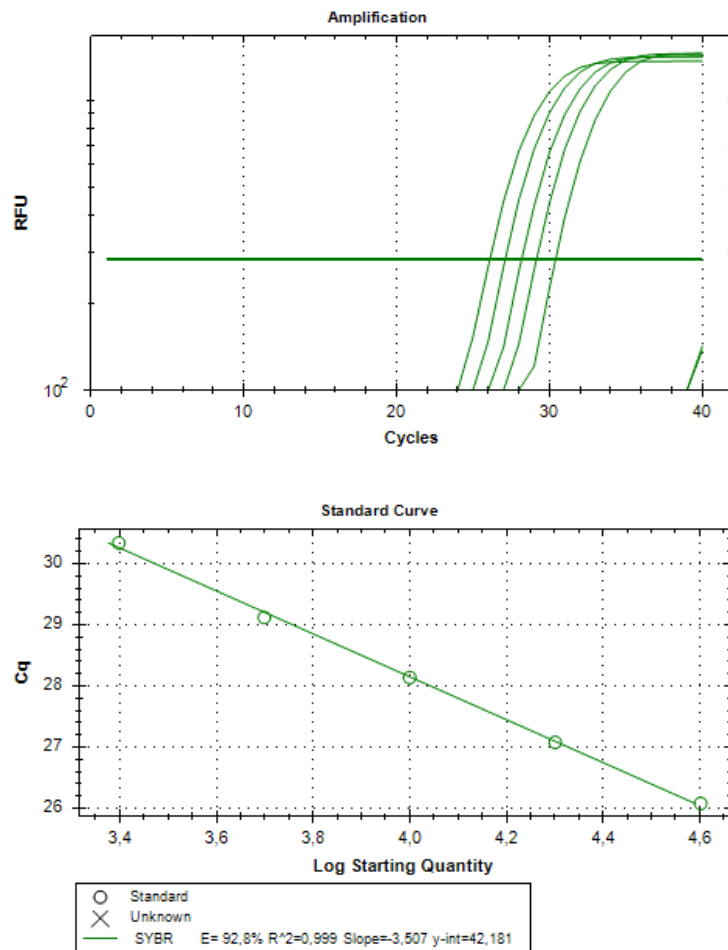


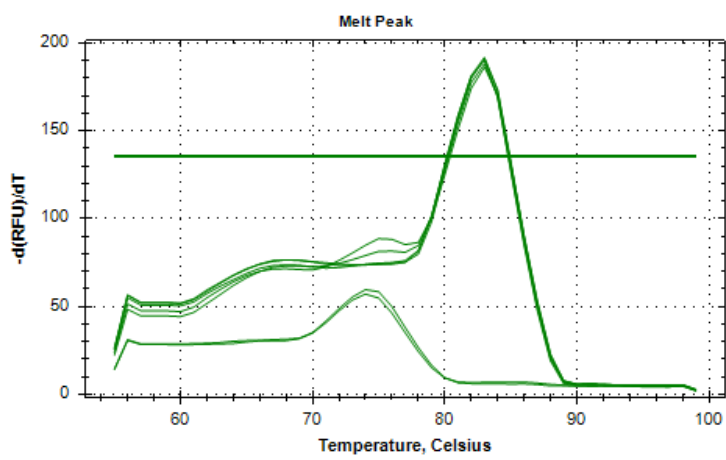
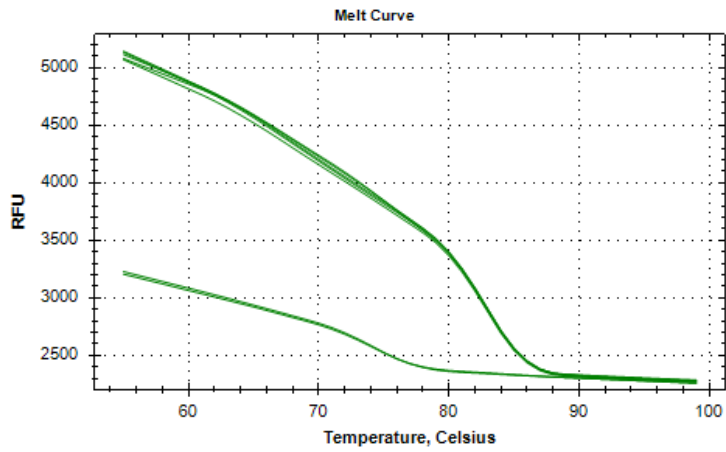
Figure E 2. Genomic DNA control PCR. 600 ng of total RNA isolates were subjected to PCR with glyceraldehyde 3-phosphate dehydrogenase (GAPDH) primers. Reaction conditions were as follows; initial denaturation at 95°C for three minutes, denaturation at 95°C for 30 seconds, annealing at 65°C for 30 seconds, extension at 72°C for 30 seconds. Denaturation, annealing and extension steps were repeated for 40 cycles with a final extension at 72°C for 10 minutes, infinite hold at 4°C. As positive control, 100 ng of genomic DNA was used in the same set of experimental PCR. Similar results were obtained for each RNA isolated. Lane 1: GeneRuler DNA Ladder Mix 100 bp-10000 bp, Thermo Scientific, USA). Lane 2: MDA-ER α 5, 6h OH treatment. Lane 3: MDA-ER α 5, 6h E2 treatment. Lane 4: MDA-ER α 11, 6h OH treatment. Lane 5: MDA-ER α 11, 6h E2 treatment. Lane 6: MDA-ER α 13, 6h OH treatment. Lane 7: MDA-ER α 13, 6h E2 treatment. Lane 8: MDA-EV2, 6h OH treatment. Lane 9: MDA-EV2, 6h E2 treatment. Lane 10: MCF7, 6h E2 treatment. Lane 11: No template control. Lane 12: 100 ng genomic DNA as template.

APPENDIX F

PERFORMANCE OF RT-qPCR REACTIONS

A representative example of the RT-qPCR reactions generated in this study. Results were shown as standard curve for *PUM1* expression in six-hour ethanol treated MCF7 cells. Similar results were obtained for *YPEL2*, *YPEL3*, *CTGF*, *TFF1/pS2*, and *CCNA1*.





Well	Fluor	Content	Sample	Cq	SQ
A01	SYBR	Std	1:5	26,08	40000,00000
B01	SYBR	Std	1:10	27,08	20000,00000
C01	SYBR	Std	1:20	28,14	10000,00000
D01	SYBR	Std	1:40	29,12	5000,00000
E01	SYBR	Std	1:80	30,34	2500,00000
C06	SYBR	NTC			
B12	SYBR	NTC			

APPENDIX G

KINETIC ANALYSIS OF CELL CYCLE HISTOGRAMS

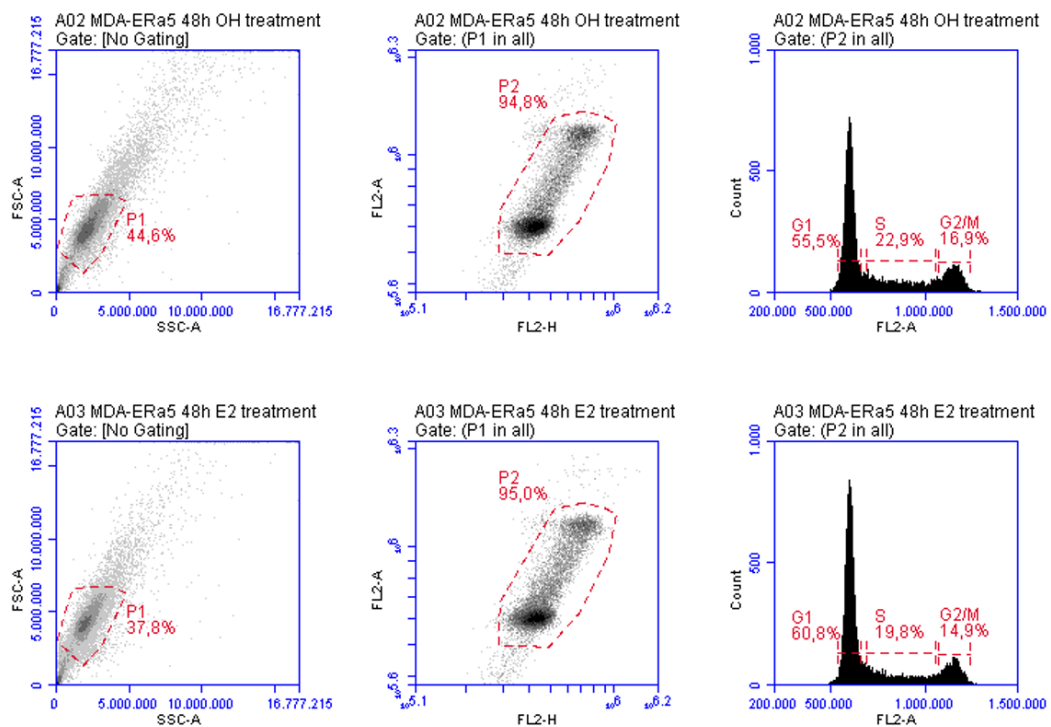


Figure G 1. Cell cycle kinetics of MDA-ER α 5 monoclonal. Cells were seeded onto six-well plates as 5×10^4 /well in CD-FBS/DMEM. 48 hours later, cells were treated with 10^{-9} M of E2 or ethanol (0.01%) as vehicle control. Cells were collected with trypsinization and washed once with PBS at room temperature 48 hours after treatment. Cells were gently re-suspended in 100 μ L of PBS and immediately fixed with ice-cold 70% ethanol diluted in distilled water. Samples were re-suspended with 200 μ L of staining buffer prepared in PBS containing propidium iodide (PI, Sigma Aldrich, Germany, P4710) with 0.02 mg/mL final concentration, RNase A (Thermo Scientific, USA, EN0531) with 200 μ g/mL final concentration, and Triton[®] X-100 (AppliChem, Germany, A4975) with 0.1% (v/v) final concentration. Cell cycle analysis was done with BD Accuri[™] C6 Cytometer (BD Biosciences). Assays were carried out as three independent experiments and similar results were obtained.

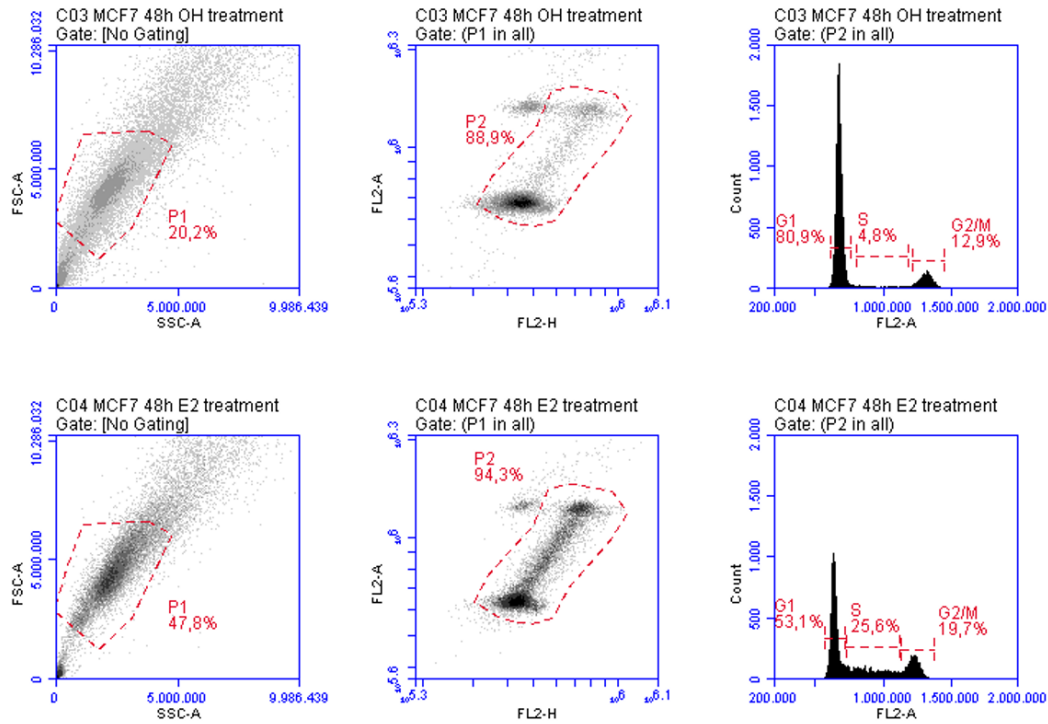


Figure G 2. Cell cycle kinetics of MCF7 cells. Cells were seeded onto six-well plates as 5×10^4 /well in CD-FBS/DMEM. 48 hours later, cells were treated with 10^{-9} M of E2 or ethanol (0.01%) as vehicle control. Cells were collected with trypsinization and washed once with PBS at room temperature 48 hours after treatment. Cells were gently re-suspended in 100 μ L of PBS and immediately fixed with ice-cold 70% ethanol diluted in distilled water. Samples were re-suspended with 200 μ L of staining buffer prepared in PBS containing propidium iodide (PI, Sigma Aldrich, Germany, P4710) with 0.02 mg/mL final concentration, RNase A (Thermo Scientific, USA, EN0531) with 200 μ g/mL final concentration, and Triton[®] X-100 (AppliChem, Germany, A4975) with 0.1% (v/v) final concentration. Cell cycle analysis was done with BD Accuri[™] C6 Cytometer (BD Biosciences). Assays were carried out as three independent experiments and similar results were obtained.

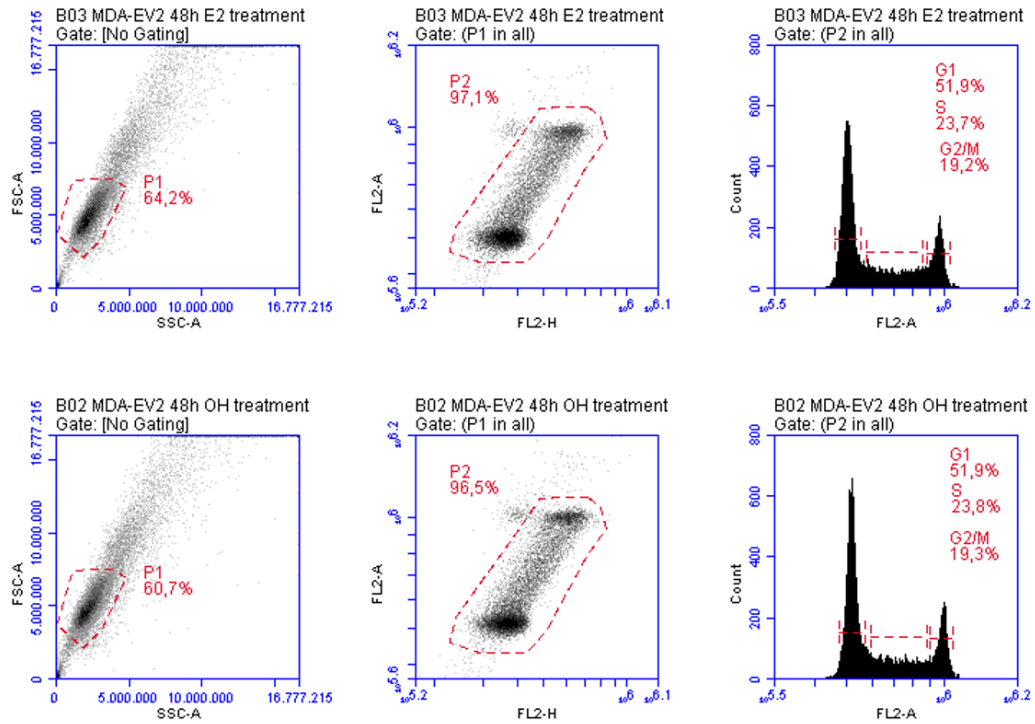


Figure G 3. Cell cycle kinetics of MDA-EV2 monoclonal. Cells were seeded onto six-well plates as 5×10^4 /well in CD-FBS/DMEM. 48 hours later, cells were treated with 10^{-9} M of E2 or ethanol (0.01%) as vehicle control. Cells were collected with trypsinization and washed once with PBS at room temperature 48 hours after treatment. Cells were gently re-suspended in 100 μ L of PBS and immediately fixed with ice-cold 70% ethanol diluted in distilled water. Samples were re-suspended with 200 μ L of staining buffer prepared in PBS containing propidium iodide (PI, Sigma Aldrich, Germany, P4710) with 0.02 mg/mL final concentration, RNase A (Thermo Scientific, USA, EN0531) with 200 μ g/mL final concentration, and Triton[®] X-100 (AppliChem, Germany, A4975) with 0.1% (v/v) final concentration. Cell cycle analysis was done with BD Accuri[™] C6 Cytometer (BD Biosciences). Assays were carried out as three independent experiments and similar results were obtained.

APPENDIX H

TOP 100 SIGNIFICANT GENOMIC REGIONS IN METYLOME ANALYSES

Table H 1. Top 100 hypermethylated genomic regions in MDA-ER α 5 cells after 6h E2 treatment.

CHROM.	START	END	STR.	PROMOTER	EXON	INTROIN	CpG ISLAND	p-VALUE	CLASSIFICATION
chr10	13537 9656	13537 9657	-	SYCE1		SYCE1	Y	1,58 E-07	stronglyHypermeth
chr11	17716 394	17716 395	+					5,09 E-07	stronglyHypermeth
chr1	15708 1740	15708 1741	-					6,4E- 07	stronglyHypermeth
chr2	19606 149	19606 150	+					1,05 E-06	stronglyHypermeth
chr9	71838 423	71838 424	+			TJP2		1,58 E-06	stronglyHypermeth
chr11	11918 7935	11918 7936	+	MCAM				1,61 E-06	stronglyHypermeth
chr1	17815 342	17815 343	-					3,13 E-06	stronglyHypermeth
chr5	17995 8765	17995 8766	+			CNOT6		3,83 E-06	stronglyHypermeth
chr8	14593 8455	14593 8456	-					4,33 E-06	stronglyHypermeth
chr1	80323 194	80323 195	-					4,34 E-06	stronglyHypermeth
chr4	18908 4674	18908 4675	+					4,34 E-06	stronglyHypermeth
chr20	48005 949	48005 950	+			KCNB1		5,23 E-06	stronglyHypermeth
chr14	58199 937	58199 938	-			SLC35F4		7,05 E-06	stronglyHypermeth
chr9	89626 710	89626 711	+			LOC440173	Y	7,94 E-06	stronglyHypermeth
chr21	42879 213	42879 214	-	TMPRS S2		TMPRS S2	Y	7,94 E-06	stronglyHypermeth

Table H 1. (continued)

CHOROM.	START	END	STR.	PROMOTER	EXON	INTRON	CpG ISLAND	P-VALUE	CLASSIFICATION
chr10	43846967	43846968	+					9,53E-06	stronglyHypemeth
chr3	46924060	46924061	-	PTH1R		PTH1R	Y	9,53E-06	stronglyHypemeth
chr5	98859823	98859824	+					1,27E-05	stronglyHypemeth
chr1	228225886	228225887	-			WNT3A		1,32E-05	stronglyHypemeth
chr7	26513287	26513288	+			LOC441204		1,45E-05	stronglyHypemeth
chr1	154540313	154540314	-	CHRN B2	CHRN B2		Y	1,45E-05	stronglyHypemeth
chr14	86736291	86736292	-					1,6E-05	stronglyHypemeth
chr13	89807423	89807424	-					1,61E-05	stronglyHypemeth
chr17	74242061	74242062	-					1,66E-05	stronglyHypemeth
chr10	44594329	44594330	-					1,91E-05	stronglyHypemeth
chr4	185949555	185949556	+					2,02E-05	stronglyHypemeth
chr5	149851663	149851664	+					2,02E-05	stronglyHypemeth
chr5	79607554	79607555	+					2,3E-05	stronglyHypemeth
chr20	19192839	19192840	+	SLC24A3			Y	2,58E-05	stronglyHypemeth
chr1	1007463	1007464	-		RNF223			2,58E-05	stronglyHypemeth
chr13	25592594	25592595	-				Y	2,58E-05	stronglyHypemeth
chr7	143066585	143066586	-					2,63E-05	stronglyHypemeth
chr4	8519775	8519776	-					2,88E-05	stronglyHypemeth
chr18	502076	502077	-					2,88E-05	stronglyHypemeth
chr20	44936622	44936623	+	CDH22		CDH22	Y	2,91E-05	stronglyHypemeth
chr9	19464207	19464208	+					3,09E-05	stronglyHypemeth
chr16	2571067	2571068	-	AMDHD2	AMDHD2		Y	3,33E-05	stronglyHypemeth
chr5	1246422	1246423	+				Y	3,33E-05	stronglyHypemeth
chr19	19649300	19649301	+	CILP2		CILP2	Y	3,39E-05	stronglyHypemeth

Table H 1. (continued)

CHOROM.	STAR T	END	ST R.	PROM OTER	EX ON	INTR ON	CpG ISLA ND	p- VAL UE	CLASSICIFI CATION
chr18	11934 724	11934 725	+					3,4E-05	stronglyHype rmeth
chr4	98947 1	98947 2	-			IDUA		4,11 E-05	stronglyHype rmeth
chr12	12634 6095	12634 6096	-				Y	4,11 E-05	stronglyHype rmeth
chr9	13521 8521	13521 8522	+			SETX		4,21 E-05	stronglyHype rmeth
chr19	49626 783	49626 784	-			PPFI A3		4,72 E-05	stronglyHype rmeth
chr1	35586 978	35586 979	+					4,72 E-05	stronglyHype rmeth
chr1	18502 33	18502 34	-	TMEM 52		TME M52	Y	4,72 E-05	stronglyHype rmeth
chr13	75149 973	75149 974	+					4,72 E-05	stronglyHype rmeth
chr10	62874 560	62874 561	+					5,14 E-05	stronglyHype rmeth
chr7	69063 535	69063 536	-	AUTS2			Y	5,36 E-05	stronglyHype rmeth
chr20	50354 818	50354 819	+			ATP9 A		5,39 E-05	stronglyHype rmeth
chr6	84419 465	84419 466	-	SNAP9 1				5,39 E-05	stronglyHype rmeth
chr14	10206 8801	10206 8802	-					5,39 E-05	stronglyHype rmeth
chr14	10206 8809	10206 8810	-					5,39 E-05	stronglyHype rmeth
chr2	12250 9962	12250 9963	+					5,39 E-05	stronglyHype rmeth
chr1	24152 0357	24152 0358	-	RGS7	RG S7		Y	5,66 E-05	stronglyHype rmeth
chr1	24152 0370	24152 0371	-	RGS7	RG S7		Y	5,66 E-05	stronglyHype rmeth
chr1	24152 0375	24152 0376	-	RGS7	RG S7		Y	5,66 E-05	stronglyHype rmeth
chr2	15969 3872	15969 3873	-					5,89 E-05	stronglyHype rmeth
chr9	96675 446	96675 447	+					6,11 E-05	stronglyHype rmeth
chr19	51830 633	51830 634	+			IGLO N5	Y	6,12 E-05	stronglyHype rmeth
chr5	95213 42	95213 43	-			SEM A5A		6,12 E-05	stronglyHype rmeth
chr19	11052 35	11052 36	-	GPX4	GP X4		Y	6,12 E-05	stronglyHype rmeth
chr9	99656 047	99656 048	+					6,12 E-05	stronglyHype rmeth

Table H 1. (continued)

CHOROM.	START	END	STR.	PROMOTER	EXON	INTRON	CpG ISLAND	p-VALUE	CLASSIFICATION
chr5	176046523	176046524	-				Y	6,12E-05	stronglyHypemeth
chr13	100553368	100553369	-					6,12E-05	stronglyHypemeth
chr14	41099053	41099054	-					6,73E-05	stronglyHypemeth
chr4	136908867	136908868	-					6,73E-05	stronglyHypermeth
chr16	29214997	29214998	-					6,73E-05	stronglyHypemeth
chr2	234664368	234664369	-	LOC100286922		UGT1A10, UGT1A8, UGT1A9, UGT1A4, UGT1A5, UGT1A6, UGT1A7, UGT1A3		6,73E-05	stronglyHypemeth
chr8	61034667	61034668	+					6,73E-05	stronglyHypemeth
chr19	30397680	30397681	+					7,14E-05	stronglyHypemeth
chr15	22683218	22683219	-					8,08E-05	stronglyHypemeth
chr7	156813955	156813956	-				Y	8,65E-05	stronglyHypemeth
chr2	901335	901336	+					9,18E-05	stronglyHypemeth
chr14	52780823	52780824	+	PTGER2			Y	9,38E-05	stronglyHypemeth
chr22	23793856	23793857	+					0,000104	stronglyHypemeth
chr12	22487824	22487825	-	ST8SIA1			Y	0,000104	stronglyHypemeth
chr11	44633075	44633076	-			CD82		0,000107	stronglyHypemeth

Table H 1. (continued)

CHOROM.	START	END	STR.	PROMOTER	EXON	INTRON	CpG ISLAND	p-VALUE	CLASSIFICATION
chr2	24220 3701	24220 3702	-			HDL BP		0,000 108	stronglyHyper meth
chr17	18467 44	18467 45	+			RTN4 RL1		0,000 119	stronglyHyper meth
chrX	48599 058	48599 059	+					0,000 125	stronglyHyper meth
chr19	58858 891	58858 892	+		A1 BG		Y	0,000 125	stronglyHyper meth
chr10	74528 33	74528 34	+	SFMB T2		SFM BT2	Y	0,000 125	stronglyHyper meth
chr10	74528 44	74528 45	+	SFMB T2		SFM BT2	Y	0,000 125	stronglyHyper meth
chr10	13198 8689	13198 8690	+				Y	0,000 125	stronglyHyper meth
chr17	16815 008	16815 009	+					0,000 125	stronglyHyper meth
chr17	25289 836	25289 837	-				Y	0,000 125	stronglyHyper meth
chr11	66165 538	66165 539	+					0,000 125	stronglyHyper meth
chr18	51109 766	51109 767	-					0,000 125	stronglyHyper meth
chr12	53317 957	53317 958	+			KRT8		0,000 125	stronglyHyper meth
chr14	10558 0297	10558 0298	-					0,000 125	stronglyHyper meth
chr13	92943 416	92943 417	+			GPC5		0,000 125	stronglyHyper meth
chr2	13783 4245	13783 4246	-			THS D7B		0,000 125	stronglyHyper meth
chr2	14061 9846	14061 9847	-					0,000 125	stronglyHyper meth
chr1	12113 7848	12113 7849	+				Y	0,000 126	stronglyHyper meth
chr1	24152 0381	24152 0382	-	RGS7	RG S7		Y	0,000 126	stronglyHyper meth
chr1	24152 0385	24152 0386	-	RGS7	RG S7		Y	0,000 126	stronglyHyper meth
chr20	21486 846	21486 847	-				Y	0,000 131	stronglyHyper meth
chr1	17199 402	17199 403	+				Y	0,000 141	stronglyHyper meth
chrX	10226 5019	10226 5020	-					0,000 141	stronglyHyper meth

Table H 2. Top 100 hypomethylated genomic regions in MDA-ER α 5 cells after 6h E2 treatment.

CHROM.	START	END	STR.	PROMOTER	EXON	INTRON	CpG ISLAND	p-VALUE	CLASSIFICATION
chr17	1627424	1627425	-	WDR81		WDR81		1,75E-09	stronglyHypometh
chr6	3940293	3940294	+					7,79E-08	stronglyHypometh
chr14	61655191	61655192	+					1,27E-07	stronglyHypometh
chr4	57703350	57703351	+					5,35E-07	stronglyHypometh
chr16	89081343	89081344	+					5,59E-07	stronglyHypometh
chr10	86499074	86499075	-					6,8E-07	stronglyHypometh
chr11	38300150	38300151	+					8,42E-07	stronglyHypometh
chr20	656137	656138	-	SCRT2	SCRT2		Y	1,02E-06	stronglyHypometh
chr8	144790758	144790759	+	CCDC166			Y	1,26E-06	stronglyHypometh
chr15	22095160	22095161	-				Y	1,45E-06	stronglyHypometh
chrX	103550540	103550541	-					1,55E-06	stronglyHypometh
chr10	122791246	122791247	-			MIR5694		2,04E-06	stronglyHypometh
chr12	127764587	127764588	+					2,07E-06	stronglyHypometh
chr12	132102658	132102659	+					6,44E-06	stronglyHypometh
chr3	124447321	124447322	+					7,69E-06	stronglyHypometh
chr3	128719584	128719585	+	EFCC1				7,94E-06	stronglyHypometh
chr1	205882081	205882082	-					9,62E-06	stronglyHypometh
chr3	59560500	59560501	+					1,22E-05	stronglyHypometh
chr1	236767602	236767603	+	HEATR1		HEATR1	Y	1,29E-05	stronglyHypometh
chr20	56558235	56558236	+					1,32E-05	stronglyHypometh
chr10	123357577	123357578	+	FGFR2	FGFR2		Y	1,34E-05	stronglyHypometh
chr22	43818167	43818168	+			MPPED1		1,34E-05	stronglyHypometh
chr1	7467117	7467118	+			CAMTA1		1,34E-05	stronglyHypometh
chr15	51483692	51483693	+					1,34E-05	stronglyHypometh

Table H 2. (continued)

CHOROM.	START	END	STR.	PROMOTER	EXON	INTRON	CpG ISLAND	P-VALUE	CLASSIFICATION
chr1	32023626	32023627	+					1,45E-05	stronglyHypometh
chr3	21983240	21983241	-					1,45E-05	stronglyHypometh
chr15	28202799	28202800	+		OCA2			1,48E-05	stronglyHypometh
chr9	130623706	130623707	+					1,55E-05	stronglyHypometh
chr17	8219410	8219411	+		ARHGEF15			1,61E-05	stronglyHypometh
chr16	879689	879690	+					1,84E-05	stronglyHypometh
chr15	98182142	98182143	+					1,84E-05	stronglyHypometh
chr15	27216305	27216306	-	GABRG3			Y	1,91E-05	stronglyHypometh
chr6	157923941	157923942	+			ZDHHC14		2,01E-05	stronglyHypometh
chr4	189278506	189278507	-					2,21E-05	stronglyHypometh
chr10	22337364	22337365	+					2,21E-05	stronglyHypometh
chr5	32711385	32711386	-	NPR3		NPR3	Y	2,21E-05	stronglyHypometh
chr8	20160814	20160815	+				Y	2,29E-05	stronglyHypometh
chr13	26733585	26733586	+					2,29E-05	stronglyHypometh
chr9	88612954	88612955	-			NAA35		2,29E-05	stronglyHypometh
chr18	76282702	76282703	-					2,58E-05	stronglyHypometh
chr5	38196303	38196304	-					2,84E-05	stronglyHypometh
chr16	85160596	85160597	-					2,88E-05	stronglyHypometh
chr17	6617210	6617211	+	SLC13A5			Y	2,88E-05	stronglyHypometh
chr2	53483462	53483463	-					2,88E-05	stronglyHypometh
chr17	74136266	74136267	+	RNF157-AS1	FOXJ1		Y	2,97E-05	stronglyHypometh
chr14	61655205	61655206	+					3,09E-05	stronglyHypometh
chr10	102505545	102505546	+	PAX2	PAX2		Y	3,33E-05	stronglyHypometh
chr7	38670779	38670780	+	AMPH		AMPH	Y	3,33E-05	stronglyHypometh

Table H 2. (continued)

CHOROM.	STAR T	END	ST R.	PROM OTER	EXO N	INTR ON	CpG ISL AND	p- VAL UE	CLASSIFICI CATION
chr1	15716 4748	15716 4749	-				Y	3,66 E-05	stronglyHypo meth
chr5	15449 4493	15449 4494	-					3,98 E-05	stronglyHypo meth
chr21	44201 548	44201 549	-					4,05 E-05	stronglyHypo meth
chr11	14689 89	14689 90	+			BRSK 2		4,11 E-05	stronglyHypo meth
chr8	11601 8565	11601 8566	+					4,16 E-05	stronglyHypo meth
chr19	54393 960	54393 961	-			PRKC G		4,72 E-05	stronglyHypo meth
chr4	11170 4819	11170 4820	+					5,39 E-05	stronglyHypo meth
chr16	85482 530	85482 531	-					5,39 E-05	stronglyHypo meth
chr1	40724 594	40724 595	+	ZMPST E24		ZMPS TE24		5,66 E-05	stronglyHypo meth
chr9	33811 366	33811 367	-					6,12 E-05	stronglyHypo meth
chr17	78067 602	78067 603	-			CCDC 40		6,12 E-05	stronglyHypo meth
chr2	21331 1911	21331 1912	-			ERBB 4		6,12 E-05	stronglyHypo meth
chr22	19584 403	19584 404	-					6,73 E-05	stronglyHypo meth
chr5	12795 6975	12795 6976	+					6,73 E-05	stronglyHypo meth
chr2	22103 8012	22103 8013	-					6,73 E-05	stronglyHypo meth
chrX	11378 4704	11378 4705	+					6,73 E-05	stronglyHypo meth
chr4	56964 997	56964 998	-					7,43 E-05	stronglyHypo meth
chr2	80136 811	80136 812	-		CTN NA2			8,08 E-05	stronglyHypo meth
chr7	14565 7507	14565 7508	+					8,46 E-05	stronglyHypo meth
chr10	10640 1369	10640 1370	+	SORCS 3	SOR CS3		Y	0,000 086	stronglyHypo meth
chr1	63637 054	63637 055	+			LINC0 0466		8,74 E-05	stronglyHypo meth
chr12	13231 4863	13231 4864	+			MMP1 7	Y	9,38 E-05	stronglyHypo meth
chr6	89827 653	89827 654	-	SRSF1 2	SRSF 12		Y	9,46 E-05	stronglyHypo meth
chr8	55371 910	55371 911	-		SOX 17		Y	0,000 104	stronglyHypo meth

Table H 2. (continued)

CHOROM.	START	END	STR.	PROMOTER	EXON	INTRON	CpG ISLAND	p-VALUE	CLASSIFICATION
chr8	55371 920	55371 921	-		SOX17		Y	0,00 0104	stronglyHypometh
chr10	64134 160	64134 161	-	ZNF365	ZNF365		Y	0,00 0104	stronglyHypometh
chr17	74273 308	74273 309	-		QRICH2			0,00 0104	stronglyHypometh
chr1	36331 233	36331 234	+					0,00 0104	stronglyHypometh
chr9	12017 5861	12017 5862	-			ASTN2	Y	0,00 0104	stronglyHypometh
chr9	12017 5887	12017 5888	-			ASTN2	Y	0,00 0104	stronglyHypometh
chr12	91160 249	91160 250	+					0,00 0106	stronglyHypometh
chr12	12042 6291	12042 6292	+					0,00 0108	stronglyHypometh
chr19	47916 481	47916 482	+			MEIS3		0,00 0112	stronglyHypometh
chr2	24214 3870	24214 3871	+			ANO7		0,00 0119	stronglyHypometh
chr3	10781 0395	10781 0396	-	CD47			Y	0,00 0122	stronglyHypometh
chr6	45983 248	45983 249	+	CLIC5	CLIC5	CLIC5	Y	0,00 0122	stronglyHypometh
chr1	95918 346	95918 347	+					0,00 0123	stronglyHypometh
chr9	13948 4811	13948 4812	-					0,00 0123	stronglyHypometh
chr20	26189 163	26189 164	-	LOC284801, MIR663A		LOC284801	Y	0,00 0125	stronglyHypometh
chr20	26189 181	26189 182	-	LOC284801, MIR663A		LOC284801	Y	0,00 0125	stronglyHypometh
chr5	13740 6520	13740 6521	-					0,00 0125	stronglyHypometh
chr5	17435 0083	17435 0084	-			FLJ16171		0,00 0125	stronglyHypometh
chr16	19463 804	19463 805	-			TMC5		0,00 0125	stronglyHypometh
chr19	39910 282	39910 283	+			PLEKHG2		0,00 0125	stronglyHypometh
chr14	84778 830	84778 831	-					0,00 0125	stronglyHypometh
chr6	15500 0958	15500 0959	+					0,00 0125	stronglyHypometh
chr22	39621 192	39621 193	-		PDGFB			0,00 0125	stronglyHypometh

Table H 2. (continued)

CHOROM.	START	END	STR.	PROMOTER	EXON	INTRON	CpG ISLAND	p-VALUE	CLASSIFICATION
chr3	16047 4371	16047 4372	+	PPM1L	PPM1L		Y	0,000 125	stronglyHypometh
chr1	32007 15	32007 16	-			PRDM16		0,000 125	stronglyHypometh
chr4	30422 626	30422 627	-					0,000 125	stronglyHypometh
chr14	44426 571	44426 572	+					0,000 131	stronglyHypometh
chr6	11228 3912	11228 3913	-					0,000 131	stronglyHypometh

Table H 3. Top 100 hypermethylated genomic regions in MCF7 cells after 6h E2 treatment.

CHROM.	START	END	STR.	PROMOTER	EXON	INTRON	CpG ISLAND	p-VALUE	CLASSIFICATION
chr7	50850611	50850612	+			GRB10	Y	7,27E-08	stronglyHypermeth
chr7	50850613	50850614	+			GRB10	Y	7,27E-08	stronglyHypermeth
chr11	8062056	8062057	+			TUB		1,58E-07	stronglyHypermeth
chr6	91005661	91005662	-	BACH2		BACH2	Y	4,03E-07	stronglyHypermeth
chr7	5811629	5811630	+			RNF216		5,1E-07	stronglyHypermeth
chr15	32179976	32179977	+					5,67E-07	stronglyHypermeth
chr10	135202521	135202522	+		PAOX			1,29E-06	stronglyHypermeth
chr11	20178718	20178719	+		DBX1		Y	1,55E-06	stronglyHypermeth
chr10	93393050	93393051	-	PPP1R3C			Y	1,58E-06	stronglyHypermeth
chr8	104153099	104153100	-	C8orf56, BAALC	BALC	C8orf56	Y	1,96E-06	stronglyHypermeth
chr10	93393030	93393031	-	PPP1R3C			Y	2,12E-06	stronglyHypermeth
chr14	52594728	52594729	+					2,63E-06	stronglyHypermeth
chr20	22549123	22549124	+			LINC00261	Y	4,33E-06	stronglyHypermeth
chr1	58524280	58524281	-			DAB1		5,98E-06	stronglyHypermeth
chr11	128419247	128419248	-			ETS1	Y	7,94E-06	stronglyHypermeth
chr1	247536436	247536437	+					8,6E-06	stronglyHypermeth
chr1	187041693	187041694	-					1,03E-05	stronglyHypermeth
chr6	76031326	76031327	-			FILIP1		1,05E-05	stronglyHypermeth
chr1	25258485	25258486	-			RUNX3	Y	1,08E-05	stronglyHypermeth
chr15	91469285	91469286	-					1,09E-05	stronglyHypermeth
chr10	93393048	93393049	-	PPP1R3C			Y	1,26E-05	stronglyHypermeth
chr4	120113618	120113619	-					1,43E-05	stronglyHypermeth
chr22	41962709	41962710	-			CSDC2		1,45E-05	stronglyHypermeth
chr2	142644823	142644824	+			LRP1B		1,45E-05	stronglyHypermeth

Table H 3. (continued)

CHOROM.	START	END	STR.	PROMOTER	EXON	INTRO	CpG ISLAND	p-VALUE	CLASSIFICATION
chr6	1391 1733 7	1391 1733 8	+	ECT2L		ECT2L	Y	1,55 E-05	stronglyHyp ermeth
chr6	9100 5663	9100 5664	-	BACH2		BACH2	Y	1,61 E-05	stronglyHyp ermeth
chr22	4866 1756	4866 1757	+					1,61 E-05	stronglyHyp ermeth
chr19	5426 4807	5426 4808	-	MIR519A2, MIR516A2				1,66 E-05	stronglyHyp ermeth
chr13	1144 8246 3	1144 8246 4	-			TMEM2 55B		1,88 E-05	stronglyHyp ermeth
chr3	7941 4812	7941 4813	+			ROBO1		2,02 E-05	stronglyHyp ermeth
chr8	1354 7629 1	1354 7629 2	+				Y	2,29 E-05	stronglyHyp ermeth
chr1	1504 9953	1504 9954	-			KAZN		2,29 E-05	stronglyHyp ermeth
chr9	1411 1136 9	1411 1137 0	+			FAM15 7B	Y	2,29 E-05	stronglyHyp ermeth
chr19	1232 7087	1232 7088	-					2,29 E-05	stronglyHyp ermeth
chr19	5448 3028	5448 3029	+			CACNG 8	Y	2,29 E-05	stronglyHyp ermeth
chr19	5448 3031	5448 3032	+			CACNG 8	Y	2,29 E-05	stronglyHyp ermeth
chr19	5448 3033	5448 3034	+			CACNG 8	Y	2,29 E-05	stronglyHyp ermeth
chr3	1263 8191 6	1263 8191 7	+	NUP210P1		NUP210 P1		2,58 E-05	stronglyHyp ermeth
chr3	5847 0884	5847 0885	+					2,83 E-05	stronglyHyp ermeth
chr1	2358 805	2358 806	-					2,92 E-05	stronglyHyp ermeth
chr2	1219 9857 8	1219 9857 9	-			TFCP2L 1		3,09 E-05	stronglyHyp ermeth
chr4	4642 166	4642 167	+			LOC100 507266		3,14 E-05	stronglyHyp ermeth
chr16	4165 511	4165 512	+	ADCY9		ADCY9	Y	3,15 E-05	stronglyHyp ermeth
chrX	6240 5618	6240 5619	-					3,66 E-05	stronglyHyp ermeth
chr17	2733 1649	2733 1650	-			SEZ6		3,72 E-05	stronglyHyp ermeth

Table H 3. (continued)

CHOROM.	START	END	STR.	PROMOTER	EXON	INTRON	CpG ISLAND	p-VALUE	CLASSIFICATION
chr2	16681 3565	16681 3566	+					3,8E-05	stronglyHypemeth
chr1	22584 321	22584 322	+					4,05E-05	stronglyHypemeth
chr7	15734 8255	15734 8256	-			PTPRN2		4,05E-05	stronglyHypemeth
chr1	15298 32	15298 33	+					4,05E-05	stronglyHypemeth
chr1	15082 8731	15082 8732	-			ARNT		4,11E-05	stronglyHypemeth
chr20	23138 369	23138 370	-					4,22E-05	stronglyHypemeth
chr2	23817 179	23817 180	+			KLHL29		4,52E-05	stronglyHypemeth
chr5	15732 9667	15732 9668	+					4,74E-05	stronglyHypemeth
chr7	29500 37	29500 38	-			CARD11		4,88E-05	stronglyHypemeth
chr11	12523 4622	12523 4623	-			PKNOX2		4,88E-05	stronglyHypemeth
chr4	83052 38	83052 39	+			HTRA3		4,97E-05	stronglyHypemeth
chr2	39855 695	39855 696	-					5E-05	stronglyHypemeth
chr2	14854 1369	14854 1370	-					5,14E-05	stronglyHypemeth
chr3	97637 97	97637 98	-			CPNE9		5,33E-05	stronglyHypemeth
chr4	14487 1174	14487 1175	-					5,38E-05	stronglyHypemeth
chr8	43132 217	43132 218	-				Y	5,39E-05	stronglyHypemeth
chr1	24514 034	24514 035	+	IFNLR1			Y	5,39E-05	stronglyHypemeth
chr1	24514 040	24514 041	+	IFNLR1			Y	5,39E-05	stronglyHypemeth
chr2	11959 9165	11959 9166	-				Y	5,39E-05	stronglyHypemeth
chr22	47184 022	47184 023	+			TBC1D22A		5,39E-05	stronglyHypemeth
chr7	98246 861	98246 862	+	NPTX2	NPTX2		Y	5,39E-05	stronglyHypemeth
chr4	70529 786	70529 787	-					6,11E-05	stronglyHypemeth
chr13	19768 595	19768 596	+					6,12E-05	stronglyHypemeth
chr5	84363 2	84363 3	+			ZDHC11	Y	6,62E-05	stronglyHypemeth

Table H 3. (continued)

CHOROM.	START	END	STR.	PROMOTER	EXON	INTRON	CpG ISLAND	P-VALUE	CLASSIFICATION
chr1	155912577	155912578	+		RXFP4			6,62E-05	stronglyHypermeth
chr2	177060386	177060387	-					6,62E-05	stronglyHypermeth
chr13	19768590	19768591	+					6,73E-05	stronglyHypermeth
chr19	30942019	30942020	-			ZNF536	Y	6,73E-05	stronglyHypermeth
chrX	48300396	48300397	-					6,73E-05	stronglyHypermeth
chr6	15222779	15222780	-					6,73E-05	stronglyHypermeth
chr2	99358949	99358950	-					6,88E-05	stronglyHypermeth
chr10	129861324	129861325	+			PTPRE		7,15E-05	stronglyHypermeth
chr16	86531849	86531850	-			FENDRR	Y	8,46E-05	stronglyHypermeth
chr19	57616167	57616168	+					8,6E-05	stronglyHypermeth
chr6	139353352	139353353	-			ABRACL		8,7E-05	stronglyHypermeth
chr8	65087536	65087537	+					8,74E-05	stronglyHypermeth
chr20	4035658	4035659	+					0,000104	stronglyHypermeth
chr1	2063874	2063875	+			PRKCZ	Y	0,000104	stronglyHypermeth
chr17	28259420	28259421	-			EFCAB5		0,000125	stronglyHypermeth
chr2	27365400	27365401	+					0,000125	stronglyHypermeth
chr13	112870346	112870347	+					0,000125	stronglyHypermeth
chr9	89101443	89101444	+					0,000125	stronglyHypermeth
chr18	29132288	29132289	-			LOC100652770		0,000125	stronglyHypermeth
chr19	45327486	45327487	+					0,000125	stronglyHypermeth
chr20	37058856	37058857	-	SNORA71C		LOC388796		0,000135	stronglyHypermeth
chr4	88607614	88607615	+					0,000141	stronglyHypermeth
chr7	2563670	2563671	-			LFNG	Y	0,000141	stronglyHypermeth
chr13	112723476	112723477	+		SOX1		Y	0,000141	stronglyHypermeth

Table H 3. (continued)

CHOROM.	START	END	STR.	PROMOTER	EXON	INTRON	CpG ISLAND	p-VALUE	CLASSIFICATION
chr21	43186 311	43186 312	+	RIPK4		RIPK4	Y	0,000 141	stronglyHyper meth
chr17	13130 69	13130 70	+					0,000 141	stronglyHyper meth
chr1	25401 235	25401 236	-					0,000 141	stronglyHyper meth
chr1	35395 483	35395 484	-				Y	0,000 141	stronglyHyper meth
chr1	55862 36	55862 37	-					0,000 153	stronglyHyper meth
chr7	28015 856	28015 857	+			JAZF1		0,000 153	stronglyHyper meth
chr16	20057 38	20057 39	-					0,000 153	stronglyHyper meth

Table H 4. Top 100 hypomethylated genomic regions in MCF7 cells after 6h E2 treatment.

CHROM.	START	END	STR.	PROMOTER	EXON	INTRON	CpG ISLAND	p-VALUE	CLASSIFICATION
chr12	75699 427	75699 428	-			CAPS2	Y	1,47 E-07	stronglyHypo meth
chr11	62101 116	62101 117	+					2,6E- 07	stronglyHypo meth
chr17	46462 37	46462 38	-			ZMYN D15		5,33 E-07	stronglyHypo meth
chr4	65506 399	65506 400	+					1,55 E-06	stronglyHypo meth
chr2	11961 5116	11961 5117	-				Y	1,55 E-06	stronglyHypo meth
chr14	68365 884	68365 885	-			RAD5 1B		3,24 E-06	stronglyHypo meth
chr18	40209 730	40209 731	-			LOC28 4260		5,03 E-06	stronglyHypo meth
chr5	21972 84	21972 85	+					5,03 E-06	stronglyHypo meth
chr6	34072 797	34072 798	+	GRM4		GRM4		6,45 E-06	stronglyHypo meth
chr7	83135 158	83135 159	-			SEMA 3E		7,03 E-06	stronglyHypo meth
chr7	26667 576	26667 577	+					7,05 E-06	stronglyHypo meth
chr11	11848 1646	11848 1647	-			PHLD B1	Y	7,42 E-06	stronglyHypo meth
chr4	10058 2618	10058 2619	-					7,43 E-06	stronglyHypo meth
chr10	72043 489	72043 490	+	NPFFR 1			Y	7,43 E-06	stronglyHypo meth
chr11	18940 13	18940 14	-			LSP1		8,05 E-06	stronglyHypo meth
chr8	93295 73	93295 74	-					1,07 E-05	stronglyHypo meth
chr12	56451 055	56451 056	+					1,14 E-05	stronglyHypo meth
chr18	29527 179	29527 180	-					1,17 E-05	stronglyHypo meth
chr6	82822 80	82822 81	+					1,17 E-05	stronglyHypo meth
chr10	72390 434	72390 435	+					1,24 E-05	stronglyHypo meth
chr19	38991 537	38991 538	+		RY R1			1,32 E-05	stronglyHypo meth
chr6	13028 9969	13028 9970	-					1,45 E-05	stronglyHypo meth
chr7	20984 563	20984 564	+					1,55 E-05	stronglyHypo meth
chr2	11960 4292	11960 4293	+		EN 1		Y	1,61 E-05	stronglyHypo meth

Table H 4. (continued)

CHOROM.	START	END	STR.	PROMOTER	EXON	INTRON	CpG ISLAND	p-VALUE	CLASSIFICATION
chr20	33246605	33246606	-			PIGU		1,77E-05	stronglyHypometh
chr1	97406295	97406296	-					2,03E-05	stronglyHypometh
chr11	4339082	4339083	+					2,03E-05	stronglyHypometh
chr5	122116452	122116453	+			SNX2		2,08E-05	stronglyHypometh
chr2	182545532	182545533	+	NEUROD1				2,22E-05	stronglyHypometh
chr13	112711313	112711314	+				Y	2,29E-05	stronglyHypometh
chr14	68195945	68195946	-		RDH12			2,29E-05	stronglyHypometh
chr5	72528289	72528290	-					2,58E-05	stronglyHypometh
chr22	37049318	37049319	+			CACNG2		2,58E-05	stronglyHypometh
chr15	32909796	32909797	+			ARHGAP11A		2,69E-05	stronglyHypometh
chr1	224200918	224200919	-					2,88E-05	stronglyHypometh
chr3	44598728	44598729	-		ZKSCAN7			2,97E-05	stronglyHypometh
chr22	49066482	49066483	-			FAM19A5		3,33E-05	stronglyHypometh
chr20	34004938	34004939	+					3,66E-05	stronglyHypometh
chr5	118539642	118539643	-			DMXL1		4,42E-05	stronglyHypometh
chr12	133192294	133192295	+					5,13E-05	stronglyHypometh
chr17	3680506	3680507	-			ITGAE		5,14E-05	stronglyHypometh
chr4	100398214	100398215	-					5,14E-05	stronglyHypometh
chr1	176685872	176685873	-			PAPPA2		5,31E-05	stronglyHypometh
chr9	16218356	16218357	+			C9orf92		5,34E-05	stronglyHypometh
chr1	2716928	2716929	-				Y	5,39E-05	stronglyHypometh
chr8	21906340	21906341	-					5,39E-05	stronglyHypometh
chr16	8873372	8873373	-		ABAT			5,39E-05	stronglyHypometh
chr7	144782789	144782790	-					5,94E-05	stronglyHypometh

Table H 4. (continued)

CHOROM.	START	END	STR.	PROMOTER	EXON	INTRON	CpG ISLAND	p-VALUE	CLASSIFICATION
chr9	10147 1920	10147 1921	+	GABBR2			Y	6,62 E-05	stronglyHypo meth
chr6	16990 2153	16990 2154	+			WDR27		6,62 E-05	stronglyHypo meth
chr4	13795 5608	13795 5609	+					6,73 E-05	stronglyHypo meth
chr4	12898 8164	12898 8165	-			LARP1B		6,73 E-05	stronglyHypo meth
chr5	12643 5375	12643 5376	-					6,73 E-05	stronglyHypo meth
chr8	12627 2469	12627 2470	-			NSMCE2		6,88 E-05	stronglyHypo meth
chr19	45737 233	45737 234	+	EXOC3L2		EXOC3L2		7,43 E-05	stronglyHypo meth
chr1	62846 019	62846 020	+					7,43 E-05	stronglyHypo meth
chr1	18958 189	18958 190	+	PAX7		PAX7	Y	7,43 E-05	stronglyHypo meth
chr17	30590 613	30590 614	+					7,43 E-05	stronglyHypo meth
chr5	15939 9438	15939 9439	+		ADRA1B		Y	7,43 E-05	stronglyHypo meth
chr3	89387 897	89387 898	+			EPHA3		8,08 E-05	stronglyHypo meth
chr12	11420 4434	11420 4435	+					8,08 E-05	stronglyHypo meth
chr6	88717 072	88717 073	+					8,74 E-05	stronglyHypo meth
chr1	22970 4106	22970 4107	-					0,000 103	stronglyHypo meth
chr15	29116 104	29116 105	+					0,000 107	stronglyHypo meth
chr9	10049 1942	10049 1943	-					0,000 115	stronglyHypo meth
chr7	65864 278	65864 279	-			LINC00174		0,000 116	stronglyHypo meth
chr7	10094 0790	10094 0791	-					0,000 119	stronglyHypo meth
chr12	13183 5367	13183 5368	-					0,000 119	stronglyHypo meth
chr22	29706 559	29706 560	+			GAS2L1	Y	0,000 119	stronglyHypo meth
chr9	84194 8	84194 9	-	DMRT1	DMRT1		Y	0,000 122	stronglyHypo meth
chr3	14095 0060	14095 0061	+	ACPL2			Y	0,000 122	stronglyHypo meth
chr2	19634 3561	19634 3562	+					0,000 125	stronglyHypo meth

Table H 4. (continued)

CHOROM.	STAR T	END	ST R.	PROM OTER	EXO N	INTR ON	CpG ISLA ND	p- VAL UE	CLASSICIFI CATION
chr2	23829 6515	23829 6516	-		COL 6A3	COL6 A3		0,000 125	stronglyHypo meth
chr17	21743 251	21743 252	+					0,000 125	stronglyHypo meth
chr22	41331 665	41331 666	-					0,000 125	stronglyHypo meth
chr20	55921 18	55921 19	+	GPCPD 1				0,000 131	stronglyHypo meth
chr11	11384 6937	11384 6938	-			HTR3 A		0,000 141	stronglyHypo meth
chr1	18367 8005	18367 8006	+			RGL1		0,000 141	stronglyHypo meth
chr1	22628 8177	22628 8178	+					0,000 141	stronglyHypo meth
chr19	39055 672	39055 673	+		RYR 1		Y	0,000 145	stronglyHypo meth
chr9	26794 667	26794 668	+					0,000 151	stronglyHypo meth
chr19	15426 89	15426 90	+					0,000 151	stronglyHypo meth
chr14	93389 563	93389 564	+	CHGA	CHG A		Y	0,000 153	stronglyHypo meth
chr15	93928 962	93928 963	+					0,000 153	stronglyHypo meth
chr1	74174 46	74174 47	-			CAM TA1		0,000 155	stronglyHypo meth
chr13	44969 567	44969 568	-			SERP 2		0,000 155	stronglyHypo meth
chr5	95953 320	95953 321	-					0,000 155	stronglyHypo meth
chr6	15963 80	15963 81	+					0,000 155	stronglyHypo meth
chr6	15963 78	15963 79	+					0,000 155	stronglyHypo meth
chr9	14002 0926	14002 0927	+					0,000 155	stronglyHypo meth
chr6	13047 2786	13047 2787	+			SAM D3		0,000 155	stronglyHypo meth
chr2	33436 12	33436 13	+			TSSC 1		0,000 155	stronglyHypo meth
chr16	44724 5	44724 6	+	NME4	NME 4		Y	0,000 165	stronglyHypo meth
chr12	11957 9258	11957 9259	-			SRR M4		0,000 17	stronglyHypo meth
chr10	28736 688	28736 689	+					0,000 178	stronglyHypo meth
chr10	13154 1061	13154 1062	+			MGM T		0,000 19	stronglyHypo meth

Table H 4. (continued)

CHOROM.	START	END	STR.	PROMOTER	EXON	INTRON	CpG ISLAND	p-VALUE	CLASSIFICATION
chr13	26024794	26024795	-			ATP8A2		0,0002	stronglyHypometh
chr13	59411138	59411139	-					0,0002	stronglyHypometh
chr6	83985434	83985435	+			ME1		0,0002	stronglyHypometh
chr9	84883191	84883192	+					0,000201	stronglyHypometh

Table H 5. Top 100 hypermethylated genomic regions in MDA-ER α 5 and MCF7 cells after 6h OH treatment.

CHOROM.	START	END	STR.	PROMOTER	EXON	INTRON	CpG ISLAND	P-VALUE	CLASSIFICATION
chr17	58217421	58217422	+				Y	9,63E-14	stronglyHypermeth
chr5	42424028	42424029	+	GHR	GHR			1,72E-13	stronglyHypermeth
chr16	68269239	68269240	-	ESRP2		ESRP2	Y	1,72E-13	stronglyHypermeth
chr5	75379450	75379451	-	SV2C		SV2C	Y	2,03E-13	stronglyHypermeth
chr17	70204582	70204583	-					2,03E-13	stronglyHypermeth
chr15	88261993	88261994	-					2,03E-13	stronglyHypermeth
chr9	29398805	29398806	-					2,03E-13	stronglyHypermeth
chr19	11009845	11009846	+			CARM1		2,03E-13	stronglyHypermeth
chr16	74701470	74701471	-	RFWD3				2,03E-13	stronglyHypermeth
chr9	140190401	140190402	+				Y	2,03E-13	stronglyHypermeth
chr12	132313551	132313552	+	MMP17		MMP17	Y	2,03E-13	stronglyHypermeth
chr12	132313555	132313556	+	MMP17		MMP17	Y	2,03E-13	stronglyHypermeth
chr13	28534568	28534569	-				Y	2,03E-13	stronglyHypermeth
chr2	176971833	176971834	+	HOXD11			Y	2,03E-13	stronglyHypermeth
chr2	176971835	176971836	+	HOXD11			Y	2,03E-13	stronglyHypermeth
chr2	176971839	176971840	+	HOXD11			Y	2,03E-13	stronglyHypermeth
chr16	3334028	3334029	+	ZNF263	ZNF263			2,19E-13	stronglyHypermeth
chr7	100876081	100876082	-			CLDN15	Y	2,22E-13	stronglyHypermeth
chr16	87739548	87739549	-					2,23E-13	stronglyHypermeth
chr16	87739696	87739697	-					2,23E-13	stronglyHypermeth
chr16	87739703	87739704	-					2,23E-13	stronglyHypermeth

Table H 5. (continued)

CHOROM.	START	END	STR.	PROMOTER	EXON	INTRON	CpG ISLAND	P-VALUE	CLASSIFICATION
chr5	176730059	176730060	+	PRELID1, RAB24	RAB24		Y	2,36E-13	stronglyHypermeth
chr16	81435009	81435010	-					2,36E-13	stronglyHypermeth
chr16	81435016	81435017	-					2,36E-13	stronglyHypermeth
chr2	99193496	99193497	-		INPP4A			2,36E-13	stronglyHypermeth
chr6	1605184	1605185	-				Y	2,41E-13	stronglyHypermeth
chr17	18585243	18585244	+	ZNF286B		ZNF286B	Y	2,47E-13	stronglyHypermeth
chr1	109203790	109203791	-	HENMT1		HENMT1	Y	2,47E-13	stronglyHypermeth
chr7	79743404	79743405	+					2,48E-13	stronglyHypermeth
chr7	100876087	100876088	-			CLDN15	Y	2,5E-13	stronglyHypermeth
chr17	36666690	36666691	-		ARHGAP23		Y	2,65E-13	stronglyHypermeth
chr16	47178560	47178561	+	NETO2				2,65E-13	stronglyHypermeth
chr20	47444429	47444430	-	PREX1			Y	2,82E-13	stronglyHypermeth
chr20	47444434	47444435	-	PREX1			Y	2,82E-13	stronglyHypermeth
chr20	47444437	47444438	-	PREX1			Y	2,82E-13	stronglyHypermeth
chr20	47444441	47444442	-	PREX1			Y	2,82E-13	stronglyHypermeth
chr20	47444461	47444462	-	PREX1			Y	2,82E-13	stronglyHypermeth
chr9	29398801	29398802	-					2,99E-13	stronglyHypermeth
chr6	27181684	27181685	-					2,99E-13	stronglyHypermeth
chr18	8263231	8263232	-			PTPRM		2,99E-13	stronglyHypermeth
chr16	31154243	31154244	+		PRSS36		Y	2,99E-13	stronglyHypermeth
chr16	31154245	31154246	+		PRSS36		Y	2,99E-13	stronglyHypermeth

Table H 5. (continued)

CHOROM.	START	END	STR.	PROMOTER	EXON	INTRON	CpG ISLAND	P-VALUE	CLASSIFICATION
chr8	107460168	107460169	-	OXR1	OXR1	OXR1		3,05E-13	stronglyHypemeth
chr3	13324663	13324664	+				Y	3,05E-13	stronglyHypemeth
chr3	13324666	13324667	+				Y	3,05E-13	stronglyHypemeth
chr3	13324668	13324669	+				Y	3,05E-13	stronglyHypemeth
chr3	13324673	13324674	+				Y	3,05E-13	stronglyHypemeth
chr3	13324676	13324677	+				Y	3,05E-13	stronglyHypemeth
chr15	63335123	63335124	-	TPM1	TPM1		Y	3,08E-13	stronglyHypemeth
chr12	133170636	133170637	+					3,08E-13	stronglyHypemeth
chr12	133170802	133170803	+					3,08E-13	stronglyHypemeth
chr10	128594996	128594997	-	DOCK1		DOCK1	Y	3,14E-13	stronglyHypemeth
chr10	128594998	128594999	-	DOCK1		DOCK1	Y	3,14E-13	stronglyHypemeth
chr17	7339951	7339952	-		TME M102		Y	3,16E-13	stronglyHypemeth
chr2	176944753	176944754	-				Y	3,16E-13	stronglyHypemeth
chr1	218330183	218330184	+					3,17E-13	stronglyHypemeth
chr20	47444432	47444433	-	PREX1			Y	3,2E-13	stronglyHypemeth
chr20	825430	825431	+	FAM110A	FAM110A		Y	3,55E-13	stronglyHypemeth
chr17	35293366	35293367	-				Y	3,55E-13	stronglyHypemeth
chr10	3280518	3280519	+					3,55E-13	stronglyHypemeth
chr10	6531592	6531593	-			PRKCQ		3,55E-13	stronglyHypemeth
chr7	23421442	23421443	+			IGF2BP3		3,55E-13	stronglyHypemeth
chr7	29603999	29604000	-	PRR15		PRR15	Y	3,55E-13	stronglyHypemeth

Table H 5. (continued)

CHOROM.	START	END	STR.	PROMOTER	EXON	INTRON	CpG ISLAND	P-VALUE	CLASSIFICATION
chr7	29604014	29604015	-	PRR15		PRR15	Y	3,55E-13	stronglyHypemeth
chr6	10417574	10417575	-			TFAP2A	Y	3,55E-13	stronglyHypemeth
chr6	10417577	10417578	-			TFAP2A	Y	3,55E-13	stronglyHypemeth
chr3	71802644	71802645	+	EIF4E3, GPR27		EIF4E3	Y	3,55E-13	stronglyHypemeth
chr20	49241284	49241285	-			FAM65C		3,65E-13	stronglyHypemeth
chr20	62103994	62103995	-	KCNQ2	KCNQ2		Y	3,65E-13	stronglyHypemeth
chr10	118032330	118032331	-	GFRA1		GFRA1	Y	3,65E-13	stronglyHypemeth
chr7	19177501	19177502	+					3,65E-13	stronglyHypemeth
chr18	6271532	6271533	-			L3MBTL4		3,65E-13	stronglyHypemeth
chr19	34113111	34113112	-	CHST8	CHST8		Y	3,65E-13	stronglyHypemeth
chr8	131455621	131455622	-	ASAP1		ASAP1	Y	4,1E-13	stronglyHypemeth
chr10	10691949	10691950	-					4,16E-13	stronglyHypemeth
chr19	4173229	4173230	+				Y	4,16E-13	stronglyHypemeth
chr16	85604269	85604270	+					4,16E-13	stronglyHypemeth
chr3	189678981	189678982	-			LEPREL1		4,44E-13	stronglyHypemeth
chrX	17673725	17673726	+			NHS	Y	4,44E-13	stronglyHypemeth
chr14	24601654	24601655	+	FITM1	FITM1		Y	4,44E-13	stronglyHypemeth
chr6	151815291	151815292	+	CCDC170	CCDC170		Y	4,44E-13	stronglyHypemeth
chr1	161695677	161695678	+		FCRLB		Y	4,44E-13	stronglyHypemeth
chr12	21471304	21471305	+			SLCO1A2		4,44E-13	stronglyHypemeth
chr8	80803317	80803318	+					4,63E-13	stronglyHypemeth

Table H 5. (continued)

CHOROM.	START	END	STR.	PROMOTER	EXON	INTRON	CpGISLAND	p-VALUE	CLASSIFICATION
chr14	61787880	61787881	+	PRKCH			Y	4,63E-13	stronglyHypemeth
chr3	13324715	13324716	-				Y	4,63E-13	stronglyHypemeth
chr3	13324727	13324728	-				Y	4,63E-13	stronglyHypemeth
chr1	109632960	109632961	+	TMEM167B				4,79E-13	stronglyHypemeth
chr19	43969883	43969884	+	LYPD3				4,97E-13	stronglyHypemeth
chr9	118339018	118339019	-					4,97E-13	stronglyHypemeth
chr17	77179279	77179280	-			RBFOX3	Y	5,65E-13	stronglyHypemeth
chr17	77179285	77179286	-			RBFOX3	Y	5,65E-13	stronglyHypemeth
chr7	4069729	4069730	-			SDK1		5,65E-13	stronglyHypemeth
chr7	37488577	37488578	-	ELMO1	ELMO1		Y	5,65E-13	stronglyHypemeth
chr7	37488594	37488595	-	ELMO1	ELMO1		Y	5,65E-13	stronglyHypemeth
chr7	37488603	37488604	-	ELMO1	ELMO1		Y	5,65E-13	stronglyHypemeth
chr1	6239840	6239841	+	CHD5		CHD5	Y	5,65E-13	stronglyHypemeth
chr1	6239844	6239845	+	CHD5		CHD5	Y	5,65E-13	stronglyHypemeth
chr6	151815525	151815526	+	CCDC170		CCDC170	Y	5,65E-13	stronglyHypemeth
chr16	28074810	28074811	+	GSG1L	GSG1L		Y	5,65E-13	stronglyHypemeth

Table H 6. Top 100 hypomethylated genomic regions in MDA-ER α 5 and MCF7 cells after 6h OH treatment.

CHOROM.	START	END	STR.	PROMOTER	EXON	INTRON	CpG ISLAND	p-VALUE	CLASSIFICATION
chr6	41604917	41604918	-				Y	1,723E-13	stronglyHypo meth
chr6	41604925	41604926	-				Y	1,723E-13	stronglyHypo meth
chr14	105559638	105559639	-				Y	1,935E-13	stronglyHypo meth
chr18	8707330	8707331	+				Y	2,031E-13	stronglyHypo meth
chr7	5467841	5467842	-				Y	2,031E-13	stronglyHypo meth
chr6	34203419	34203420	+				Y	2,031E-13	stronglyHypo meth
chr16	677701	677702	-		RAB40C		Y	2,031E-13	stronglyHypo meth
chr11	30424685	30424686	+			MPPED2		2,031E-13	stronglyHypo meth
chr11	30424687	30424688	+			MPPED2		2,031E-13	stronglyHypo meth
chr3	13301007	13301008	+					2,031E-13	stronglyHypo meth
chr2	19558313	19558314	-	OSR1	OSR1		Y	2,031E-13	stronglyHypo meth
chr2	19558322	19558323	-	OSR1	OSR1		Y	2,031E-13	stronglyHypo meth
chr16	21532887	21532888	+					2,189E-13	stronglyHypo meth
chr11	67887507	67887508	-			CHKA		2,189E-13	stronglyHypo meth
chr12	118490247	118490248	-		WSB2			2,189E-13	stronglyHypo meth

Table H 6. (continued)

CHOROM.	START	END	STR.	PROMOTER	EXON	INTRON	CpG ISLAND	P-VALUE	CLASSIFICATION
chr12	118490251	118490252	-		WSB2			2,189E-13	stronglyHypometh
chr17	45357974	45357975	-			ITGB3		2,189E-13	stronglyHypometh
chr6	41604931	41604932	-				Y	2,297E-13	stronglyHypometh
chr1	6795593	6795594	+					2,297E-13	stronglyHypometh
chr15	67413603	67413604	-			SMAD3		2,297E-13	stronglyHypometh
chr12	66219959	66219960	-	RPSAP52		RPSAP52, HMGA2	Y	2,356E-13	stronglyHypometh
chr6	34203420	34203421	-				Y	2,407E-13	stronglyHypometh
chr2	10673877	10673878	+					2,407E-13	stronglyHypometh
chr3	9988248	9988249	+	PRRT3-AS1	PRRT3		Y	2,471E-13	stronglyHypometh
chr3	9988250	9988251	+	PRRT3-AS1	PRRT3		Y	2,471E-13	stronglyHypometh
chr20	56273742	56273743	-			PMEPA1		2,65E-13	stronglyHypometh
chr10	131477100	131477101	+			MGMT		2,65E-13	stronglyHypometh
chrX	152658485	152658486	+					2,65E-13	stronglyHypometh
chr14	74100945	74100946	-				Y	2,65E-13	stronglyHypometh
chr7	1607829	1607830	-			PSMG3		2,987E-13	stronglyHypometh
chr12	124870112	124870113	-			NCOR2		3,045E-13	stronglyHypometh
chr19	8245850	8245851	+					3,045E-13	stronglyHypometh

Table H 6. (continued)

CHOROM.	START	END	STR.	PROMOTER	EXON	INTRON	CpG ISLAND	p-VALUE	CLASSIFICATION
chr21	36042601	36042602	-	CLIC6	CLIC6		Y	3,081E-13	stronglyHypometh
chr3	128151940	128151941	-				Y	3,081E-13	stronglyHypometh
chr3	128151944	128151945	-				Y	3,081E-13	stronglyHypometh
chr10	77103109	77103110	+			ZNF503-AS1		3,136E-13	stronglyHypometh
chr16	80966860	80966861	-					3,155E-13	stronglyHypometh
chr9	92292556	92292557	-			UNQ6494		3,155E-13	stronglyHypometh
chr17	48619617	48619618	+		EPN3		Y	3,155E-13	stronglyHypometh
chr17	48619671	48619672	+		EPN3		Y	3,155E-13	stronglyHypometh
chr17	66309007	66309008	-			ARSG		3,155E-13	stronglyHypometh
chr2	16053516	16053517	+					3,155E-13	stronglyHypometh
chr14	104443644	104443645	-			TDRD9		3,155E-13	stronglyHypometh
chr1	229893921	229893922	+					3,547E-13	stronglyHypometh
chr3	194014818	194014819	+				Y	3,547E-13	stronglyHypometh
chr12	56325496	56325497	+	DGKA		DGKA		3,547E-13	stronglyHypometh
chr9	116311190	116311191	+			RGS3		3,547E-13	stronglyHypometh
chr2	88582947	88582948	-					3,547E-13	stronglyHypometh

Table H 6. (continued)

CHOROM.	STAR T	END	ST R.	PROM OTER	EXO N	INTRO N	CpG ISLAND	P- VAL UE	CLASSIFICATI ON
chr22	33931798	33931799	+			LARGE		3,547E-13	stronglyHypometh
chr14	89017810	89017811	-			PTPN21	Y	3,547E-13	stronglyHypometh
chr6	39161965	39161966	+		KCNK5			3,648E-13	stronglyHypometh
chr16	678028	678029	-		RAB40C		Y	3,648E-13	stronglyHypometh
chr2	128158906	128158907	-				Y	3,648E-13	stronglyHypometh
chr3	54373066	54373067	-			CACNA2D3		3,648E-13	stronglyHypometh
chr17	79316595	79316596	-				Y	3,748E-13	stronglyHypometh
chr11	62369802	62369803	+	MTA2	EML3		Y	3,905E-13	stronglyHypometh
chr6	2857948	2857949	-			MGC39372		4,101E-13	stronglyHypometh
chr10	98050261	98050262	-					4,101E-13	stronglyHypometh
chr10	87373300	87373301	+		GRI D1			4,101E-13	stronglyHypometh
chr10	87373309	87373310	+		GRI D1			4,101E-13	stronglyHypometh
chr10	123774785	123774786	-			TACC2		4,101E-13	stronglyHypometh
chr15	23661937	23661938	+					4,101E-13	stronglyHypometh
chr9	93601740	93601741	-			SYK		4,101E-13	stronglyHypometh
chr2	29338137	29338138	-	CLIP4			Y	4,101E-13	stronglyHypometh

Table H 6. (continued)

CHOROM.	START	END	STR.	PROMOTER	EXON	INTRON	CpGISLAND	P-VALUE	CLASSIFICATION
chr14	104613379	104613380	+			KIF26A		4,101E-13	stronglyHypometh
chr17	1390511	1390512	+			MYO1C	Y	4,16E-13	stronglyHypometh
chr18	13137097	13137098	-				Y	4,435E-13	stronglyHypometh
chr18	13137103	13137104	-				Y	4,435E-13	stronglyHypometh
chr18	77245574	77245575	-			NFATC1		4,435E-13	stronglyHypometh
chr6	7051662	7051663	-				Y	4,435E-13	stronglyHypometh
chr6	7051665	7051666	-				Y	4,435E-13	stronglyHypometh
chr1	16159209	16159210	-					4,435E-13	stronglyHypometh
chr21	42798586	42798587	+	MX1		MX1	Y	4,435E-13	stronglyHypometh
chr17	76567759	76567760	-		DNAH17			4,435E-13	stronglyHypometh
chr4	15780539	15780540	-	CD38		CD38	Y	4,435E-13	stronglyHypometh
chr6	160769428	160769429	-	SLC22A3	SLC22A3		Y	4,435E-13	stronglyHypometh
chr6	160769432	160769433	-	SLC22A3	SLC22A3		Y	4,435E-13	stronglyHypometh
chr6	160769435	160769436	-	SLC22A3	SLC22A3		Y	4,435E-13	stronglyHypometh
chr12	111847269	111847270	+			SH2B3		4,443E-13	stronglyHypometh
chr12	111847275	111847276	+			SH2B3		4,443E-13	stronglyHypometh

Table H 6. (continued)

CHOROM.	START	END	STR.	PROMOTER	EXON	INTRON	CpG ISLAND	p-VALUE	CLASSIFICATION
chr17	40573821	40573822	+			PTRF	Y	4,629E-13	stronglyHypometh
chr9	132601310	132601311	+			USP20		4,969E-13	stronglyHypometh
chr17	38717305	38717306	+			CCR7		4,969E-13	stronglyHypometh
chr19	38904011	38904012	-			RASGRP4		4,969E-13	stronglyHypometh
chr7	55088018	55088019	-			EGFR	Y	5,653E-13	stronglyHypometh
chr7	55088022	55088023	-			EGFR	Y	5,653E-13	stronglyHypometh
chr7	55088024	55088025	-			EGFR	Y	5,653E-13	stronglyHypometh
chr7	55088035	55088036	-			EGFR	Y	5,653E-13	stronglyHypometh
chr7	55088037	55088038	-			EGFR	Y	5,653E-13	stronglyHypometh
chr22	40635357	40635358	-			TNRC6B		5,653E-13	stronglyHypometh
chr10	72218292	72218293	-				Y	5,668E-13	stronglyHypometh
chr12	124864613	124864614	+			NCOR2		5,668E-13	stronglyHypometh
chr20	6749019	6749020	-	BMP2	BMP2		Y	5,678E-13	stronglyHypometh
chr20	6749022	6749023	-	BMP2	BMP2		Y	5,678E-13	stronglyHypometh
chr5	153569241	153569242	-					5,678E-13	stronglyHypometh
chr5	153569246	153569247	-					5,678E-13	stronglyHypometh

Table H 6. (continued)

CHOROM.	START	END	STR.	PROMOTER	EXON	INTRON	CpG ISLAND	P-VALUE	CLASSIFICATION
chr5	17102 3801	17102 3802	+					5,67 8E- 13	stronglyHypo meth
chr3	13925 8657	13925 8658	+	RBP1	RBP1		Y	5,67 8E- 13	stronglyHypo meth
chr11	58967 192	58967 193	-		DTX4			5,67 8E- 13	stronglyHypo meth
chr11	65478 316	65478 317	-					5,67 8E- 13	stronglyHypo meth

Table H 7. Top 100 hypermethylated genomic regions in MDA-ER α 5 and MCF7 cells after 6h E2 treatment.

CHOROM.	START	END	STR.	PROMOTER	EXON	INTRON	CpGISLAND	p-VALUE	CLASSIFICATION
chr20	55841259	55841260	-	BMP7	BMP7		Y	9,634E-14	stronglyHypermeth
chr19	34287927	34287928	+	KCTD15		KCTD15	Y	1,935E-13	stronglyHypermeth
chr11	69632333	69632334	-			FGF3	Y	1,935E-13	stronglyHypermeth
chr19	41119496	41119497	+			LTP4	Y	2,031E-13	stronglyHypermeth
chr22	46932330	46932331	-	CELSR1	CELSR1		Y	2,031E-13	stronglyHypermeth
chr17	69777628	69777629	+					2,031E-13	stronglyHypermeth
chr17	72919814	72919815	+	OTOP2,USH1G			Y	2,031E-13	stronglyHypermeth
chr16	74701461	74701462	-	RFWD3				2,031E-13	stronglyHypermeth
chr16	74701482	74701483	-	RFWD3				2,031E-13	stronglyHypermeth
chr16	74701487	74701488	-	RFWD3				2,031E-13	stronglyHypermeth
chr6	27840104	27840105	+	HIST1H3I				2,031E-13	stronglyHypermeth
chr18	25323653	25323654	-					2,031E-13	stronglyHypermeth
chr7	8482633	8482634	-			NXP1	Y	2,189E-13	stronglyHypermeth
chr6	34112513	34112514	+			GRM4	Y	2,231E-13	stronglyHypermeth
chr6	34520750	34520751	+			SPDEF		2,231E-13	stronglyHypermeth

Table H 7. (continued)

CHOROM.	START	END	STR.	PROMOTER	EXON	INTRON	CpG ISLAND	p-VALUE	CLASSIFICATION
chr18	27419017	27419018	+					2,297E-13	stronglyHypermeth
chr20	59933806	59933807	+			CDH4		2,356E-13	stronglyHypermeth
chr17	35295063	35295064	-	LHX1	LHX1		Y	2,356E-13	stronglyHypermeth
chr15	42500723	42500724	+	VPS39				2,356E-13	stronglyHypermeth
chr1	245878313	245878314	-					2,407E-13	stronglyHypermeth
chr16	74701470	74701471	-	RFWD3				2,483E-13	stronglyHypermeth
chr2	71355856	71355857	-			MCE		2,65E-13	stronglyHypermeth
chr17	68388034	68388035	+					2,65E-13	stronglyHypermeth
chr17	68388038	68388039	+					2,65E-13	stronglyHypermeth
chr10	133999539	133999540	-	DPYSL4			Y	2,65E-13	stronglyHypermeth
chr18	25865539	25865540	-					2,65E-13	stronglyHypermeth
chr7	45613832	45613833	-	ADCY1			Y	2,65E-13	stronglyHypermeth
chr7	45613858	45613859	-	ADCY1			Y	2,65E-13	stronglyHypermeth
chr18	25323656	25323657	-					2,987E-13	stronglyHypermeth
chr1	201583538	201583539	-					3,045E-13	stronglyHypermeth
chr1	218330092	218330093	+					3,081E-13	stronglyHypermeth
chr1	218330104	218330105	+					3,081E-13	stronglyHypermeth
chr12	49109356	49109357	+			CCNT1		3,081E-13	stronglyHypermeth

Table H 7. (continued)

CHOROM.	START	END	STR.	PROMOTER	EXON	INTRON	CpG ISLAND	p-VALUE	CLASSIFICATION
chr12	49109359	49109360	+			CCNT1		3,081E-13	stronglyHypemeth
chr2	219724427	219724428	+	WNT6			Y	3,081E-13	stronglyHypemeth
chr2	219724441	219724442	+	WNT6			Y	3,081E-13	stronglyHypemeth
chr14	87326588	87326589	-					3,081E-13	stronglyHypemeth
chr14	105993511	105993512	+	TMEM121		TMEM121	Y	3,081E-13	stronglyHypemeth
chr17	78450145	78450146	-	NPTX1	NPTX1		Y	3,081E-13	stronglyHypemeth
chr16	330695	330696	-	ARHGDIG	ARHGDIG		Y	3,081E-13	stronglyHypemeth
chr16	330697	330698	-	ARHGDIG	ARHGDIG		Y	3,081E-13	stronglyHypemeth
chr3	192289263	192289264	-			FGF12		3,136E-13	stronglyHypemeth
chr1	6531218	6531219	+			PLEKHG5	Y	3,136E-13	stronglyHypemeth
chr1	6531220	6531221	+			PLEKHG5	Y	3,136E-13	stronglyHypemeth
chr1	6531232	6531233	+			PLEKHG5	Y	3,136E-13	stronglyHypemeth
chr14	95236197	95236198	-	GSC	GSC		Y	3,136E-13	stronglyHypemeth
chr18	8151788	8151789	+			PTPRM		3,136E-13	stronglyHypemeth
chr7	24143950	24143951	-					3,136E-13	stronglyHypemeth
chr2	44108896	44108897	+					3,155E-13	stronglyHypemeth

Table H 7. (continued)

CHOROM.	START	END	STR.	PROMOTER	EXON	INTRON	CpG ISLAND	p-VALUE	CLASSIFICATION
chr12	112574709	112574710	-			TRAFD1		3,155E-13	stronglyHypemeth
chr19	15619401	15619402	+	CYP4F22		CYP4F22	Y	3,155E-13	stronglyHypemeth
chr19	15619403	15619404	+	CYP4F22		CYP4F22	Y	3,155E-13	stronglyHypemeth
chr19	15619405	15619406	+	CYP4F22		CYP4F22	Y	3,155E-13	stronglyHypemeth
chr17	37862112	37862113	+			ERBB2		3,155E-13	stronglyHypemeth
chr8	80272552	80272553	+					3,169E-13	stronglyHypemeth
chr8	106154924	106154925	-					3,169E-13	stronglyHypemeth
chr1	244340418	244340419	-					3,547E-13	stronglyHypemeth
chr7	150675352	150675353	-	KCNH2	KCNH2		Y	3,547E-13	stronglyHypemeth
chr21	44494812	44494813	-			CBS	Y	3,547E-13	stronglyHypemeth
chr19	1749277	1749278	+				Y	3,547E-13	stronglyHypemeth
chr19	39226762	39226763	-		CAPN12		Y	3,547E-13	stronglyHypemeth
chr22	28197426	28197427	-	MN1	MN1		Y	3,547E-13	stronglyHypemeth
chr17	5404267	5404268	-	LOC78392	LOC78392		Y	3,547E-13	stronglyHypemeth
chr17	74864933	74864934	+	MGAT5B	MGAT5B		Y	3,547E-13	stronglyHypemeth
chr17	74864942	74864943	+	MGAT5B	MGAT5B		Y	3,547E-13	stronglyHypemeth

Table H 7. (continued)

CHOROM.	START	END	STR.	PROMOTER	EXON	INTRON	CpG ISLAND	p-VALUE	CLASSIFICATION
chr17	74864949	74864950	+	MGAT5B	MGAT5B		Y	3,547E-13	stronglyHypermeth
chr11	33397664	33397665	-				Y	3,547E-13	stronglyHypermeth
chr11	33397666	33397667	+				Y	3,547E-13	stronglyHypermeth
chr11	33397667	33397668	-				Y	3,547E-13	stronglyHypermeth
chr9	14018992	14018993	-				Y	3,547E-13	stronglyHypermeth
chr17	35295091	35295092	-	LHX1	LHX1		Y	3,648E-13	stronglyHypermeth
chr11	370212	370213	+	B4GALNT4		B4GALNT4		3,648E-13	stronglyHypermeth
chr9	137248969	137248970	+			RXRA		3,648E-13	stronglyHypermeth
chr7	27183054	27183055	-	HOXA5	HOXA5	HOXAAS3	Y	3,648E-13	stronglyHypermeth
chr8	129165586	129165587	+					3,905E-13	stronglyHypermeth
chr15	63335990	63335991	-		TPM1	TPM1	Y	3,905E-13	stronglyHypermeth
chr17	58217409	58217410	+				Y	4,001E-13	stronglyHypermeth
chr17	58217454	58217455	+				Y	4,001E-13	stronglyHypermeth
chr14	100771168	100771169	-			SLC25A29		4,084E-13	stronglyHypermeth
chr16	90038569	90038570	+	CENPBD1, AFG3L1P	CENPBD1		Y	4,16E-13	stronglyHypermeth

Table H 7. (continued)

CHOROM	START	END	STR.	PROMOTER	EXON	INTRON	CpG ISLAND	p-VALUE	CLASSIFICATION
chr16	90038571	90038572	+	CENPBD1,AFG3L1P	CENPBD1		Y	4,16E-13	stronglyHypermeth
chr16	90038582	90038583	+	CENPBD1,AFG3L1P	CENPBD1		Y	4,16E-13	stronglyHypermeth
chr16	90038586	90038587	+	CENPBD1,AFG3L1P	CENPBD1		Y	4,16E-13	stronglyHypermeth
chr16	90038590	90038591	+	CENPBD1,AFG3L1P	CENPBD1		Y	4,16E-13	stronglyHypermeth
chr16	90038606	90038607	+	CENPBD1,AFG3L1P	CENPBD1		Y	4,16E-13	stronglyHypermeth
chr16	90038712	90038713	+	CENPBD1,AFG3L1P	CENPBD1		Y	4,16E-13	stronglyHypermeth
chr15	83348891	83348892	+			LOC283692,AP3B2	Y	4,16E-13	stronglyHypermeth
chr1	158986434	158986435	-		IFI16	IFI16		4,435E-13	stronglyHypermeth
chr7	113778705	113778706	-			FOXP2		4,435E-13	stronglyHypermeth
chr20	35064610	35064611	-		DLGAP4		Y	4,435E-13	stronglyHypermeth
chr3	48700288	48700289	+	CELSR3	CELSR3		Y	4,435E-13	stronglyHypermeth
chr3	48700291	48700292	+	CELSR3	CELSR3		Y	4,435E-13	stronglyHypermeth
chr17	54912213	54912214	-	DGKE,C17orf67	DGKE		Y	4,435E-13	stronglyHypermeth
chr9	120176994	120176995	-	ASTN2	ASTN2		Y	4,435E-13	stronglyHypermeth
chr4	2464090	2464091	-			LOC402160	Y	4,435E-13	stronglyHypermeth

Table H 7. (continued)

CHOROM.	START	END	STR.	PROMOTER	EXON	INTRON	CpGISLAND	p-VALUE	CLASSIFICATION
chr4	4671072	4671073	-			LOC100507266		4,435E-13	stronglyHypemeth
chr4	8582469	8582470	-	GPR78	GPR78	GPR78	Y	4,435E-13	stronglyHypemeth
chr7	15117797	15117798	+					4,435E-13	stronglyHypemeth
chr7	27183057	27183058	+	HOXA5	HOXA5	HOXA-AS3	Y	4,435E-13	stronglyHypemeth
chr18	8151915	8151916	+			PTPRM		4,443E-13	stronglyHypemeth

Table H 8. Top 100 hypomethylated genomic regions in MDA-ER α 5 and MCF7 cells after 6h E2 treatment.

CHOROM.	START	END	STR.	PROMOTER	EXON	INTRON	CpG ISLAND	p-VALUE	CLASSIFICATION
chr6	14977 1931	14977 1932	-		ZC3H 12D		Y	1,72 3E- 13	stronglyHypo meth
chr6	14977 1933	14977 1934	-		ZC3H 12D		Y	1,72 3E- 13	stronglyHypo meth
chr7	15262 0136	15262 0137	+					2,03 1E- 13	stronglyHypo meth
chr19	34354 12	34354 13	+			NFIC	Y	2,03 1E- 13	stronglyHypo meth
chr3	18758 0328	18758 0329	-					2,03 1E- 13	stronglyHypo meth
chr3	18758 0340	18758 0341	-					2,03 1E- 13	stronglyHypo meth
chr4	81294 33	81294 34	+			ABLI M2		2,03 1E- 13	stronglyHypo meth
chr5	16783 6834	16783 6835	-			WW C1		2,03 1E- 13	stronglyHypo meth
chr15	89991 120	89991 121	-					2,03 1E- 13	stronglyHypo meth
chr3	99885 90	99885 91	-	PRRT3- AS1	PRRT 3		Y	2,18 9E- 13	stronglyHypo meth
chr3	99882 44	99882 45	+	PRRT3- AS1	PRRT 3		Y	2,18 9E- 13	stronglyHypo meth
chr3	18554 4050	18554 4051	+				Y	2,18 9E- 13	stronglyHypo meth
chr6	13137 16	13137 17	+		FOX Q1		Y	2,18 9E- 13	stronglyHypo meth
chr6	13137 18	13137 19	+		FOX Q1		Y	2,18 9E- 13	stronglyHypo meth
chr20	42069 445	42069 446	+					2,35 6E- 13	stronglyHypo meth

Table H 8. (continued)

CHOROM.	START	END	STR.	PROMOTER	EXON	INTRON	CpGISLAND	p-VALUE	CLASSIFICATION
chr19	3509670	3509671	+			FZR1		2,356E-13	stronglyHypometh
chr14	101640912	101640913	-					2,356E-13	stronglyHypometh
chr14	101640944	101640945	-					2,356E-13	stronglyHypometh
chr6	74290152	74290153	+					2,407E-13	stronglyHypometh
chr12	107767582	107767583	-			BTBD11		2,471E-13	stronglyHypometh
chr19	10015452	10015453	+			OLFM2		2,483E-13	stronglyHypometh
chr9	133788419	133788420	+			FIBCD1		2,65E-13	stronglyHypometh
chr12	52800086	52800087	+	KRT82	KRT82			2,65E-13	stronglyHypometh
chr14	99687256	99687257	-			BCL11B		2,65E-13	stronglyHypometh
chr1	18053114	18053115	+					2,65E-13	stronglyHypometh
chr8	124552733	124552734	+	FBXO32		FBXO32	Y	2,65E-13	stronglyHypometh
chr8	124552784	124552785	+	FBXO32		FBXO32	Y	2,65E-13	stronglyHypometh
chr4	6570822	6570823	-					2,65E-13	stronglyHypometh
chr5	107005257	107005258	-			EFNA5	Y	2,65E-13	stronglyHypometh
chr5	178585254	178585255	+			ADAMTS2		2,65E-13	stronglyHypometh
chr15	67356672	67356673	-					2,65E-13	stronglyHypometh
chr18	13439098	13439099	+			LDLRAD4		2,987E-13	stronglyHypometh
chr18	21270092	21270093	+	LAMA3		LAMA3	Y	2,987E-13	stronglyHypometh

Table H 8. (continued)

CHOROM.	START	END	STR.	PROMOTER	EXON	INTRON	CpG ISLAND	p-VALUE	CLASSIFICATION
chr14	10294 9439	10294 9440	-			TEC PR2		2,98 7E- 13	stronglyHypo meth
chr1	11042 0157	11042 0158	-					2,98 7E- 13	stronglyHypo meth
chr10	12702 4907	12702 4908	+					2,98 7E- 13	stronglyHypo meth
chr2	27938 580	27938 581	-					3,08 1E- 13	stronglyHypo meth
chr6	39161 959	39161 960	+		KC NK5			3,08 1E- 13	stronglyHypo meth
chr6	39161 965	39161 966	+		KC NK5			3,08 1E- 13	stronglyHypo meth
chr7	25019 109	25019 110	+	OSBPL 3		OSB PL3	Y	3,08 1E- 13	stronglyHypo meth
chr7	25019 115	25019 116	+	OSBPL 3		OSB PL3	Y	3,08 1E- 13	stronglyHypo meth
chr12	94541 919	94541 920	-	PLXNC 1			Y	3,13 6E- 13	stronglyHypo meth
chr8	12912 1439	12912 1440	-					3,13 6E- 13	stronglyHypo meth
chr9	98279 049	98279 050	-	PTCH1	PTC H1		Y	3,15 5E- 13	stronglyHypo meth
chr9	98279 059	98279 060	-	PTCH1	PTC H1		Y	3,15 5E- 13	stronglyHypo meth
chr9	98279 061	98279 062	-	PTCH1	PTC H1		Y	3,15 5E- 13	stronglyHypo meth
chr20	56283 944	56283 945	-			PME PA1	Y	3,15 5E- 13	stronglyHypo meth
chr7	10168 8721	10168 8722	-			CUX 1		3,15 5E- 13	stronglyHypo meth
chr17	76312 264	76312 265	-					3,15 5E- 13	stronglyHypo meth

Table H 8. (continued)

CHROM.	START	END	STR.	PROMOTER	EXON	INTRON	CpG ISLAND	p-VALUE	CLASSIFICATION
chr22	30652615	30652616	+					3,155E-13	stronglyHypometh
chr1	110420154	110420155	+					3,155E-13	stronglyHypometh
chr1	110420189	110420190	+					3,155E-13	stronglyHypometh
chr1	17994232	17994233	+			ARHGEF10L		3,155E-13	stronglyHypometh
chr3	155454914	155454915	+					3,155E-13	stronglyHypometh
chr8	124173268	124173269	-				Y	3,155E-13	stronglyHypometh
chr16	70222557	70222558	+				Y	3,155E-13	stronglyHypometh
chr11	69063297	69063298	+		MYEOV			3,155E-13	stronglyHypometh
chr10	131504532	131504533	+			MGMT		3,155E-13	stronglyHypometh
chr9	91792668	91792669	-			SHC3	Y	3,547E-13	stronglyHypometh
chr9	91792673	91792674	-			SHC3	Y	3,547E-13	stronglyHypometh
chr9	91792792	91792793	-	SHC3		SHC3	Y	3,547E-13	stronglyHypometh
chr9	91792801	91792802	-	SHC3		SHC3	Y	3,547E-13	stronglyHypometh
chr11	2178778	2178779	-			INS-IGF2		3,547E-13	stronglyHypometh
chr4	141217788	141217789	-			SCOC,LOC100129858		3,547E-13	stronglyHypometh
chr17	42082135	42082136	-	PYY,NAGS	NAGS		Y	3,547E-13	stronglyHypometh

Table H 8. (continued)

CHOROM.	START	END	STR.	PROMOTER	EXON	INTRON	CpG ISLAND	p-VALUE	CLASSIFICATION
chr17	42082137	42082138	-	PYY,NAGS	NAGS		Y	3,547E-13	stronglyHypometh
chr18	77218649	77218650	+			NFACT1	Y	3,547E-13	stronglyHypometh
chr22	40635356	40635357	+			TNRC6B		3,547E-13	stronglyHypometh
chr14	101617896	101617897	-					3,547E-13	stronglyHypometh
chr1	39183905	39183906	+					3,547E-13	stronglyHypometh
chr3	149374823	149374824	+	WWTR1	WWTR1		Y	3,547E-13	stronglyHypometh
chr10	33625946	33625947	+				Y	3,547E-13	stronglyHypometh
chr10	33625970	33625971	+				Y	3,547E-13	stronglyHypometh
chr16	699539	699540	-	WDR90		WDR90	Y	3,547E-13	stronglyHypometh
chr16	1312334	1312335	-					3,547E-13	stronglyHypometh
chr7	2349791	2349792	-			SNX8		3,547E-13	stronglyHypometh
chr1	203598492	203598493	+			ATP2B4	Y	3,547E-13	stronglyHypometh
chr1	203598494	203598495	+			ATP2B4	Y	3,547E-13	stronglyHypometh
chr1	203598505	203598506	+			ATP2B4	Y	3,547E-13	stronglyHypometh
chr1	203598651	203598652	-			ATP2B4	Y	3,547E-13	stronglyHypometh
chr1	203598674	203598675	-			ATP2B4	Y	3,547E-13	stronglyHypometh

Table H 8. (continued)

CHOROM.	START	END	STR.	PROMOTER	EXON	INTRON	CpG ISLAND	p-VALUE	CLASSIFICATION
chr19	34394603	34394604	+					3,648E-13	stronglyHypometh
chr14	74101177	74101178	-				Y	3,648E-13	stronglyHypometh
chr8	131369612	131369613	+			ASAPI		3,648E-13	stronglyHypometh
chr5	177263962	177263963	-					3,648E-13	stronglyHypometh
chr10	125672174	125672175	+					3,648E-13	stronglyHypometh
chr10	131504036	131504037	-			MGMT		3,648E-13	stronglyHypometh
chr7	5469231	5469232	-				Y	3,648E-13	stronglyHypometh
chr19	17414194	17414195	+	ABHD8	ABHD8		Y	4,084E-13	stronglyHypometh
chr3	187580339	187580340	+					4,084E-13	stronglyHypometh
chr20	20846128	20846129	-					4,101E-13	stronglyHypometh
chr2	232478863	232478864	+				Y	4,101E-13	stronglyHypometh
chr17	76354946	76354947	+		SOC S3		Y	4,101E-13	stronglyHypometh
chr17	76354954	76354955	+		SOC S3		Y	4,101E-13	stronglyHypometh
chr17	76354964	76354965	+		SOC S3		Y	4,101E-13	stronglyHypometh
chr2	16212378	16212379	+					4,101E-13	stronglyHypometh
chr14	52294996	52294997	+					4,101E-13	stronglyHypometh

Table H 8. (continued)

CHOROM.	START	END	STR.	PROMOTER	EXON	INTRON	CpG ISLAND	p-VALUE	CLASSIFICATION
chr8	12892 9888	12892 9889	-			PVT1		4,10 1E- 13	stronglyHypo meth
chr5	17867 8600	17867 8601	-			ADAMTS2		4,10 1E- 13	stronglyHypo meth
chr7	75524 084	75524 085	+					4,10 1E- 13	stronglyHypo meth

APPENDIX I

LINKS FOR METHYLATION TRACKS

MDA-ER α 5 6h OH treatment:

```
track      name='zr1134_1      CpG      methylation      track'  
bigDataUrl=https://s3.amazonaws.com/epiquest/epiquest_zr1134/VYDFJXA2MT8  
GDJLBF7EZRZEXJCY6J7BN/Analysis/browserTracks/zr1134_1_CpG_meth.bb  
type=bigBed itemRgb=On visibility=3
```

MDA-ER α 5 6h E2 treatment:

```
track      name='zr1134_2      CpG      methylation      track'  
bigDataUrl=https://s3.amazonaws.com/epiquest/epiquest_zr1134/VYDFJXA2MT8  
GDJLBF7EZRZEXJCY6J7BN/Analysis/browserTracks/zr1134_2_CpG_meth.bb  
type=bigBed itemRgb=On visibility=3
```

MCF7 6h OH treatment:

```
track      name='zr1134_3      CpG      methylation      track'  
bigDataUrl=https://s3.amazonaws.com/epiquest/epiquest_zr1134/VYDFJXA2MT8  
GDJLBF7EZRZEXJCY6J7BN/Analysis/browserTracks/zr1134_3_CpG_meth.bb  
type=bigBed itemRgb=On visibility=3
```

MCF7 6h E2 treatment:

```
track      name='zr1134_4      CpG      methylation      track'  
bigDataUrl=https://s3.amazonaws.com/epiquest/epiquest_zr1134/VYDFJXA2MT8  
GDJLBF7EZRZEXJCY6J7BN/Analysis/browserTracks/zr1134_4_CpG_meth.bb  
type=bigBed itemRgb=On visibility=3
```


APPENDIX J

GENES SHOWING SIGNIFICANT CHANGES IN TRANSCRIPTOMIC ANALYSES

Table J 1. Genes showing significant changes in transcriptomic analysis of MDA-ER α 5 monoclonal after 6h E2 treatment compared to ethanol group.

GENE_ID	GENE	LOCUS	p-VALUE
ENSG00000138131.3	LOXL4	chr10:98247689-98268250	0
ENSG00000198406.7	BZW1P2	chr3:115802362-117139389	0
ENSG00000225178.5	RPSAP58	chr19:23762943-23874701	0
ENSG00000232024.2	LSM12P1	chr8:35235456-35796550	0
ENSG00000239899.3	RN7SL674P	chr2:11482340-11642788	0
ENSG00000241175.3	RN7SL494P	chr15:50241946-50266026	0
ENSG00000242071.3	RPL7AP6	chr14:69854130-70032366	1,33227E-15
ENSG00000225573.4	RPL35P5	chr7:66606737-66607107	2,90434E-13
ENSG00000179542.15	SLITRK4	chrX:143622789-143635777	2,33584E-11
ENSG00000237330.2	RNF223	chr1:1070965-1074307	6,21967E-11
ENSG00000198774.4	RASSF9	chr12:85800696-85836570	1,12152E-10
ENSG00000226085.3	UQCRC1P1	chr22:39743043-39893864	4,23036E-09
ENSG00000101230.5	ISM1	chr20:13221770-13300651	9,47252E-09

Table J 1. (continued)

GENE_ID	GENE	LOCUS	p-VALUE
ENSG00000163083.5	INHBB	chr2:120346142-120351808	8,49427E-08
ENSG00000185090.14	MANEAL	chr1:37793801-37801137	8,92019E-08
ENSG00000152137.6	HSPB8	chr12:119178641-119221131	1,49842E-07
ENSG00000188483.7	IER5L	chr9:129175551-129210548	4,95103E-07
ENSG00000237991.3	RPL35P1	chr1:236981338-236981708	9,13474E-07
ENSG00000214900.8	LINC01588	chr14:49981711-50092643	5,03365E-06
ENSG00000230629.2	RPS23P8	chrX:70962963-70963293	7,9036E-06
ENSG00000116774.11	OLFML3	chr1:113979390-114035572	9,9005E-06
ENSG00000206625.1	RNU6-1	chr15:67819703-67873866	4,72998E-05
ENSG00000180720.7	CHRM4	chr11:46385097-46386608	5,91255E-05

Table J 2. Genes showing significant changes in transcriptomic analysis of MCF7 cells after 6h E2 treatment compared to ethanol group.

GENE_ID	GENE	LOCUS	p-VALUE
ENSG00000141753.6	IGFBP4	chr17:40443460-40457731	0
ENSG00000152137.6	HSPB8	chr12:119178641-119221131	0
ENSG00000162891.10	IL20	chr1:206865353-206869223	0
ENSG00000189343.7	RPS2P46	chr17:19417803-19492991	0
ENSG00000214391.3	TUBAP2	chr11:90251231-90915052	0
ENSG00000232024.2	LSM12P1	chr8:35235456-35796550	0
ENSG00000241175.3	RN7SL494P	chr15:50241946-50266026	0
ENSG00000242071.3	RPL7AP6	chr14:69854130-70032366	0
ENSG00000163485.15	ADORA1	chr1:203090653-203167405	6,88E-15
ENSG00000213694.3	S1PR3	chr9:88990862-89005010	1,89E-14
ENSG00000150594.6	ADRA2A	chr10:111077162-111080907	2,2E-14
ENSG00000109321.10	AREG	chr4:74445133-74455009	6,95E-14
ENSG00000107562.16	CXCL12	chr10:44370164-44386493	1,17E-13
ENSG00000205363.5	C15orf59	chr15:73735430-73770613	3,54E-13
ENSG00000142619.4	PADI3	chr1:17249097-17284233	8,38E-13
ENSG00000139211.6	AMIGO2	chr12:47075706-47236662	2,28E-12
ENSG00000180530.9	NRIP1	chr21:14818842-15065000	2,7E-12
ENSG00000197977.3	ELOVL2	chr6:10980758-11078226	5,75E-12
ENSG00000153165.18	RGPD3	chr2:106382170-106468376	6,94E-12

Table J 2. (continued)

GENE_ID	GENE	LOCUS	p-VALUE
ENSG00000239887.4	C1orf226	chr1:162069773-162386818	1,05E-11
ENSG00000225840.2	AC010970.2	chrY:10197255-10199103	1,6E-11
ENSG00000134996.11	OSTF1	chr9:75088542-75147265	2,1E-11
ENSG00000183779.6	ZNF703	chr8:37695750-37700021	4,46E-11
ENSG00000169908.10	TM4SF1	chr3:149369021-149386583	1,67E-10
ENSG00000086062.12	B4GALT1	chr9:33104081-33179983	1,69E-10
ENSG00000174977.8	AC026271.5	chr17:18635005-18682262	2,39E-10
ENSG00000163659.12	TIPARP	chr3:156671861-156706770	3,85E-10
ENSG00000100234.11	TIMP3	chr22:32512551-33058372	5,8E-10
ENSG00000135547.8	HEY2	chr6:125578557-125761269	5,92E-10
ENSG00000136574.17	GATA4	chr8:11676958-11760002	8,8E-10
ENSG00000237330.2	RNF223	chr1:1070965-1074307	1,24E-09
ENSG00000182704.7	TSKU	chr11:76782250-76798154	1,67E-09
ENSG00000185697.16	MYBL1	chr8:66562174-66614247	1,96E-09
ENSG00000277483.1	RN7SL321P	chr3:48372218-48401259	2,81E-09
ENSG00000164626.8	KCNK5	chr6:39188972-39229450	8,8E-09
ENSG00000106733.20	NMRK1	chr9:75060572-75088217	9,5E-09
ENSG00000184454.6	NCMAP	chr1:24556110-24609328	3,14E-08
ENSG00000180730.4	SHISA2	chr13:26044596-26051031	3,31E-08
ENSG00000108551.4	RASD1	chr17:17494436-17496395	6,28E-08

Table J 2. (continued)

GENE_ID	GENE	LOCUS	p-VALUE
ENSG00000224040.1	HMGN1P4	chr1:182899864-182953525	8,54E-08
ENSG00000135549.14	PKIB	chr6:122471916-122726373	8,77E-08
ENSG00000154553.13	PDLIM3	chr4:185500659-185535612	8,81E-08
ENSG00000119669.4	IRF2BPL	chr14:77024542-77031572	1,04E-07
ENSG00000099812.8	MISP	chr19:751125-764318	1,54E-07
ENSG00000137441.7	FGFBP2	chr4:15960242-16084378	1,57E-07
ENSG00000146242.8	TPBG	chr6:82363205-82370828	1,7E-07
ENSG00000138764.13	CCNG2	chr4:77157150-77494286	1,94E-07
ENSG00000176532.3	PRR15	chr7:29563810-29567295	2,08E-07
ENSG00000181788.3	SIAH2	chr3:150741126-150763477	2,32E-07
ENSG00000134830.5	C5AR2	chr19:47332146-47347327	2,33E-07
ENSG00000069188.16	SDK2	chr17:73334383-73644089	2,34E-07
ENSG00000164761.8	TNFRSF11B	chr8:118923556-118952200	2,61E-07
ENSG00000177519.3	RPRM	chr2:153420676-153593288	2,9E-07
ENSG00000221866.9	PLXNA4	chr7:132123331-132648688	2,94E-07
ENSG00000168306.12	ACOX2	chr3:58505135-58537319	3,59E-07
ENSG00000165732.12	DDX21	chr10:68956127-68985073	4,48E-07
ENSG00000117479.12	SLC19A2	chr1:169463908-169486003	4,75E-07
ENSG00000244211.3	PDZK1P1	chr1:147993861-148014956	5,01E-07
ENSG00000125968.8	ID1	chr20:31605282-31606515	5,03E-07

Table J 2. (continued)

GENE_ID	GENE	LOCUS	p-VALUE
ENSG00000003137.8	CYP26B1	chr2:72129237-72148038	5,19E-07
ENSG00000237350.1	CDC42P6	chr4:22692913-22819575	7,98E-07
ENSG00000138829.10	FBN2	chr5:128257908-129033642	8,15E-07
ENSG00000271254.6	AC240274.1	KI270711.1:4611-29626	1,05E-06
ENSG00000135625.7	EGR4	chr2:73290928-73293705	1,48E-06
ENSG00000161031.12	PGLYRP2	chr19:15468644-15498956	2,01E-06
ENSG00000141384.11	TAF4B	chr18:26225935-26391685	3,91E-06
ENSG00000111907.20	TPD52L1	chr6:125119048-125302078	3,99E-06
ENSG00000175906.4	ARL4D	chr17:43398958-43401137	5,51E-06
ENSG00000106789.12	CORO2A	chr9:98120974-98192640	5,62E-06
ENSG00000189143.9	CLDN4	chr7:73799541-73832693	6,72E-06
ENSG00000175264.7	CHST1	chr11:45648876-45665622	6,76E-06
ENSG00000226887.7	ERVMER34-1	chr4:52722617-52751640	7,43E-06
ENSG00000109062.9	SLC9A3R1	chr17:74670577-74769353	7,59E-06
ENSG00000160183.13	TMPRSS3	chr21:42371889-42396846	7,75E-06
ENSG00000170629.14	DPY19L2P2	chr7:103175132-103280410	9,59E-06
ENSG00000164128.6	NPY1R	chr4:163323960-163351934	9,89E-06
ENSG00000144655.14	CSRNP1	chr3:39141854-39154562	0,0000105
ENSG00000160182.2	TFF1	chr21:42362281-42366594	0,0000111
ENSG00000140465.13	CYP1A1	chr15:74719541-74725610	0,0000157

Table J 2. (continued)

GENE_ID	GENE	LOCUS	p-VALUE
ENSG00000226085.3	UQCRFS1P1	chr22:39743043-39893864	0,0000162
ENSG00000178695.5	KCTD12	chr13:76880165-76886400	0,0000163
ENSG00000082175.14	PGR	chr11:101029623-101209591	0,0000175
ENSG00000275342.4	SGK223	chr8:8317735-8386498	0,0000203
ENSG00000188211.8	NCR3LG1	chr11:17351725-17377341	0,0000207
ENSG00000147041.11	SYTL5	chrX:37349274-38688920	0,0000225
ENSG00000196126.10	HLA-DRB1	chr6:32552712-32589848	0,0000291
ENSG00000163823.3	CCR1	chr3:46163603-46266706	0,0000295
ENSG00000201289.1	RN7SKP76	chr16:61647241-62037035	0,0000351
ENSG00000198797.6	BRINP2	chr1:177171496-177282422	0,0000419
ENSG00000186603.5	HPDL	chr1:45326904-45328533	0,0000426
ENSG00000117318.8	ID3	chr1:23557917-23559794	0,0000429
ENSG00000164687.10	FABP5	chr8:81279870-81284777	0,0000444
ENSG00000056736.9	IL17RB	chr3:53846579-53865800	0,0000468
ENSG00000100290.2	BIK	chr22:43110747-43129712	0,0000475
ENSG00000115844.10	DLX2	chr2:172099438-172102900	0,0000487
ENSG00000165731.17	RET	chr10:43077026-43130351	0,0000587
ENSG00000052344.15	PRSS8	chr16:31131432-31135762	0,0000656
ENSG00000118523.5	CTGF	chr6:131948175-132077393	0,0000667
ENSG00000148344.10	PTGES	chr9:129738330-129753047	0,0000671

Table J 2. (continued)

GENE_ID	GENE	LOCUS	p-VALUE
ENSG00000196136.16	SERPINA3	chr14:94561090-94624646	0,0000686
ENSG00000121966.6	CXCR4	chr2:136114348-136118165	0,0000936
ENSG00000146278.10	PNRC1	chr6:89080750-89085160	0,0000988
ENSG00000148488.15	ST8SIA6	chr10:17318382-17454330	0,0001043
ENSG00000174453.9	VWC2L	chr2:213284378-214684246	0,0001096
ENSG00000235123.5	DSCAM-AS1	chr21:40010998-40847139	0,0001099
ENSG00000120149.8	MSX2	chr5:174724532-174730893	0,00011
ENSG00000149328.14	GLB1L2	chr11:134331873-134378341	0,0001107
ENSG00000116774.11	OLFML3	chr1:113979390-114035572	0,0001107
ENSG00000247626.4	MARS2	chr2:197693105-197786762	0,0001155
ENSG00000174827.13	PDZK1	chr1:145670851-145708148	0,0001187
ENSG00000129159.6	KCNC1	chr11:17734811-17783055	0,0001416
ENSG00000124496.12	TRERF1	chr6:42224930-42452051	0,0001423
ENSG00000157514.16	TSC22D3	chrX:107713220-107777342	0,0001521
ENSG00000186212.3	SOWAHB	chr4:76894927-76898147	0,0001547
ENSG00000124216.3	SNAI1	chr20:49982998-49988886	0,0001564
ENSG00000151835.13	SACS	chr13:23328822-23433728	0,0001674
ENSG00000176907.4	C8orf4	chr8:40153454-40155308	0,0001848
ENSG00000143473.11	KCNH1	chr1:210678314-211134115	0,0001934
ENSG00000186665.8	C17orf58	chr17:67991100-67993649	0,000195

Table J 2. (continued)

GENE_ID	GENE	LOCUS	p-VALUE
ENSG00000149218.4	ENDOD1	chr11:95089809-95132645	0,0002148
ENSG00000124664.10	SPDEF	chr6:34537801-34556333	0,0002179
ENSG00000118513.18	MYB	chr6:135181314-135219173	0,0002244
ENSG00000225431.1	AP001626.1	chr21:42599279-42615058	0,0002248
ENSG00000185090.14	MANEAL	chr1:37793801-37801137	0,0002255
ENSG00000197308.8	GATA3-AS1	chr10:8050449-8053484	0,0002255
ENSG00000214389.2	RPS3AP26	chr7:98252378-98401068	0,0002307
ENSG00000054598.6	FOXC1	chr6:1609971-1613897	0,0002476
ENSG00000159335.15	PTMS	chr12:6747995-6770952	0,0002548
ENSG00000111845.4	PAK1IP1	chr6:10671417-10709782	0,0002584
ENSG00000168209.4	DDIT4	chr10:72273919-72276036	0,0002718
ENSG00000204386.10	NEU1	chr6:31857658-31862906	0,000284
ENSG00000198488.10	B3GNT6	chr11:77034397-77041973	0,000293
ENSG00000134533.6	RERG	chr12:15107782-15597399	0,0003211
ENSG00000267056.2	AC005336.4	chr19:15910581-15911824	0,000341
ENSG00000179542.15	SLITRK4	chrX:143622789-143635777	0,0003417
ENSG00000104998.3	IL27RA	chr19:14031747-14053216	0,0003595
ENSG00000164120.13	HPGD	chr4:174490176-174523154	0,0003914
ENSG00000155090.14	KLF10	chr8:102648778-102655902	0,0004034
ENSG00000239398.3	RN7SL342P	chr18:59972913-59973207	0,0004068

Table J 2. (continued)

GENE_ID	GENE	LOCUS	p-VALUE
ENSG00000233621.1	LINC01137	chr1:37454878- 37474411	0,0004153